Repair of Damaged Strip and Stirrup Confined Beam Column Joints Using Carbon Fiber Reinforced Polymer

Muhammad Arshad

NUST-2014-64393-MMCE-10614F

Supervisor

Dr. Muhammad Rizwan

MILITARY COLLEGE OF ENGINEERING

NATIONAL UNIVERSITY OF SCIENCES AND TECHNOLOGY, RISALPUR

AUGUST, 2018

Repair of Damaged Strip and Stirrup Confined Beam Column Joints Using Carbon Fiber Reinforced Polymer

Submitted by

MUHAMMAD ARSHAD

NUST-2014-64393-MMCE-10614F

A thesis submitted in partial fulfillment of the requirements for the degree of

MS Structural Engineering

Thesis Supervisor:

DR. M. RIZWAN

Thesis Supervisor's Signature:_____

MILITARY COLLEGE OF ENGINEERING

NATIONAL UNIVERSITY OF SCIENCES AND TECHNOLOGY, RISALPUR

AUGUST, 2018

Declaration

I certify that this research work titled "*Repair of Damaged Strip and Stirrup Confined Beam Column Joints Using Carbon Fiber Reinforced Polymer"* is my own work. The work has not been presented elsewhere for assessment. The material that has been used from other sources it has been properly acknowledged / referred.

MUHAMMAD ARSHAD

NUST-2014-64393-MMCE-10614F

Language Correctness Certificate

This thesis has been read by an English expert and is free of typing, syntax, semantic, grammatical and spelling mistakes. Thesis is also according to the format given by the university.

Signature of Student

MUHAMMAD ARSHAD

Registration Number

NUST-2014-64393-MMCE-10614F

Signature of Supervisor

Copyright Statement

Acknowledgements

I am thankful to my Creator Allah Subhana-Watala to have guided me throughout this work at every step and for every new thought which You setup in my mind to improve it. Indeed, I could have done nothing without Your priceless help and guidance. Whosoever helped me throughout the course of my thesis, whether my parents or any other individual was Your will, so indeed none be worthy of praise but You.

I am profusely thankful to my beloved parents who raised me when I was not capable of walking and continued to support me throughout in every department of my life.

I would also like to express special thanks to my supervisor **Dr. Muhammad Rizwan** for his help throughout my thesis. I can safely say that I haven't learned any other engineering subject in such depth than the ones which he has taught.

I would also like to pay special thanks to **Dr. Fiaz Tahir** and **Engr. Syed Saqib Mehboob** for their tremendous support and cooperation. Each time I got stuck in something, they came up with the solution. Without their help I wouldn't have been able to complete my thesis. I appreciate their patience and guidance throughout the whole thesis.

Finally, I would like to express my gratitude to all the individuals who have rendered valuable assistance to my study.

Dedicated to my exceptional parents whose tremendous support and cooperation led me to this wonderful accomplishment

Abstract

The performance of column-beam joints has been recognized as an important factor since long affecting the overall behavior of reinforced framed structures subjected to large scale lateral loading during earthquakes. Different repairing techniques are being used to retrofit column-beam joints weakened by seismic excitations. This study is a part of ongoing research to develop efficient retrofitting techniques.

As a part of research work, twelve pre-damaged specimens were repaired. The specimens were divided into two majors group based on strength. The characteristics compressive strength of first group was 28 MPa and that for the second was 21 MPa. Each group was further divided into three sub-groups numbered one, two and three, and designated as conventionally reinforced concrete joint CRCJ, strip confined joint SRCJ and strip confined beam. Group one was consisting of Grade 40, 10 mm diameter bar as stirrups. In group two and group three steel strips was used as stirrups. Gage of group two strip was 14 and that of group three was 18. The total area of stirrups remained constant which was 0.11 mm^2. The basic idea behind using the strips as stirrups was to check the performance of strips as stirrups in order to avoid congesting of steel bars at joint. Cracks in the sample were filled with epoxy resins and joints were repaired with CFRP laminates. Joints were tested under cyclic axial loads to investigate seismic performance.

Quasi static load was applied during testing of repaired specimens. During the conduct of test the compressive load was kept constant on the column, thus nullifying the chance of column movement. Loads were applied using hydraulic jack and proving ring of 500 kN capacity was used as load cell. Deflection gages were mounted to record defection under applied loads. Cyclic loads were applied until 20 % degradation was achieved in the samples. Following parameters were examined and compared; yield load displacement, peak load displacement, ultimate load, residual displacement, energy dissipation, ductility and stiffness.

Key Words: *Column-Beam Joint, Seismic Excitations, Retrofitting, Cyclic loads, Finite Element Modeling*

Table of Contents

List of Figures

List of Tables

Chapter 1

INTRODUCTION

1.1. Introduction

Due to devastating earth quakes such as, Kobe (Japan) 1995, the Kocaeli (Turkey), 1999 and Boumerdes (Algeria) 2003, seismic performance of existing structures has become a great matter of concern. Structures built as per previous design aids are the most vulnerable, for these sorts of repeated events. Therefore, they contribute to higher seismic hazard, predominantly in big metropolitan zones. The exposure of building structures to earthquake has remained an important region for the researchers in order to curtail the hazards of earthquake as much as possible. As the buildings/ structures have to resist huge lateral load reversals through an event of earthquake, appropriate reinforced concrete beam column joint detailing in structures is of great importance. Beam-column joint is one of the structural components to transfer loads to soil through foundations. Beam-column joints, being the lateral as well as vertical load carrying members are predominantly subject to failure during seismic excitation and hence their rehabilitation is a major concern for successful rehabilitation strategy. One of the techniques followed up for the repair and strengthening the reinforced concrete structures is confining the RC member using composite enclosure. Reinforced structural members subjected to confinement introduces deformability in reinforced concrete structural elements. The yield strength, configuration and spacing of transverse reinforcement have considerable influence on the stress strain relationship of confined concrete members.

Typically, columns have minimum cross-sectional dimensions, this results in a weak column-strong beam construction that, under seismic loads, may lead to the formation of local hinges in the column. Although hinge zones of beam and columns, in reinforced concrete frames, are often well confined. However, higher ductility requirements of the system can only be met if the stress path of moment reversals occurring at the face of supports exists through the joint. The joints are often congested. An interior joint, of intermediate floor, is required to accommodate reinforcement of at least six structural components. Due to congestion it is difficult to add confining reinforcement in the joints. In this project, a proposed technique to confine beam-column joints using steel strips will be implemented and examined. The technique uses contact area of steel strips to provide confinement and economize on the overall

volume of confining reinforcement provided in the joints. The behavior of steel-strip-confined beam-column joints will be studied in the form of load-displacement curves.

Number of technical solutions have been proposed with the aim to improve the seismic performance of deficient RC structures. However, in gravity load-designed structures the ductility of columns is insufficient, because the joint-panel makes the next weakest element in the structure either due to transverse reinforcement, discontinuity of the beam bottom reinforcement, improper and non-ductile detailing. These arrangements of detailing in beam-column joints results in collapse of structural integrity. Therefore, beam column joint is considered as a vital element in structures exposed to seismic effects.

1.2. Background, scope and motivation

If a reinforced concrete structure is designed to withstand seismic effects it must show satisfactory performance under severe load conditions. To withstand lateral load without severe damage, structure needs strength as well as energy absorption capacity. Moreover, it is advised to design a stable RC structure having the most economical design. Therefore, the necessity for strength and ductility needs to be considered against economic restraints.

Many of RC structures when subjected to seismic loadings fail in shear at beam column joints, due to non-ductile detailing at joints, or weak column/beam structure design without seismic provisions in design codes. A joint with under a severe earthquake, undergoes a large amount of shear stress concentration over the joint zone, and it may lead to total collapse of the structure if the joint shear capacity is inadequate. The kocaeli earthquake, in Turkey (1999) is one practical evidence of such sort of failures. If a situation of this type arises it is necessary to determine whether it is more economical to strengthen the existing structure or to replace it, and strengthening is much more complicated in some cases.

Improving the strength of beam column joint is the most viable solution to avoid structural failures because of localized defects. Various techniques are available to assimilate already constructed weak beam column joints. Alcocer and Jirsa experimented reinforced concrete jackets and steel jackets for improving the strength of RC joints. However, this technique is labor demanding, costlier and requires highly skilled workers. This method increases the dead load and dimensions of the joint. Steel plates fixed with epoxy or a bolt is another method to increase the strength and ductility of concrete. Alternatively, fiber-reinforced polymers (FRP) can be used in RC members at critical locations. These polymers act as external reinforcement

which is attached on to the members. FRP is also a good strengthening technique. Use of fiber-reinforced polymer (FRP) is grownup its acceptance over the past decade, appreciated for higher strength-to-weight ratios, corrosion-resistant, adaptability, and constructability. The FRP composite materials are light weight and have more strength as compared to steel; they are non-corroding and non-conducting. Moreover, the load carrying capacity of the structure is increased using FRP composite materials. In order to overcome shear deficiency in beam-column joints Antonopoulos and Triantafillou tested various configurations of FRP sheets and strips. Externally bonded FRP technique improved the strength, energy dissipation and stiffness of the poorly detailed joints.

1.3. Conventional repair methods

The following are some of the methods used to rehabilitate RC structures:

Bonded steel plates

A steel composite system is formed by the help of steel plates which are connected using epoxy adhesives.

Section enlargement or Jacketing

In this method additional reinforcement with stirrups is provided right from the base.

Grouting process

Grouting is a process of increasing the load bearing capacity of the structure by filling a material into the cavities in the concrete.

Application of epoxy resins

In this method an epoxy adhesive is used for the rehabilitation of RC structure.

Post tensioning

It includes external pre-stressing methods to correct the deflections in RC structures.

1.7. Problem statement

The northern area of Pakistan is covered by World's three largest mountain ranges that are Hindu Kush, Himalayan and Karakoram ranges and these ranges are located over the tectonic plate boundaries. Large region of Pakistan is seismically active. Numbers of earthquakes are

recorded each year. These earthquakes cause large damages to property/ infrastructure and loss of lives. Design of structures which can achieve desired performance levels as required by prevailing building codes is necessary. Therefore, such projects aimed in the area of performance based seismic design are important and will help in mitigating the effects of earthquakes.

Thus, a requirement arises to compare the variation in ductility and ultimate strength under cyclic loading of steel strips confined joints with joints confined by steel stirrups as transverse reinforcements.

1.8. Aims and objectives

The project has the following objectives:

i. To find the efficacy of CFRP repaired beam column joint confined with steel stirrups and strips against cyclic loading.
ii. To evaluate the ultimate strength, ductility factor and stiffness of CFRP repaired joints at different damage levels.

1.9. Research Utilization

This experimental work on joint repair will be helpful to strengthen the shear and improve bond slip resistance in order to overcome brittle failures. Study will be useful for research community to address joint performance with special reference to CFRP application in seismically affected areas. It will be beneficial to restore the joints to their desired capacity with a very practical, light weight, corrosion resistant, fast, easy to apply and efficient repair technique.

1.10 Chapter Organization

The thesis work is comprised of five chapters. Introduction of research work, problem statement, and objectives of research work are given in first chapter. Literature review on application of different types of repair methods including CFRP repair for strengthening and retrofitting of different RC structural elements is presented in second chapter.

In third chapter, complete experimental program, conducted for repair of beams column joints (BCJ) with CFRP sheets, is presented including material properties of concrete, material properties of CFRP sheets and epoxy adhesives, geometry/cross sections of beams, mixing

proportions of concrete, damaging/testing of beams column joints, repair configuration of joints and repair procedure of joints with CFRP.

Fourth chapter contains results discussion and conclusions drawn for CFRP repaired joints. In last chapter (fifth) test results recommendations are developed after complete analysis of test program.

Chapter 2

LITERATURE REVIEW

2.1. Introduction

Natural calamities such as earthquakes always cause devastating effects on the mankind as well as the physical structures. Natural disasters are unpredictable and unavoidable and cause a sudden destruction.

For example, at 11th of April in 2012, when two earthquakes 8.2 and 8.6 magnitude hit the west coast of Indonesia 100 to 200 km in northern Sumatra (southwest of major subduction zone), that was one of its kind, resulted due to strike-slip faulting at oceanic lithosphere in Indo-Australia plate and caused a huge destruction.

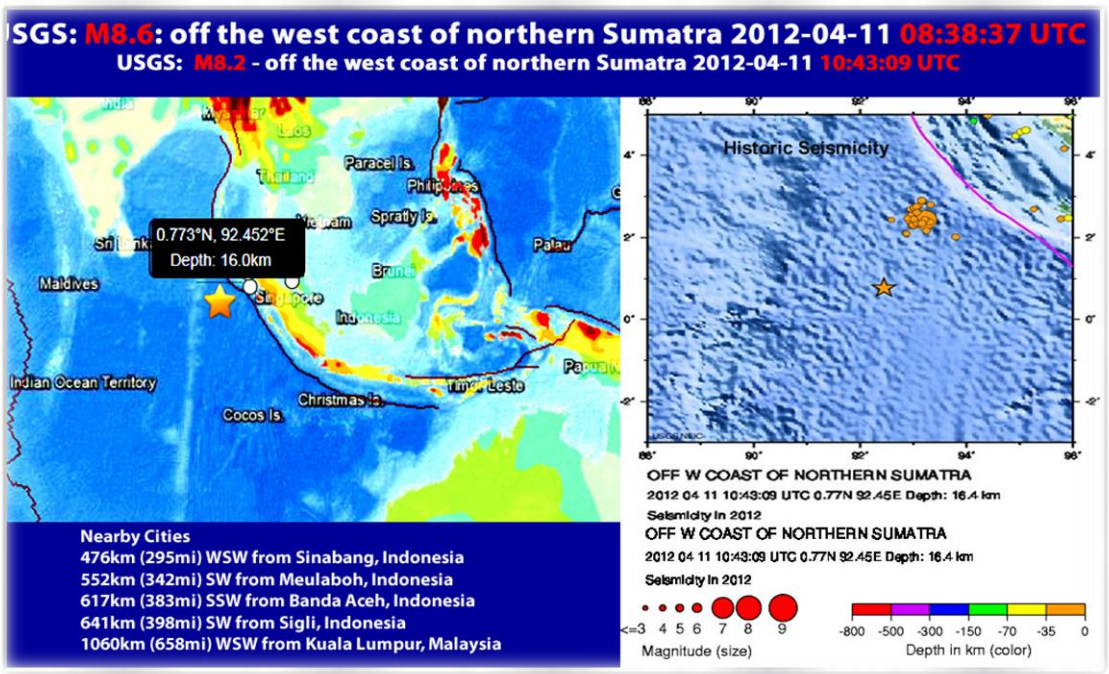

Figure 2.1 Seismic events in Indonesia April, 2011

Design life of buildings is normally kept 50 - 100 years, but they are designed and detailed to withstand major earthquakes which may occur in 100 – 1000 years. This is because the damages caused are intense and too expensive. Hence, the major requirement is to construct earthquake resistant buildings/ structures, which can withstand the enormous force of an earthquake. During earthquake buildings are designed not to collapse, however severe damage

is expected. Thus, the human being safety and contents is guaranteed in earthquake resistant structures. Seismic provisions and codes are used in world to achieve this objective.

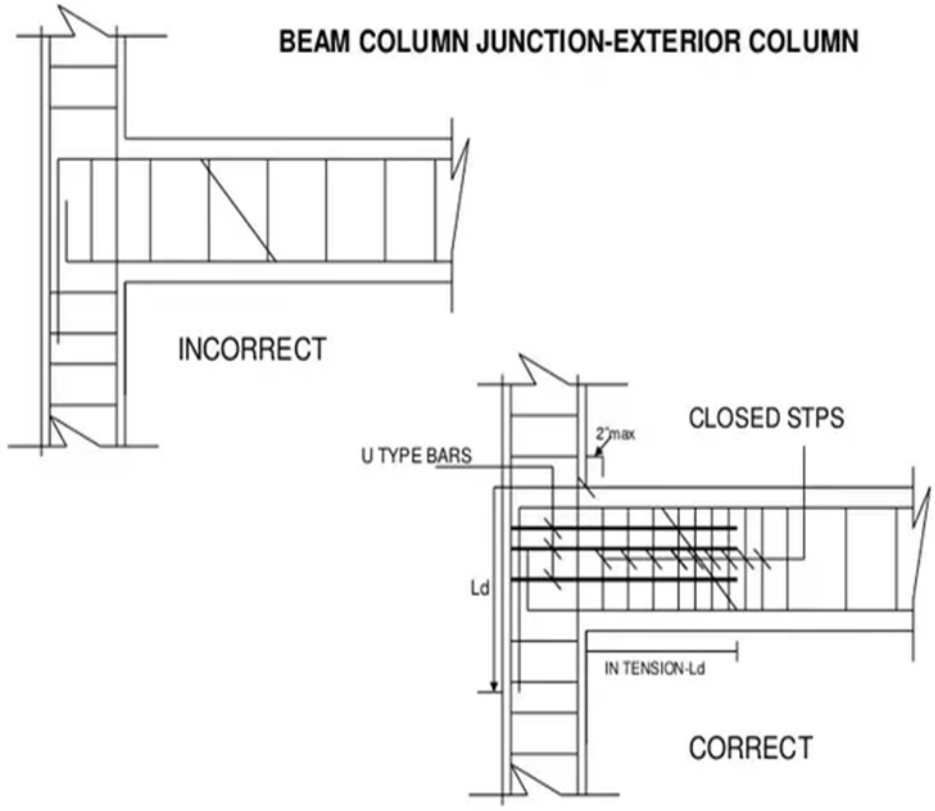

Figure 2.2 A typical beam-column joint (exterior)

Portion of column within the beam is called as Beam Column Joints (BCJ). Their design was limited to prove passable anchorage for the main rebars, but it has become more important with the increasing use of high strength concrete, this resulted in reduction of member dimensions and increase in the area of steel reinforcement.

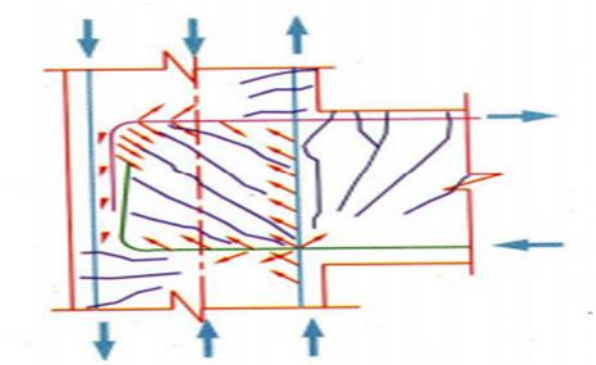

Figure 2.3 Free body diagram of loads acting on a typical joint

The poor design practice in RC beam-column joint is compounded when ever higher demand of adjoining beam and column members is raised, that mobilize the inelastic capacity of RC members to dissipate their seismic energy. To understand joints behavior under seismic excitation, numerous researches are carried out experimentally and analytically.

In recent years, a lot of non-conventional techniques have been suggested to enhance the performance of RC joints (BCJ) under seismic excitations, for example joints reinforced with steel jackets and fiber-reinforced polymer (FRP). The failure of structure during an earthquake is normally subjected to the failure of joints.

Figure 2.4 A typical failure of Beam-Column joint

The major objective of the ACI code is to design structures with adequate strength and ductility. Ductility is the ability of a member to endure large deformations without rupture during failure. Ductile member may bend or deform excessively under load but it remains by and large intact. This capability prevents total structure collapse and provides protection/ reaction time to the occupants of the building. Ductile structures undergo large deformations before collapse and

provide visible evidences of impending failure and give opportunity to relieve the distress by reducing loads. Brittle members fail explosively or suddenly, completely and without warning thus not allowing any remedial measures to be taken. When a brittle member fails it usually disintegrates and may damage adjacent portion of the structure or overload the member bringing an additional failure. A collapse in which the effect of local failure is spread to the entire structure or to a significant portion of the structure is known as progressive collapse.

2.2. Previous research on repair of beam column joint

G. Maariappan & R. Singaravadivelan (2013) - RCC Beam-Column Joint Retrofitted with Basalt Fiber Reinforced Polymer Sheet:

In this study failed specimens were retrofitted to make new specimens. At the failure zone concrete was detached and cement paste was applied, again the portion was repaired with the same type of concrete. Curing time for the specimens was kept to be 28 days. After completely filling all voids with putty; a two-component primer was applied and cured for 24 hours. Basalt fiber sheet was rapped over the joint after the application two component epoxy coating.

The testing involved deflecting the beam using the push pull jack up to control deflection of 75mm. The strength and ductility of reinforced concrete columns was effectively improved by the use of the reinforcing technique and was proved after the analysis.

Paul J. Granata and Azadeh Parvin – Strengthening of beam column connection:

This experiment demonstrated the property of FPR fabrics to enhance the moment capacity of RC joints. A number of six exterior joints (BCJ) were tested. The beam and column wrap thickness were considered a variable. Joints were tested by applying a vertical load at the free end of the beam and its deflection was measured by using simple dial gauge. It was observed that 60 percent of the moment capacity was increased using the FPR fabrics.

Jianchun Li, Bijan Samali, Lin Ye, and Steve Bakoss - beam–column connections reinforced with hybrid FRP sheet:

In this experiment, three concrete frame beam column joint specimens were used.

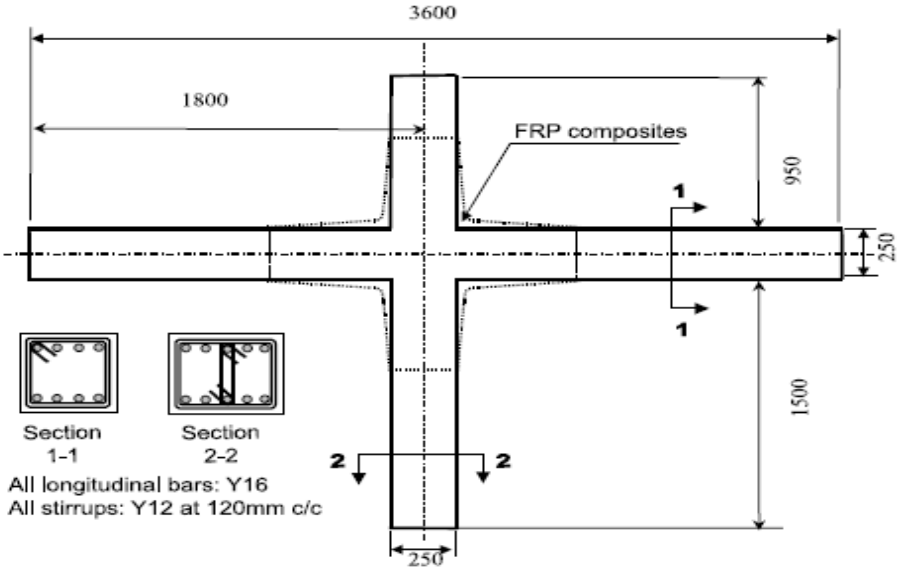

Figure 2.5 Reinforced Concrete Beam Column Joint

Comparison of load-deflection curves for FRP and non-FRP joints after 100 cycles of fatigue loading was made, as shown below

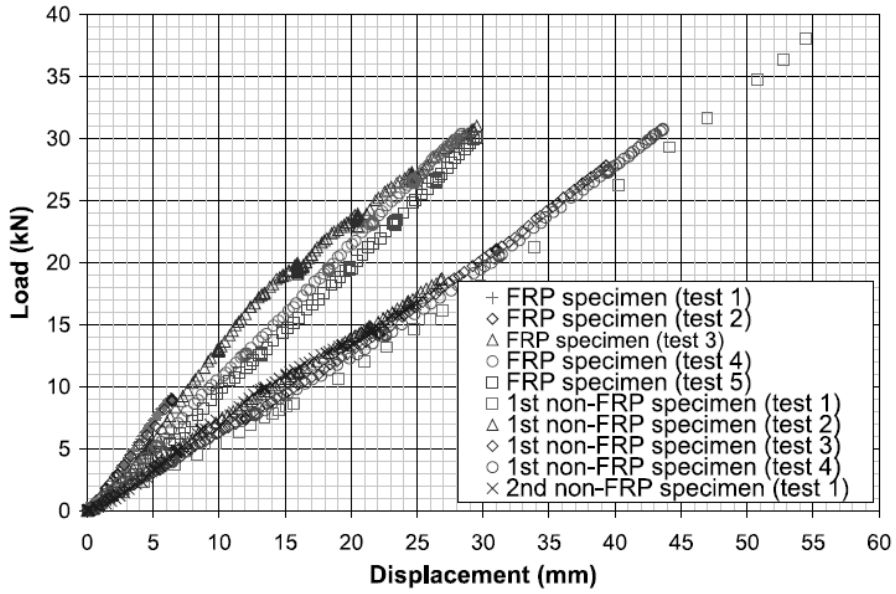

Figure 2.6 Load Deflection Curve for FRP and Non FRP Joints

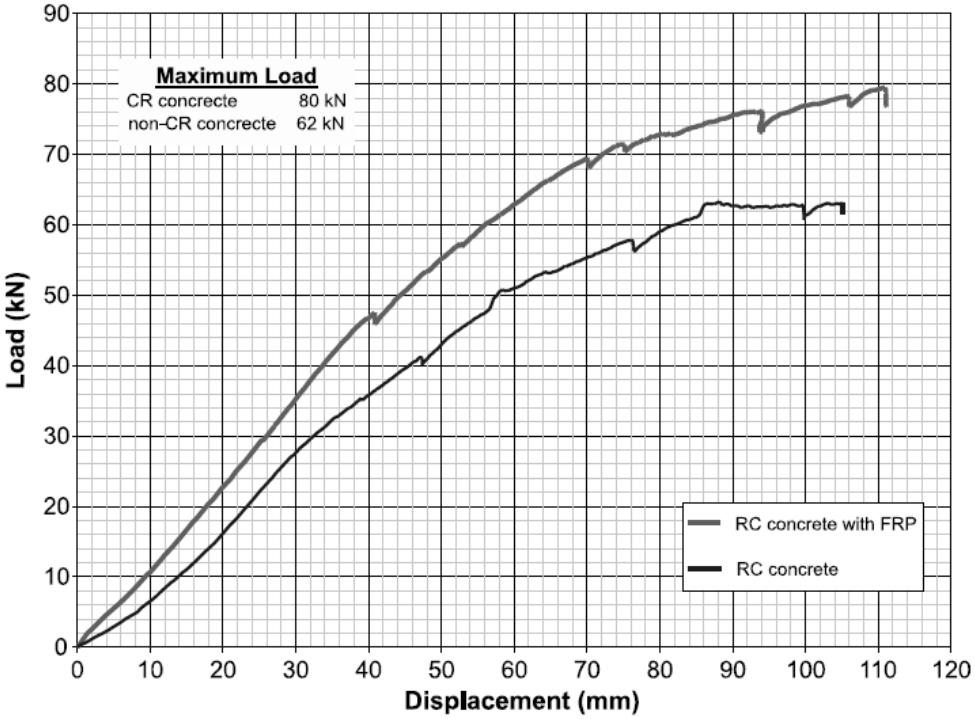

Figure 2.7 RC Beam Column Joint Repaired with CFRP

The results of the experiment showed 45% increase in the stiffness due to the presence of FRP.

Hasan Moghaddam (2010) - Axial compressive behavior of concrete actively confined by metal strips; part A: experimental study:

In this experimental study the concrete specimens were retrofitted by use of a strapping technique to enhance their compressive strength.

High strength metal strips were post tensioned around RC columns. This study consisted of 72 cylindrical and prismatic compressive specimens for axial compressive tests, these samples were dynamically confined by metal strips and these strips were post tensioned, thus increasing confining pressure. The influence of different parameters on ductility and strength of confined concrete and confining strips were noted. Longitudinal and lateral strains in both, concrete as well as strips were studied. It was noted that ductility of confining material is significant for increase in concrete ductility. The increase in strength was found relying on the effective mechanical volumetric ratio of confining strips.

Seismic Behavior of RC Beam-Wide Column Joints (RC) Retrofitted with CFRP:

Four beam column joints not conforming to seismic code provisions were designed constructed and tested.

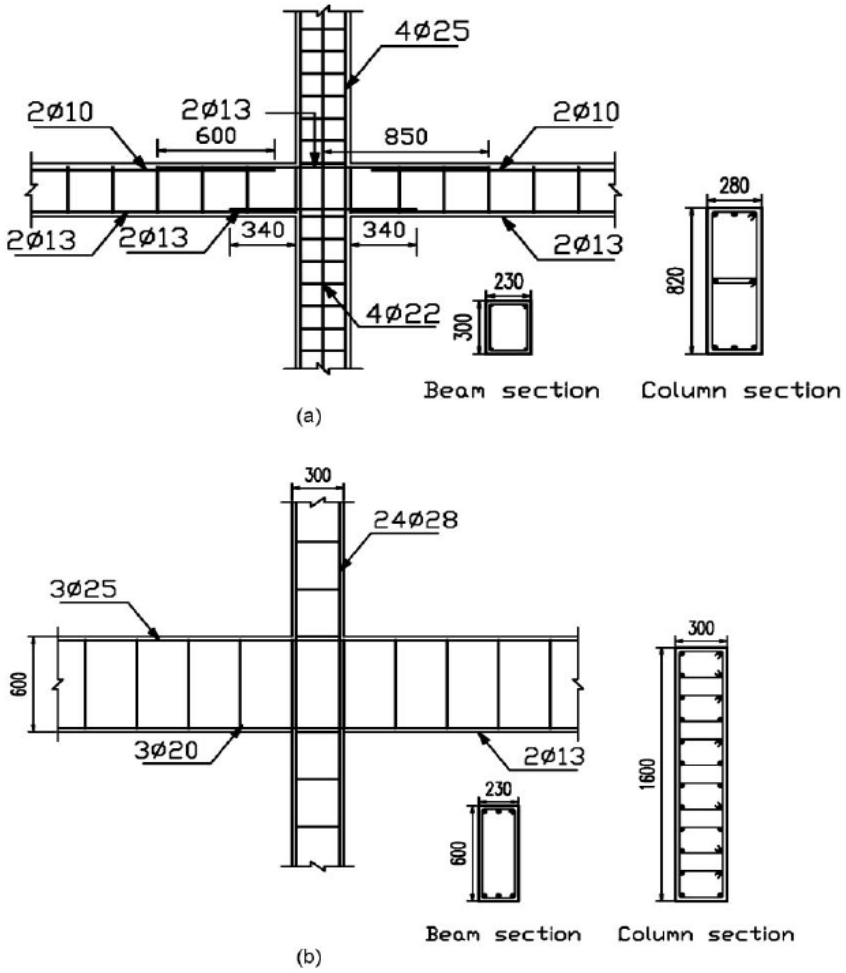

Figure 2.6 Cross Sectional Details for RC Beam Column Joints

At the top end of the column a reversible horizontal load was applied through a 1,000 kN stroke dynamic actuator. Hydraulic jacks were used to apply constant axial load. No significant affect in lateral resisting capacity was observed during axial compression loading of the specimens.

Pasala Nagaprasad (2009) - Seismic strengthening of RC columns using external steel cage:

RC columns of rectangular cross sections are strengthened using steel caging technique. Angle sections of steel cages are placed corners and tightened by battens at constant intervals along the cross-sectional height. Effectiveness of the proposed model was studied and results proved increase in flexural strength, lateral stiffness, energy dissipation and ductility. Proposed model

was found to be reasonably predicting the moment capacities in conformity with tested experimental values.

Rajagopal and Prabavathy (2013) – Enhancement of Seismic strength of beam-column joints using Reinforcement Anchorage:

Performance of exterior beam-column joint was enhanced and studied by using reinforcement anchorage. Anchorages were installed according to ACI specifications as ACI-352 (Mechanical anchorage), ACI-318 (90^o Standard bent anchorage), and IS-456 (Full anchorage). By using mechanical anchorages plus hair clip bars, the seismic performance, strength and ductility was greatly enhanced. But this was proposed only for those areas which are highly susceptible to seismicity.

Dr Muhammad Fiaz Tahir (2015) - Response of Seismically Detailed Beam Column Joints Repaired with CFRP Under Cyclic Loading:

6 x beam column joints were fabricated and tested in this experimental study. Quasi-static monotonic loading was applied on the casted samples. The samples were tested up till failure point, the damaged samples were retrofitted with carbon fiber reinforced polymer/ laminates. The retrofitted samples are again subjected to the same type of loading. The experiment results indicated an increase of 8.6, 6.7% in the ultimate strength of sample 1 and 2 and an increase of 54.6, 51.2% in the ultimate deflection. However, a reduction of 49, 48; 24.8, 25.6; 60.6, 51.7 % was observed in the ductility, ductility factor and stiffness of retrofitted specimens respectively.

2.3. Finite Element Modeling (FEM)

Wolanski (2004) performed a study to investigate the load-deflection response of reinforced concrete beams using finite element modelling. A reinforced concrete beam model was analyzed and compared with experimental data. The results matched well with the experimental and manually calculated data. Buckhouse (1997) formulated a method to reinforce the reinforced concrete beam in flexure strength using peripheral structural steel channels. The research comprised experimental testing of control beams in laboratory that could be used as subsequent for calibration of finite element modelling. Two load cells of 50-kip capability were located at third points, or 5 ft. from end-span supports with the help steel bearing plates as shown in Figure 2.9. Data logger was used to plot the relations between the applied load, mid-

span deflection of beam, and strains in the main steel reinforcement simultaneously. The beam was loaded up to the flexural failure point as shown in Figure 2.9.

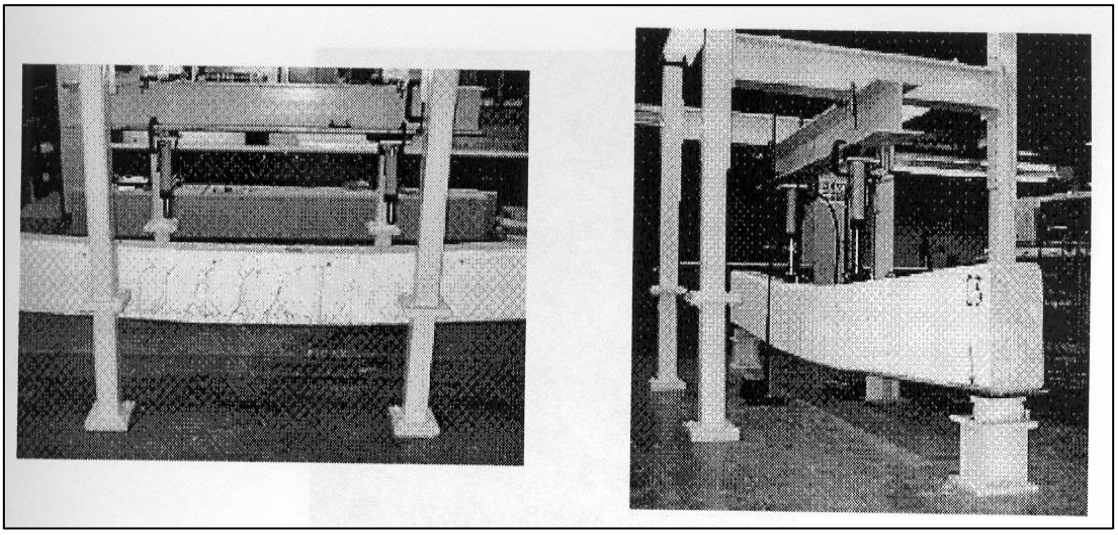

Figure 2.9: Loading setup and supports arrangement for the beam (Buckhouse 1997)

The concrete material was modelled using SOLID65 element. A SOLID45 element was used to model the steel plates for the application of loads. LINK8 element was used to model steel reinforcement. Discrete reinforcement modelling approach was applied in the present research work. The concrete in beam, steel plates, and supports were modelled using volume command. In the present research only quarter portion of the beam was modelled. Boundary conditions needed to be defined at points of requirements to confirm that the model perform in the same manner as was the experimental beam. The FEM model was though a simple beam under transverse loading. Static analysis type was applied to investigate the behavior of beam. In the present case the analysis type was small displacement and static. The FEM analysis of the model was established to inspect three different types of behaviors: preliminary cracking of the beam, yielding of the steel bars, and the strength limit capacity of the beam. The objective of the assessment of the FE model and the beam from Buckhouse (1997) was to confirm that the elements choosen, material properties, real constants and the convergence criteria were acceptable to model the behavior of the reinforced concrete beam. The load-deformation behavior investigated using the FEM is plotted against the experimental behavior from Buckhouse (1997). This then gave an enormous confidence in the approach of ANSYS and the methodology formulated.

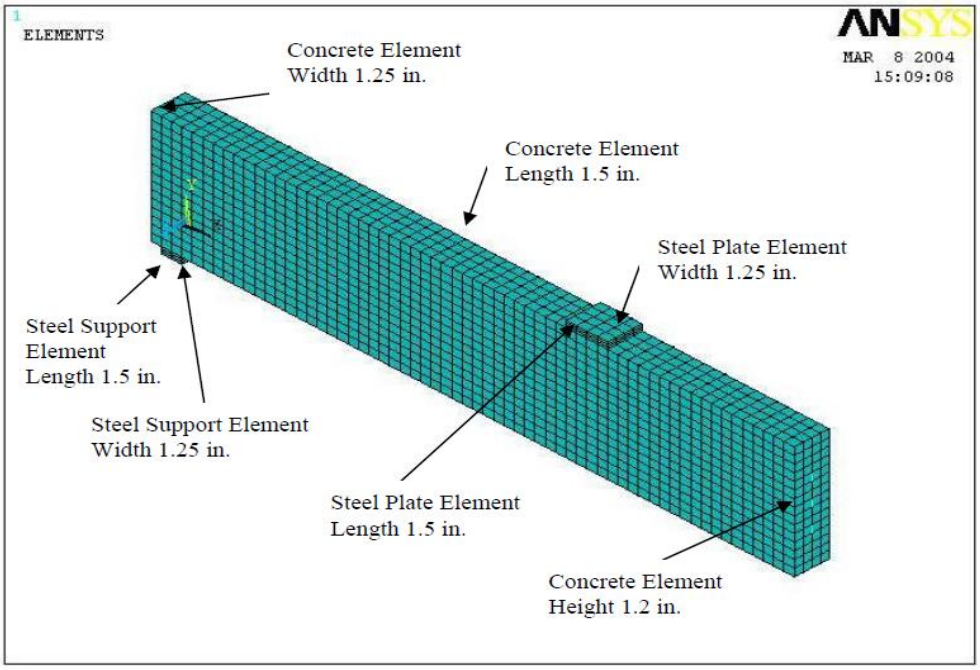

Figure 2.10: Mesh of the reinforced concrete beam

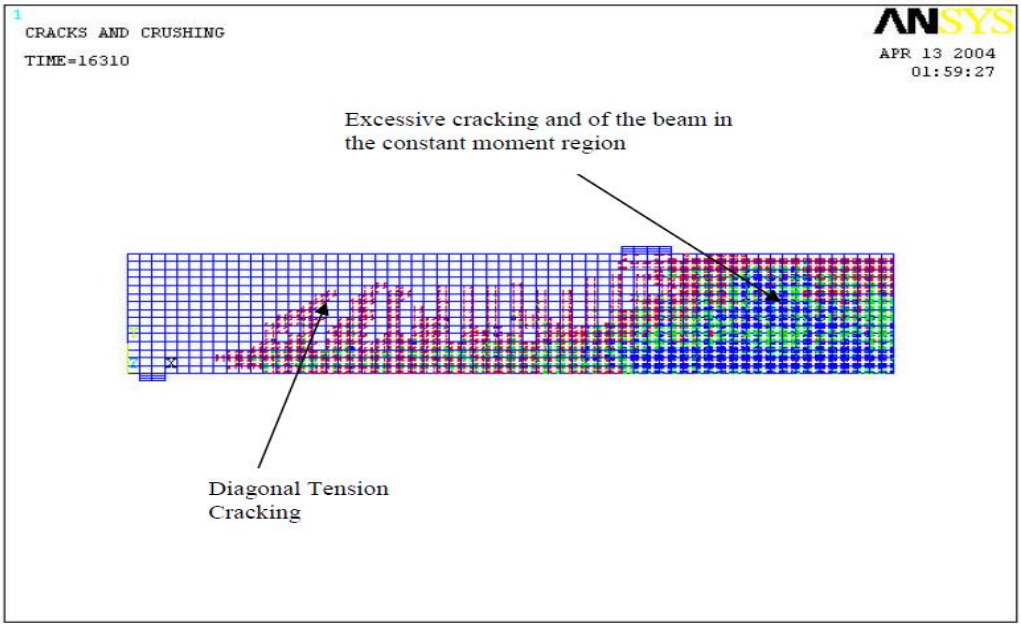

Figure 2.11: Failure of the Concrete Beam

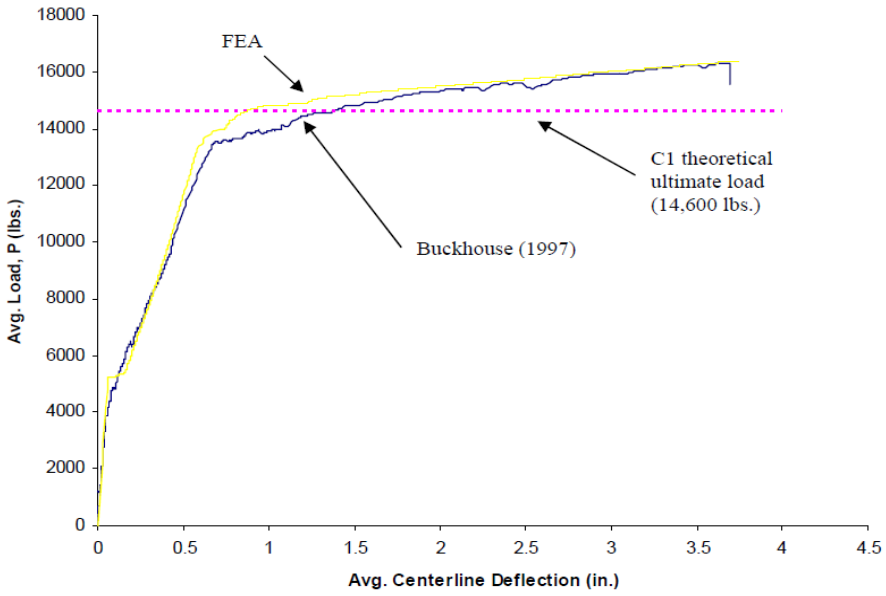

Figure 2.12: Comparison of load-deflection curve between ANSYS and Buckhouse (1997)

Kachlakev and Miller (2001) developed models for linear and non-linear finite element modelling for a reinforced concrete beam strengthened with the help of fiber reinforced polymer composites in ANSYS. Simulation from ANSYS were found to be in conformity with the experimental results**.** Only quarter of the full-sized beam was modelled because of symmetry. Hence the effort to model the beam and the time for non-linear solution has significantly reduced by modelling only the quarter portion of the beam.

An eight-node solid element, Solid65, was experimented to stimulate the behaviour of concrete. A Link8 element was used to model the behaviour of steel reinforcement. An eight-node solid element, Solid45, was used for the modelling of steel plates at the supports in the beam. The ultimate concrete's compressive and tensile strengths were determined from the elastic modulus which was calculated with the help of pulse velocity method by equations developed by ACI 318, 1999. The reinforced concrete beam was mesh into element sizes which was determined after an enormous research on the size of elements mesh. The four full-size beams were tested in third point loading. The finite element models were loaded at the same locations and manner as the full-size beams in laboratory to have approximate results. To measure deflections for the experimental beams at mid-span bottom face, direct current displacement transducers (DCDTs) were used. IN ANSYS, deflections were also recorded at the same location as in experimental beams. Figure 2.35 shows the load-deflection plot from the FEM and the experimental results for the control beam. It shows that the load-deflection plot from the FEM agreed well with the experimental results for the control beam. Crack patterns

obtained from the finite element analyses at the last converged load steps are compared to failure photographs from the actual beams. For the Control Beam, Figure 2.13, the crack pattern from ANSYS and the actual beam agree very well.

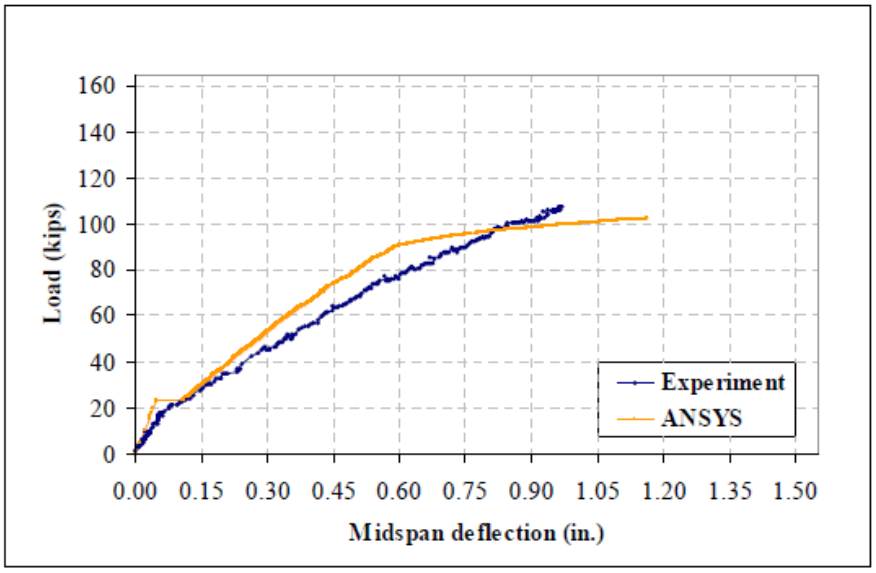

Figure 2.13: Load-deflection plot for control beam

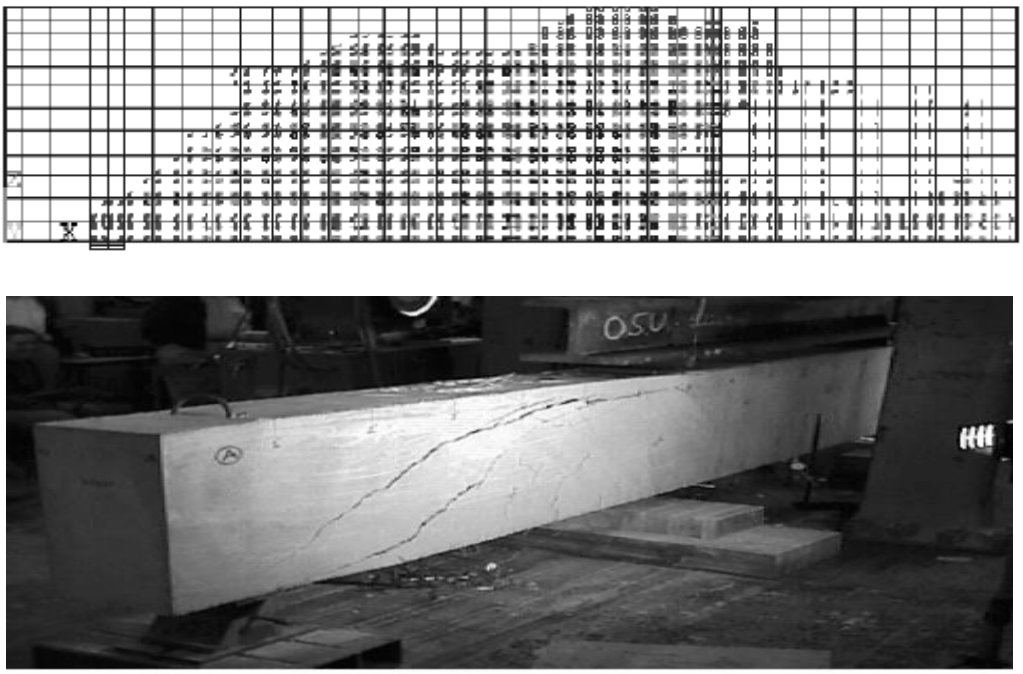

Figure 2.14: Crack patterns at failure of Finite element model and Actual experimental beam

Chapter 3

EXPERIMENTAL PROGRAM

The experimental program was carried out to study the response of CFRP repair on pre-damaged beam column joints. The methodology was to repair of beam column joints (BCJ) (12 x pre-damaged samples, with 4 x control samples that were confined with steel stirrups and 8 x samples confined with steel strips). Already tested/damaged joints under cyclic loading were re-analyzed after CFRP repair to evaluate effectiveness of proposed repair technique.

3.1. Specification of Pre-Damaged Joints

In this investigation totally twelve pre-damaged joints for the repaired with CFRP. Two groups of six joints, each with 21MPa and 28MPa with same cross-sectional dimensions of 250 x 200 mm were utilized. Column length at joint was 800 mm, beam cantilever was also 800 mm from face of the column. 60 Grade rebars were there for main reinforcement and 40 grade stirrups were used for six pre-damaged conventionally reinforced concrete joints (CRCJ). In replacement of stirrup, 14 gauge and 18 gauge strip confinement was there as an alternate arrangement for transverse reinforcement in steel strip confined joints (SSCJ). Cross sectional area of one stirrup was 0.11 in^2. Same cross-sectional area was kept for both types of strips (14 and 18 gauge). Strips of 1.3mm thickness were used in six beam column joints specimens confined with 18 gauge and strips of 2mm strips were there in six specimens confined with 14 gauges. In all joints four #6 bars were provided in columns where as in the beam, three #4 bars were used on tension face and two #3 were provided on the compression side. Structural details along with nomenclature of pre-damaged joints is as follows.

Table 3.1 Specification and Cut length of bars required

S. No	Type	Cut Length	No. of Bars	Grade
1	#3 Deformed	40 in	120	40
2	#3 Deformed	27.5 in	48	60
3	#6 Deformed	30.5 in	48	60
4	#4 Deformed	30.5 in	36	60

Table 3.2: Strips details

S. No	**Strip Type**	**Length (in)**	**Thickness (mm)**	**Thickness (in)**	**Width (im)**	**Area (in)**
1	A	40	2 (14 gauge)	0.07875	36	0.11
2	B	40	1.3 (18 gauge)	0.0512	54	0.11

Table 3.3 Specimen Details

Group/ Set	Ratio	Long Rft (Beam/ Column)	Transverse Rft	Name	No. of Specimen
1	1:1.25:3	3#4 + 2#3/ 4#6	#3@ 63mm c/c	Control Specimen	2
1	1:1.25:3	3#4 + 2#3/ 4#6	1.3mm x 54mm @ 63mm c/c	18 Gauge Specimen	2
1	1:1.25:3	3#4 + 2#3/ 4#6	2.0 mm x 36 mm @ 63mm c/c	14 Gauge Specimen	2
2	1:2:4	3#4 + 2#3/ 4#6	#3@ 63mm c/c	Control Specimen	2
2	1:2:4	3#4 + 2#3/ 4#6	1.3mm x 54mm @ 63mm c/c	18 Gauge Specimen	2
2	1:2:4	3#4 + 2#3/ 4#6	2.0mm x 36 mm @ 63mm c/c	14 Gauge Specimen	2
Total					12 Specimens

c/c = center to center distance

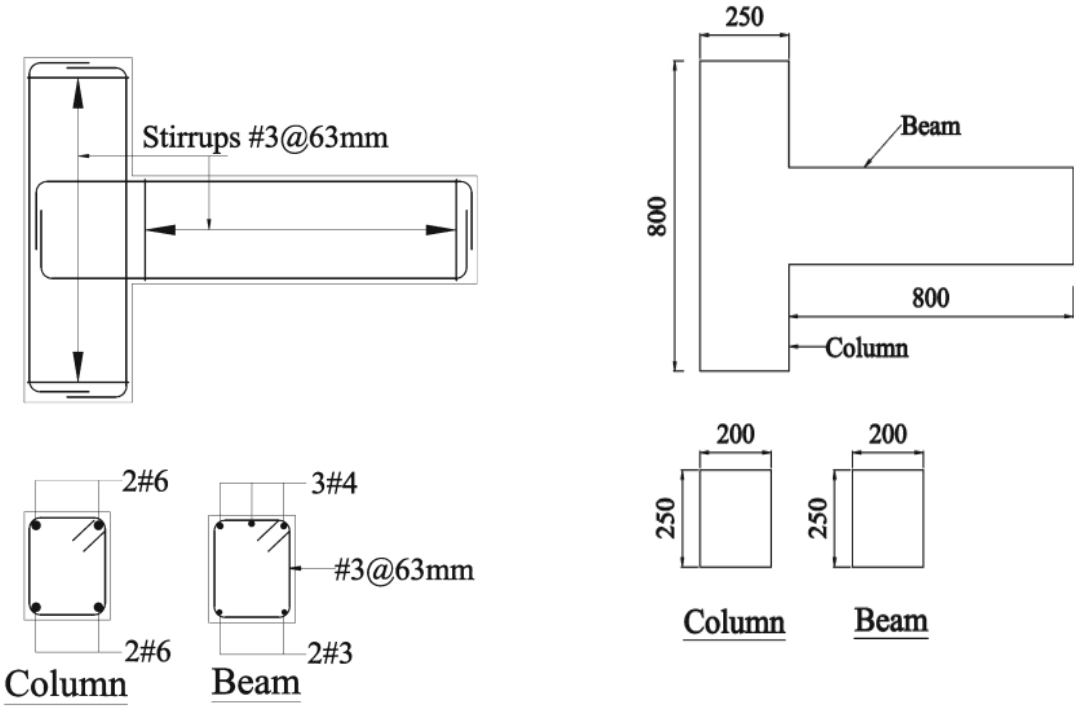

Figure 3.1 Structural details of pre-damaged joints

Coded Name	Type	Code Description
CRCJ	1-4-#3	Specimen no.1 having 28 MPa (4ksi) strength with #3 stirrups as transverse reinforcement
	2-4-#3	Specimen no.2 having 28 MPa (4ksi) strength with #3 stirrups as transverse reinforcement
SSCJ-02	1-4-14	Specimen no.1 having 28 MPa (4ksi) strength with transverse reinforcement as 2mm thick strip (14 gauge)
	2-4-14	Specimen no.2 having 28 MPa (4ksi) strength with transverse reinforcement as 2mm thick strip (14 gauge)
SSCJ-1.3	1-4-18	Specimen no.1 having 28 MPa (4ksi) strength with transverse reinforcement as 1.3mm thick strips (18 gauge)
	2-4-18	Specimen no.2 having 28 MPa (4ksi) strength with transverse reinforcement as 1.3mm thick strips (18 gauge)
CRCJ	1-3-#3	Specimen no.1 having 21 MPa (3ksi) strength with #3 stirrups as transverse reinforcement
	2-3-#3	Specimen no.2 having 21 MPa (3ksi) strength with #3 stirrups as transverse reinforcement
SSCJ-02	1-3-14	Specimen no.1 having 21 MPa (3ksi) strength with transverse reinforcement as 2mm thick strip (14 gauge)
	2-3-14	Specimen no.2 having 21 MPa (3ksi) strength with transverse reinforcement as 2mm thick strip (14 gauge)
SSCJ-1.3	1-3-18	Specimen no.1 having 21 MPa (3ksi) strength with transverse reinforcement as 1.3mm thick strips (18 gauge)
	2-3-18	Specimen no.2 having 21 MPa (3ksi) strength with transverse reinforcement as 1.3mm thick strips (18 gauge)

Table 3.4 Nomenclatures of Joints

CRCJ = Conventionally Reinforced Concrete joint **SSCJ-02** = Steel Strip Confined Joint-2 mm thick

SSCJ-1.3 = Steel Strip Confined Joint-1.3 mm thick

3.2 Experimental Program for repair:

3.2.1 Repairing of specimen after testing:

There were three main stages of repair after testing

Filling of cracks

Pre-damaged joints loaded up to 20% degradation in strength were repaired using carbon fiber reinforced polymer.

Following steps are performed for filling of cracks;

i. First of all, joints surfaces with cracks were washed with the help of brush or air pressure.
ii. When the cracks were washed joints were made completely wet.
iii. After that resin was made and put it in the cracks so that each crack was completely filled so that no crack space was kept free. And after that these were dried before testing

Figure 3.2 Joints repair work using non-shrink grout Chemdur-31

Applying the Resins

After filing the cracks resins is applied. There are many types of resins but some are described below:

Figure 3.3 Filling of joint cracks using resins

Chemdur – 30

It is solvent free, thixotropic, epoxy based two component adhesive mortar. It is used as adhesive bonding carbon fiber reinforcement, adhesive mortar for concrete, steel, epoxy & bridges segments.

Chemdur -31

It is solvent free, thixotropic, epoxy mortar based on a combination of epoxy resins. It can be used as concrete repairs, blow hole filling, cracks and surface filling, structural adhesive for precast concrete elements, columns.

Chemdur - 52

It is 2 component solvent free, low viscosity epoxies for injection based on high strength resins. It is used to fill cavities & cracks in structural components such as bridges, columns, beams, foundation walls and floors. It also bonds the concrete sections together.

Chemrite AG-200

It is highly effective liquid superplasticizer for the production of free-flowing concrete which prolongs slump reactions at

low water cement ratio. It is used in concrete works such as slabs, foundations, walls, columns, hot weather concreting, pre-cast concrete, pre-stressed concrete, bridges, roads & pavements.

Figure 3.4 CFRP being applied to damaged specimen

To ensure the bond between concrete surface and CFRP wrap, epoxy adhesive was utilized. Properties of CFRP composite and epoxy adhesive used for strengthening and retrofitting are presented earlier in Table 3.1 to 3.4.

Table 3.5 Properties of CFRP

Fiber Type	High Strength Carbon Fibers
Fiber Orientation	Unidirectional
Areal Weight (g / m^2)	225 ± 5
Fiber Density (g / cm^3)	1.77
Thickness per ply, t_f (mm)	0.115
Ultimate Tensile strength, f_{fu} (N / mm^2)	4150
Tensile E-Modulus of Fibers (N / mm^2)	231,500
Strain at break of fibers, ε_{fu} (%)	1.68

Table 3.6 Properties of primary base material

Colour	Comp. A+ B mixed: light grey
Mix ratio	Comp. A + B = 2:1 by weight and volume
Density	1.76 Kg/Lit. (mixed)
Pot life	45 minutes. (at +36°C) 90 min. (at + 16°C)
Open time	35 minutes (at +36°C)
Application Temperature	Substrate and ambient: + 12°C to +35°C
Adhesive Tensile Strength on steel	To sandblasted substrate: 30 N/mm^2
Coefficient of thermal Expansion	8.90 x 10^{-5} per °C
Consistency	Comp. A + B mixed: creamy paste

Table 3.7 Properties of thin adhesive epoxy for retrofitting

Color (mixture)	Yellowish		
Mix ratio	Comp. A: B = 2:1 parts by volume and weight		
Density (20°C)	Comp. A: 4.0 Kg/L Comp. B: 0.5 Kg/L Comp. A+B: 4.5 Kg/L (mixed)		
Pot life (2 Kg)		Normal Type	L.P. Type
	5°C	75 min.	-
	10°C	55 min.	-
	20°C	20 min.	60 min.
	30°C	10 min.	30 min.
	40°C	-	15 min.
Coefficient of thermal expansion	89 x 10^{-6} per °C		
Viscosity (mPa's)		Normal Type	L.P. Type
	10°C	1000	-
	20°C	500	290
	30°C	250	130

Application Temperature	Substrate and ambient temperature: +15°C to 35°C.
Mechanical Strengths (at 20°C and 65% r.h.)	after 10 days . Compressive strength 55 N/mm^2 . Flexural strength 50 N/mm^2 . Tensile strength 25 N/mm^2 . Bond strength to concrete 4 N/mm^2 (concrete failure) . Bond strength to steel 12 N/mm^2 (DIN 53232)

3.2.2 Testing of specimen

After filling the cracks and applying resins the CFRP was applied as per configuration shown specimen were tested

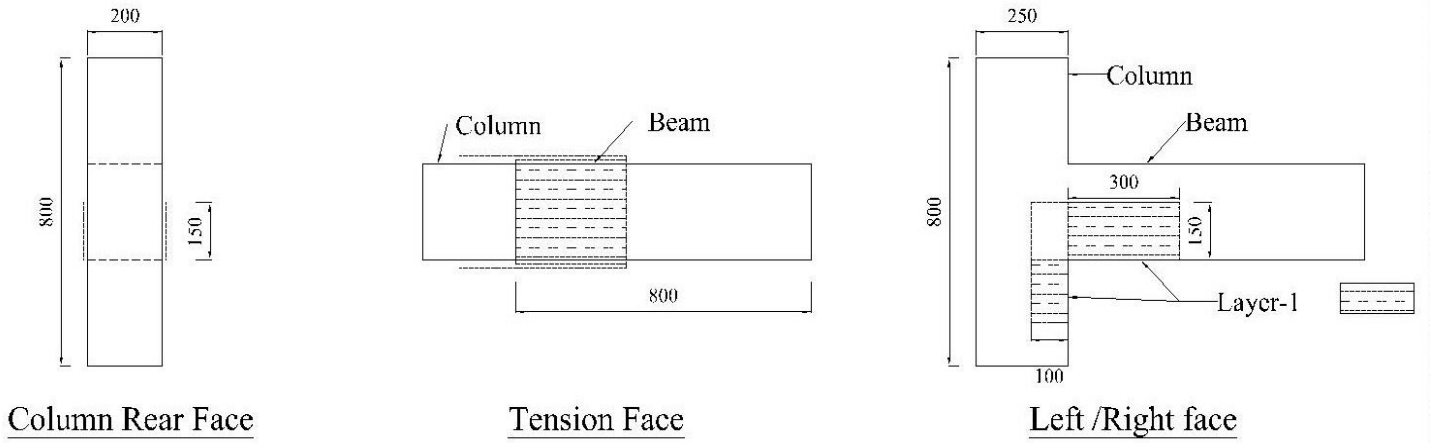

Figure 3.5 Configuration of applied CFRP laminate

Specimen and Loading Arrangement

Steel band around column ends were used in order to ensure that there is no damage/ crushing to the ends of the column. The column was applied with axial compressive force so that no movement of column occurs. The reinforcement has been provided at 63 mm c/c. The test was carried out by applying cyclic load on the beam end and displacement was measured. Drifts

levels for the first cycle were 0.25% and second at 0.5%. A 0.5% increment in drift levels was used up till 5% drift level, after that the reduction in increment was to 0.25%. The concluding drift level of 5.5% was kept repetitive until we achieved 20% degradation in strength.

During the conduct of test the compressive load was kept constant on the column, thus nullifying any chance of column movement. The nomenclature assigned to beam column joints is discussed above. CRCJ represents Conventionally Reinforced Concrete Joints and SSCJ represents Steel Strip Confined Joints. A load cell was placed over a hydraulic jack and this arrangement was placed under the free end of the beam. Load on beam was then applied through the jack.

Figure 3.6 Joints repaired using CFRP

Instrumentation

The displacements were measured by means of Deflection gauge installed at free end of the beam, where there is maximum deflection. A hydraulic jack was used for load application and was placed under the free end of the beam. A load cell placed between the hydraulic jack and the beam. The displacement caused due to load was measured by use of deflection gauge. The details of instrumentation are shown in Figure 19 and Table 10.

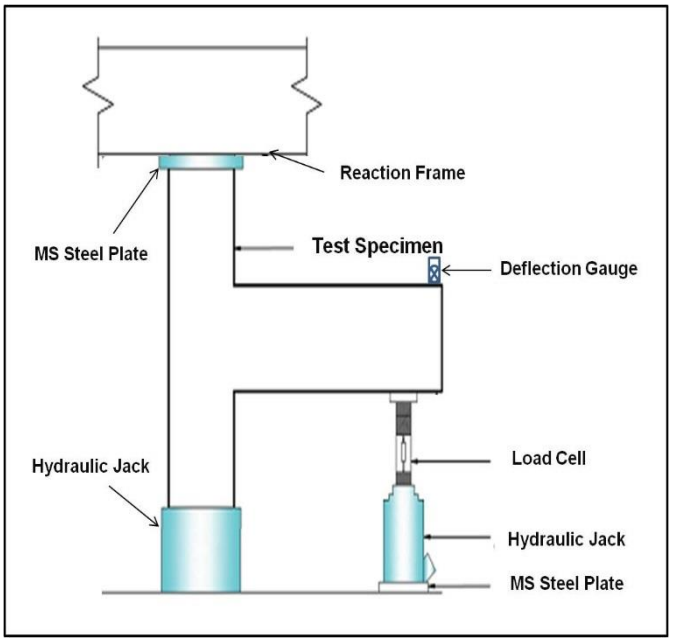

Figure 3.7: Line Diagram of Test Setup

SER	INSTRUMENTS
1	Hydraulic jack for column axial compressive loading
2	Hydraulic jack for loading of beam
3	Deflection gauge at top, free end of beam to measure displacement
4	Load cell to measure the load in positive and negative direction on beam
5	Load lifter

Table 3.8: Detail of instrumentation

Testing Setup

Standard test assembly was used with arrangements for static cyclic loading. The shear block was properly fixed to the floor. Load was applied axially with the help of hydraulic jack assembly to ensure no movement of column. Column ends were fitted with steel collars and steel plates were used at column ends to ensure uniform compressive load. The test setup is shown in Figure 20.

Testing of specimen

12 x beam column joints were tested using the test setup. The test was conducted up till 20% degradation level. Data of deflection gauges fixed at top of beam near it's the free end and the load cell was recorded. The deflection was measured in mm and the load was measured in KN (after necessary conversion of load cell readings to KN). The data recorded was used to make the backbone curves and the hysteresis loops (using Excel). This data will be presented and analyzed in this paper.

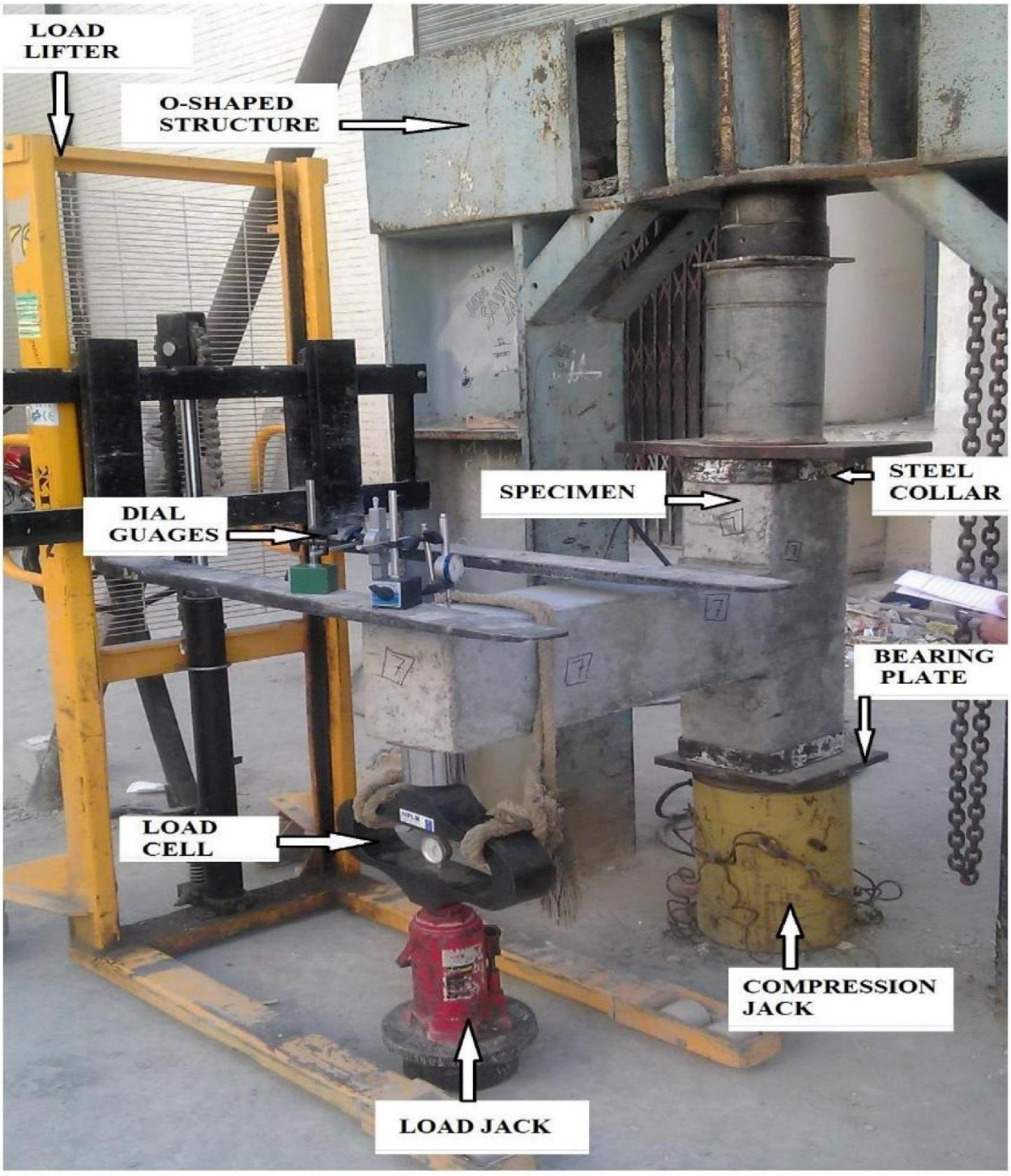

Figure 3.8: General layout of test conditions

Figure 3.9: Placing of repaired specimen for test

Figure 3.10: Collars Installed at Column Ends

Figure 3.11: Steel plate at Column Ends

The procedure followed for conduct of test is as under:

a. The specimens were placed near the shear frame after identification of specimen markings/ coding. They were checked for any visual imperfections.

b. The steel collars were installed on column ends, thus nullifying any chance of column crushing at the ends.

c. The lifter was used to lift the specimen to the required position on the shear frame.

d. The specimen was than fixed inside the shear frame and compressive load was applied on column with the help of hydraulic jack, this ensures vertical stability of the sample. Moreover, steel plates were placed on column ends for even distribution of load.

e. Deflection gauge was fixed at free end of beam on the top face in vertical position to measure the upward deflection as shown.

f. Another hydraulic jack was placed below the beam at its free end, this arrangement can apply load on the beam.

g. Between the hydraulic Jack and beam a load cell was placed to measure the magnitude of load being applied on the sample.

h. The load cell and the deflection gauge were calibrated before the start of test.

i. Load was then applied on the beam and the deflection was measured. The cyclic load was applied very slowly keeping the deflections at 1mm, 2mm, 4mm and so on. After every cycle load was released and the residual displacement was measured.

j. This procedure was repeated until failure of the joint was achieved (20 % degradation)

k. The cracks were observed and marked against the corresponding load/ deflections.

l. After testing the samples were again marked and retested after repair in concrete Laboratory at UET Taxila.

Chapter 4

RESULTS & DISCUSSION

In this chapter the results from experimental study are discussed. The comparison of results between pre-damaged and repaired joints was made through load deflection plots, loads at first crack, failure loads and crack patterns. Load deflection curve, hysteresis curves. In the tables of comparison, gain and loss of a specific parameter for the joint being compared is indicated with a positive or negative sign respectively. CFRP repaired joint from 28 MPa and 21 MPa samples are compared with control specimen and average values of same type of samples in each group are used.

4.1 Load deflection Plots

4.1.1 Load deflection and hysteresis behavior

Testing of CRCJ (1-4-#3)

In 7th cycle of loading 20% degradation was achieved. The deformation in the joint started at 12.5 KN load during the 1st cycle and achieved a displacement of 4 mm, while for repaired specimen at the load of 16 KN displacement was 6mm, with the appearance of a hair line crack at a distance of 2 mm from joint. In the 7th cycle peak load of 52 KN was recorded, while in case of repaired peak load was 63KN. The residual displacements became significant after 4th cycle. The residual displacement was 8.6 mm at the completion of test. The hysteresis response and backbone curve are shown below.

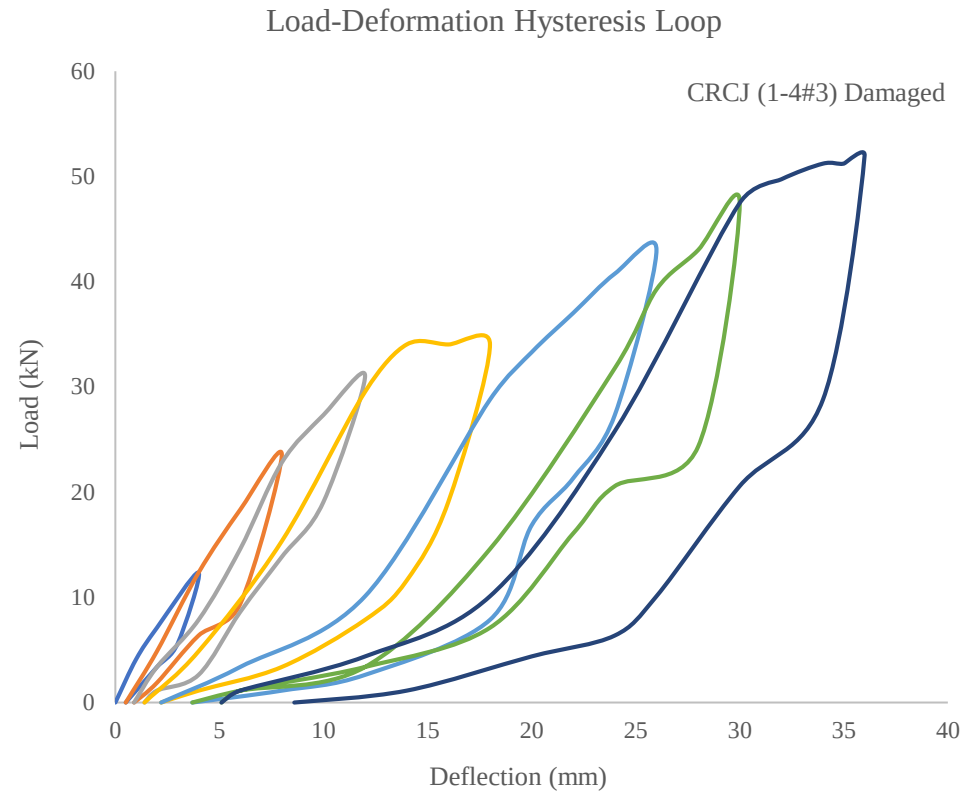
Load-Deformation Hysteresis Loop
CRCJ (1-4#3) Damaged
Load (kN)
Deflection (mm)
0
10
20
30
40
50
60
0
5
10
15
20
25
30
35
40

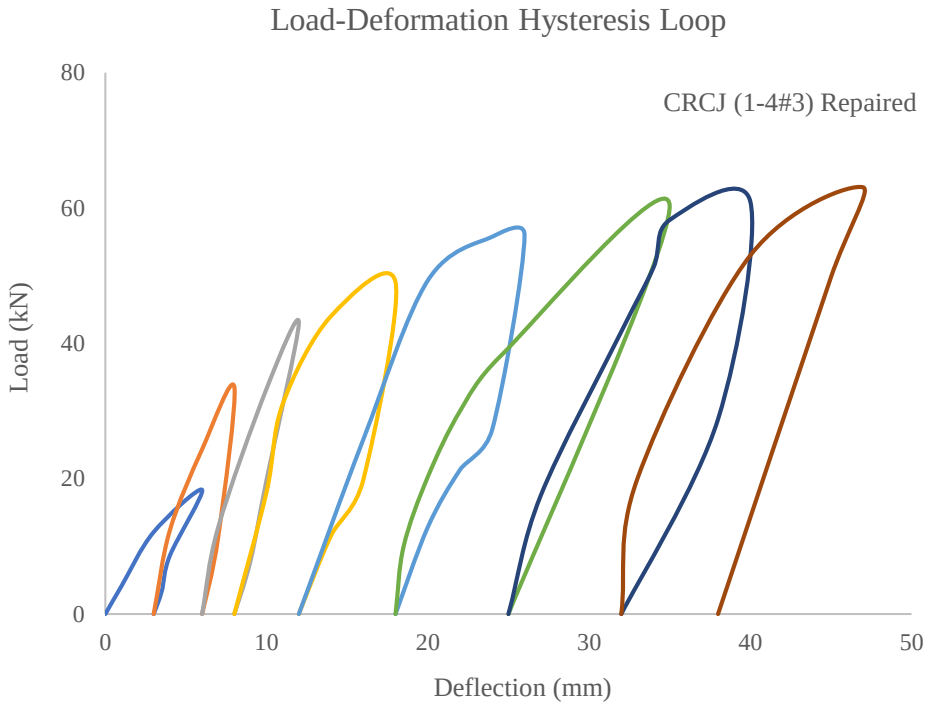
Load-Deformation Hysteresis Loop
CRCJ (1-4#3) Repaired
Load (kN)
Deflection (mm)
0
20
40
60
80
0
10
20
30
40
50

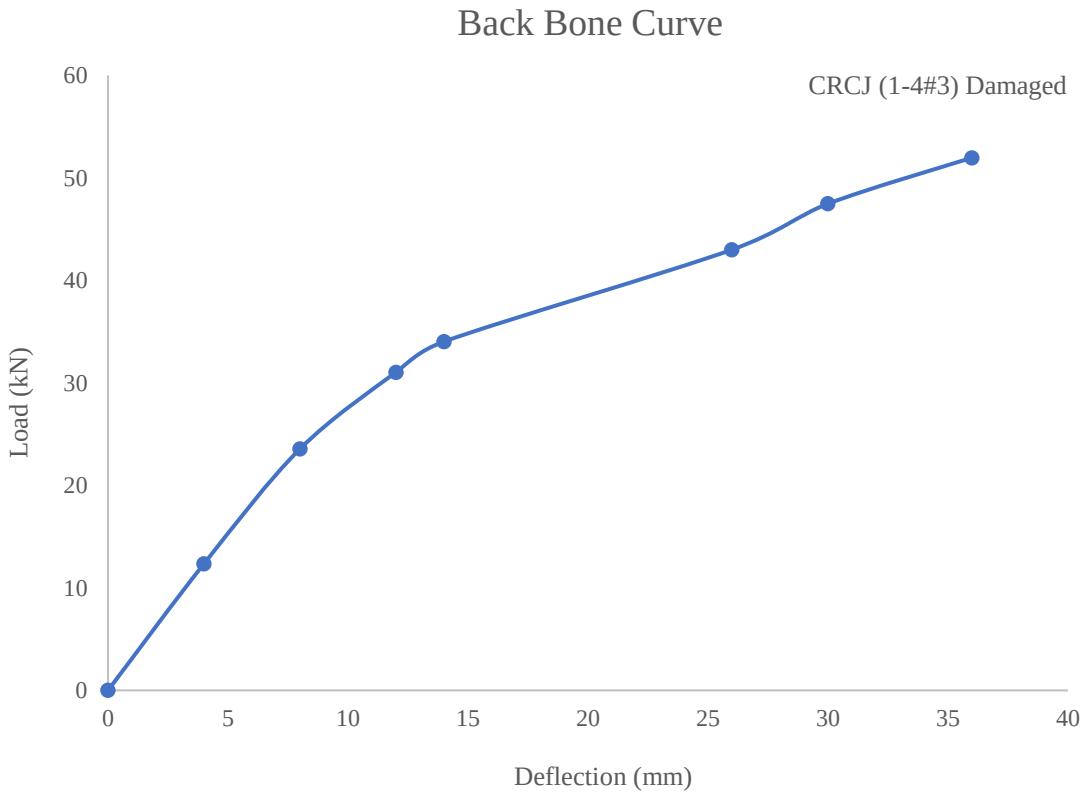

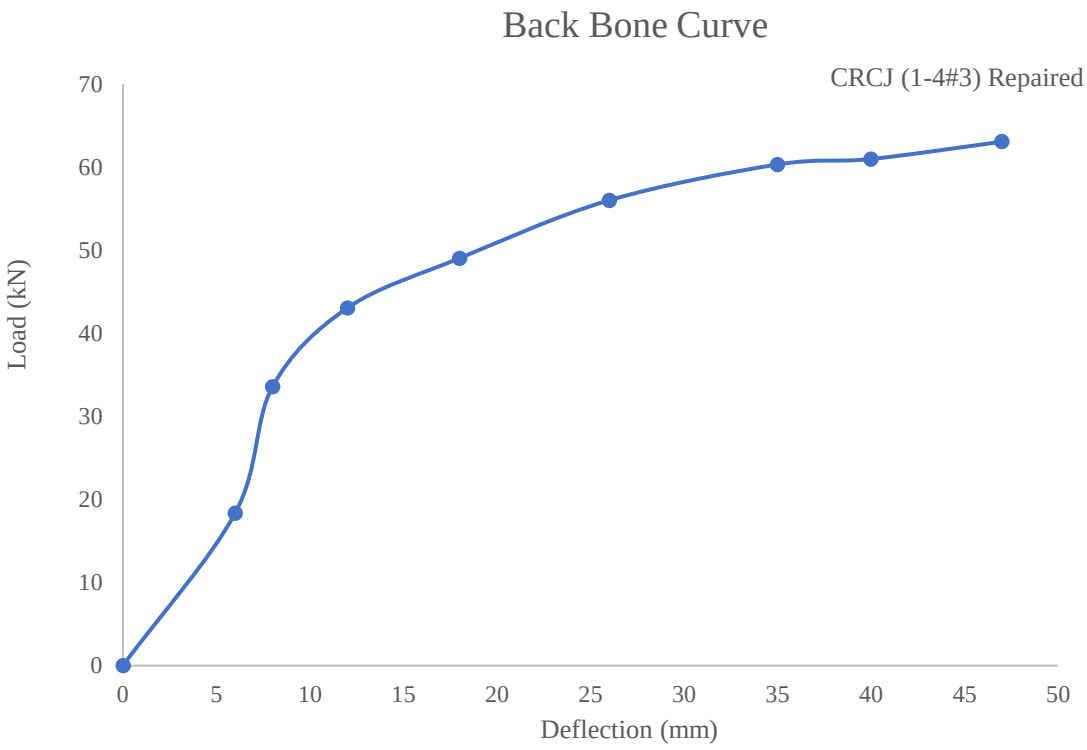

Figure 4.1: CRCJ (1-4-#3) Curves

Testing of CRCJ (2-4-#3)

In 9th cycle of loading 20% degradation was achieved. The deformation in the joint started at 18 KN load during the 1st cycle and achieved a displacement of 2 mm, while for repaired specimen at the load of 18 KN displacement was 2mm, with the appearance of a hair line crack at a distance of 6 mm from joint. In the 9th cycle peak load of 53 KN was recorded, while in case of repaired peak load was 62 KN. The residual displacements became significant after 4th cycle. The residual displacement was 10.2 mm at the completion of test. The hysteresis response and backbone curve are shown below.

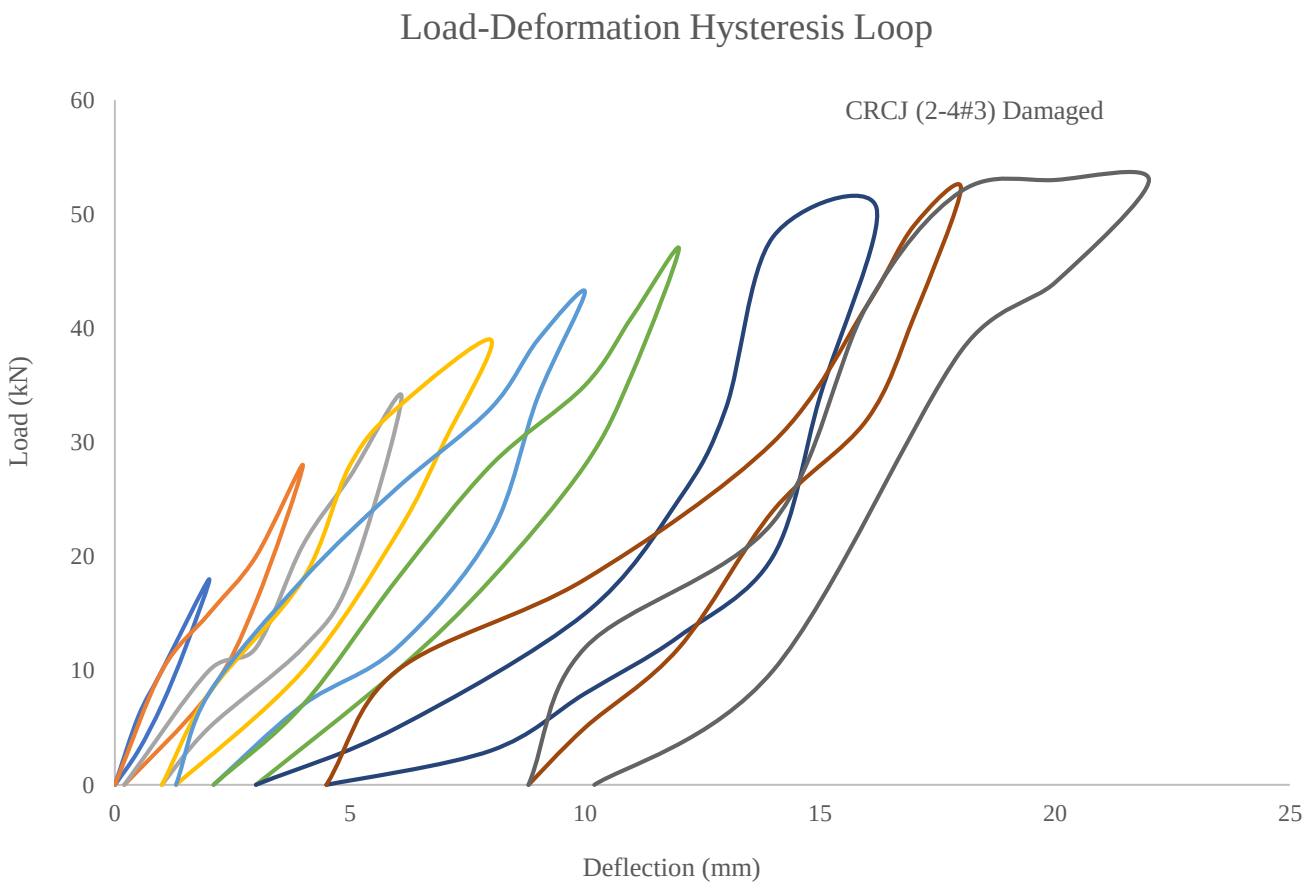

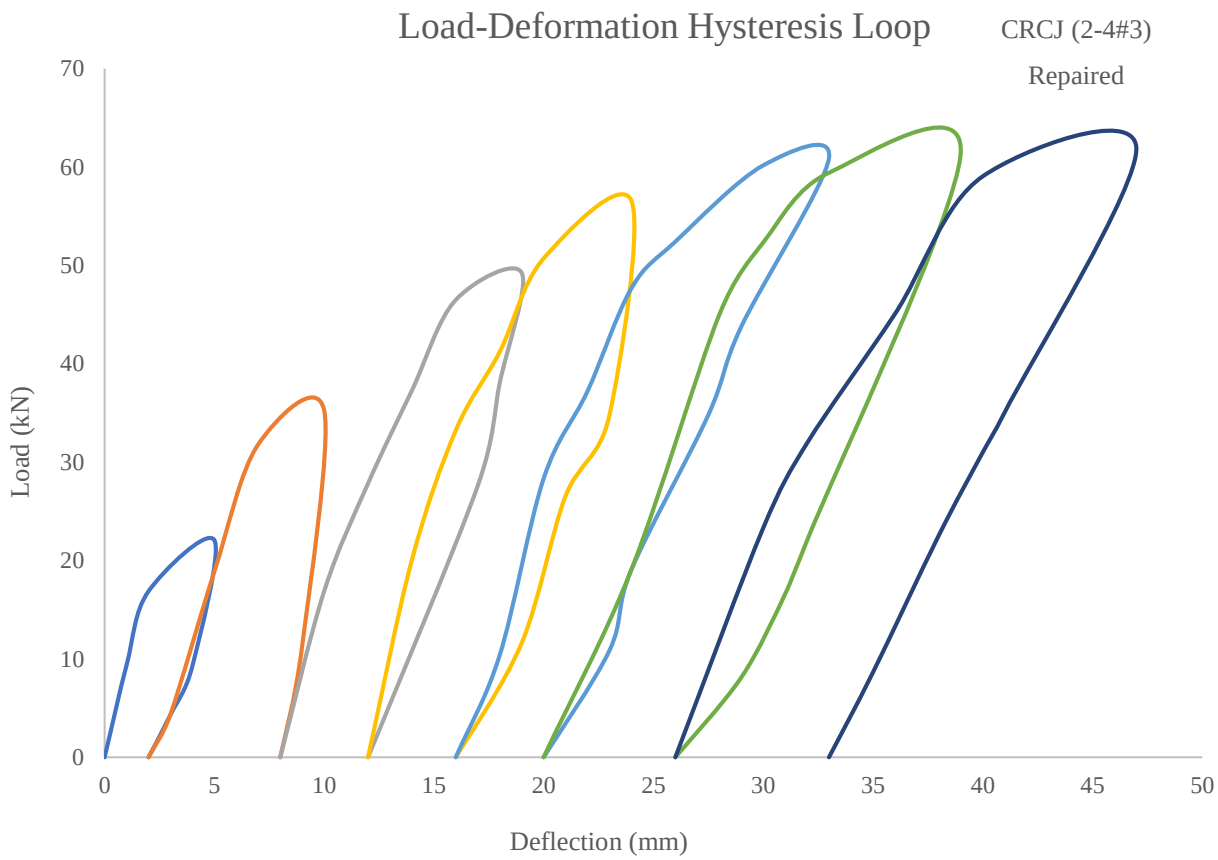
Load-Deformation Hysteresis Loop
CRCJ (2-4#3)
Repaired
Load (kN)
70
60
50
40
30
20
10
0
0
5
10
15
20
25
30
35
40
45
50
Deflection (mm)

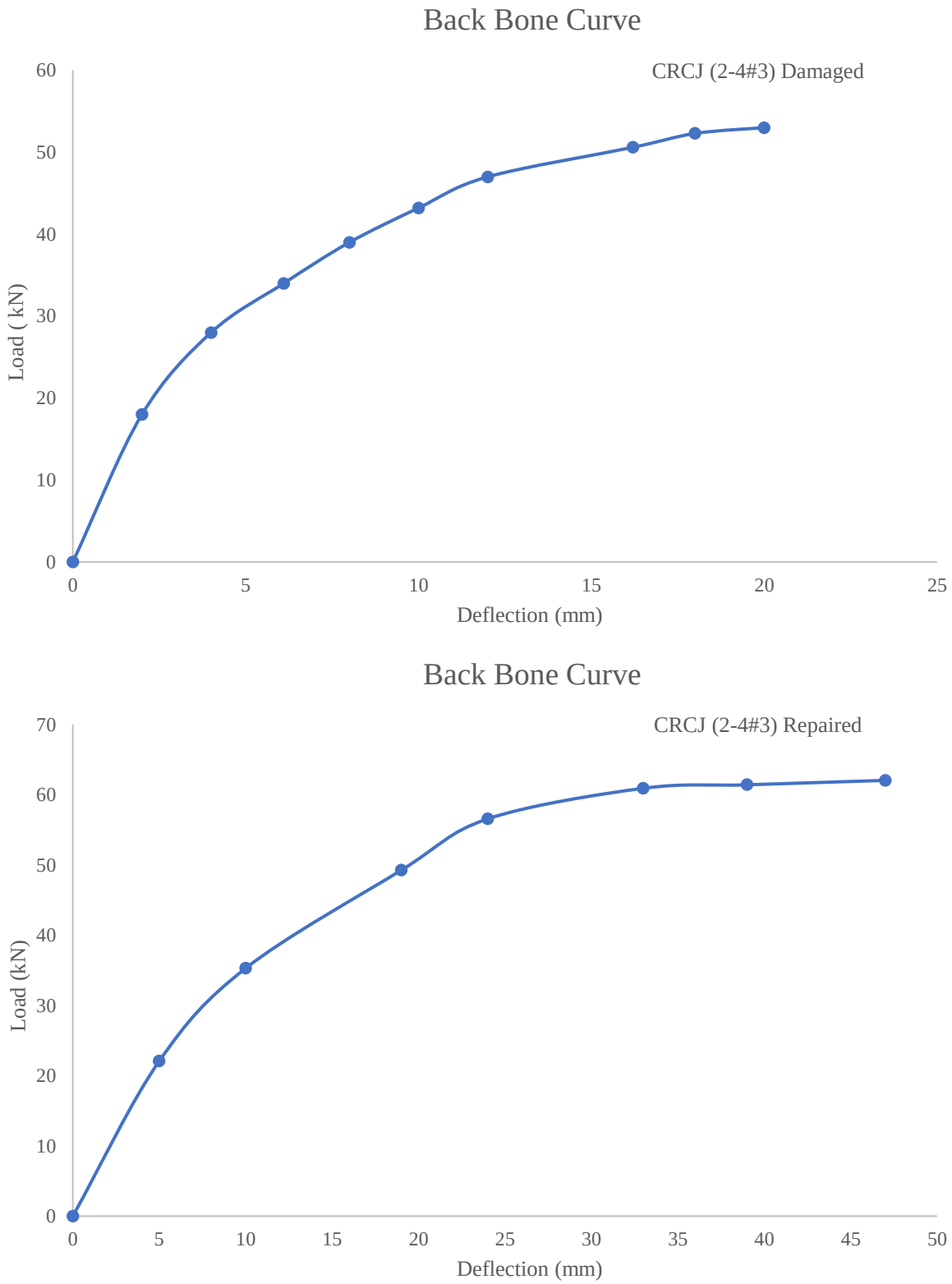

Figure 4.2: CRCJ (2-4-#3) Curves

Testing of SSCJ 02 (1-4-14)

In 9th cycle of loading 20% degradation was achieved. The deformation in the joint started at 18 KN load during the 1st cycle and achieved a displacement of 1 mm, while for repaired specimen at the load of 20 KN displacement was 3mm, with the appearance of a hair line crack at a distance of 9 mm from joint. In the 9th cycle peak load of 59 KN was recorded, while for repaired peak load was 69 KN. The residual displacements became significant after 5th cycle. The residual displacement was 14.5 mm at the completion of test. The hysteresis response and backbone curve are shown below.

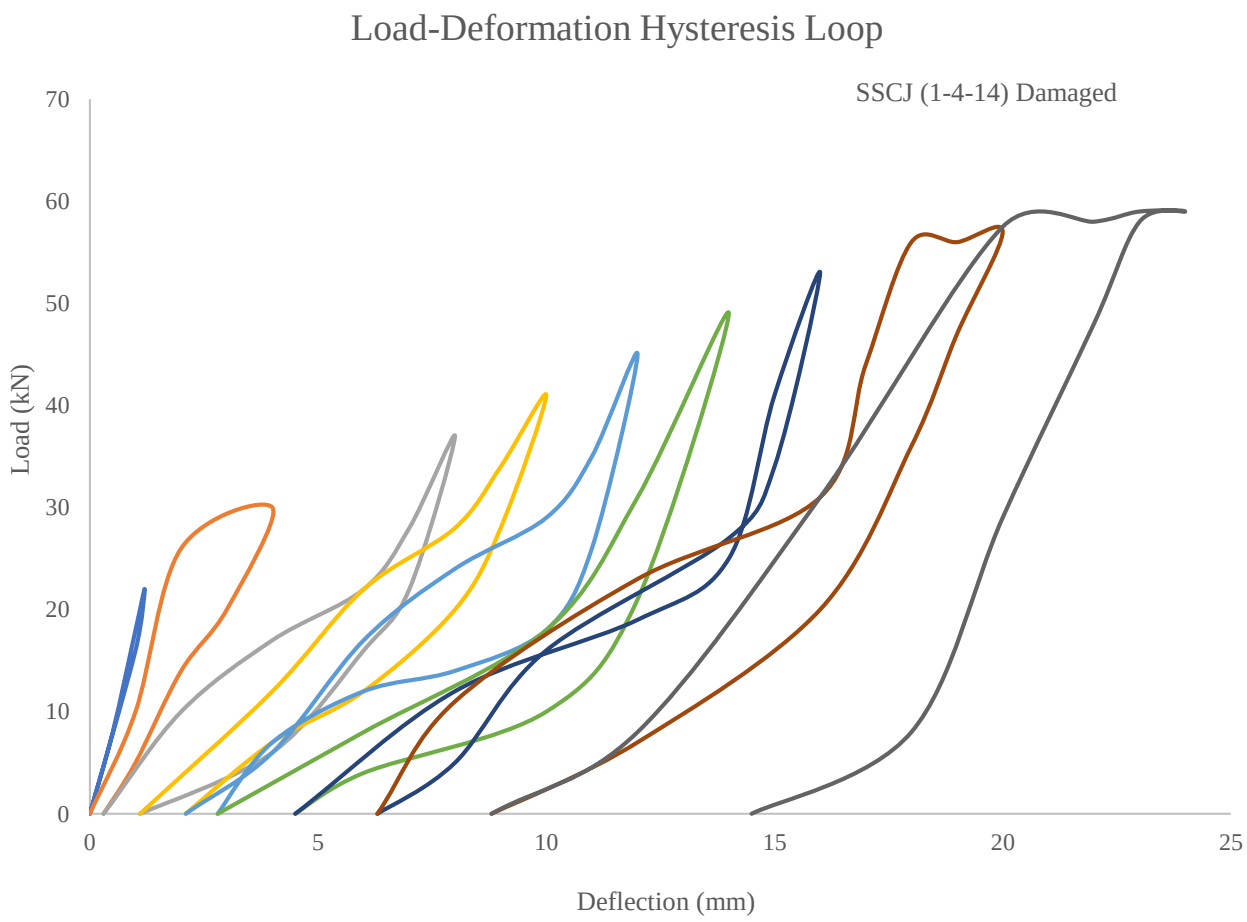

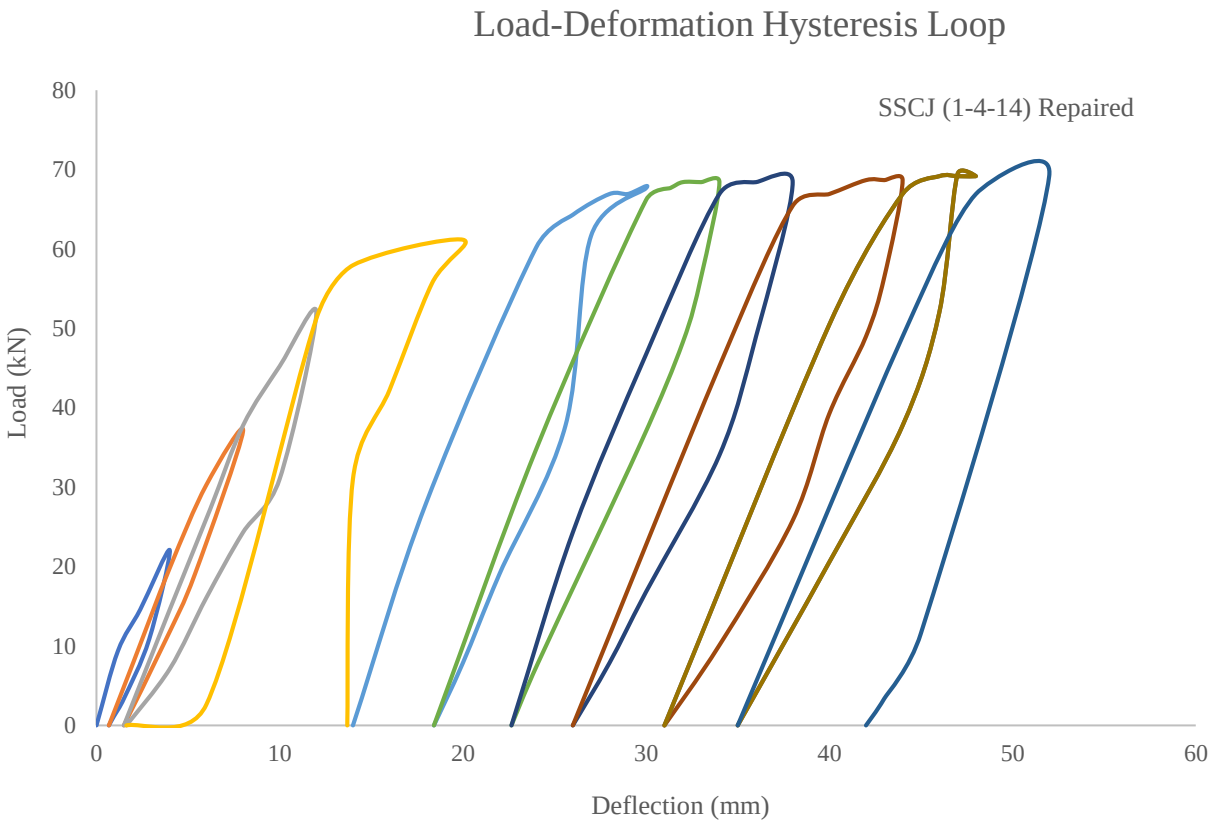
Load-Deformation Hysteresis Loop
SSCJ (1-4-14) Repaired
Load (kN)
80
70
60
50
40
30
20
10
0
0
10
20
30
40
50
60
Deflection (mm)

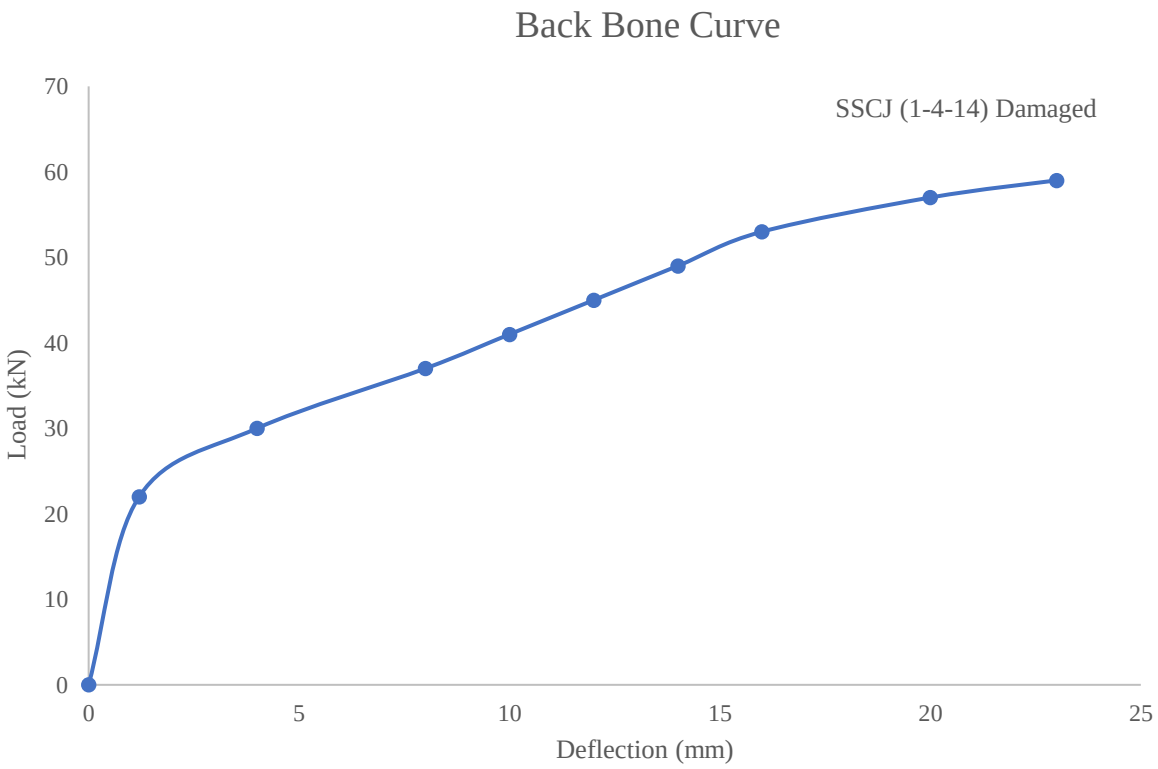
Back Bone Curve
SSCJ (1-4-14) Damaged
Load (kN)
70
60
50
40
30
20
10
0
0
5
10
15
20
25
Deflection (mm)

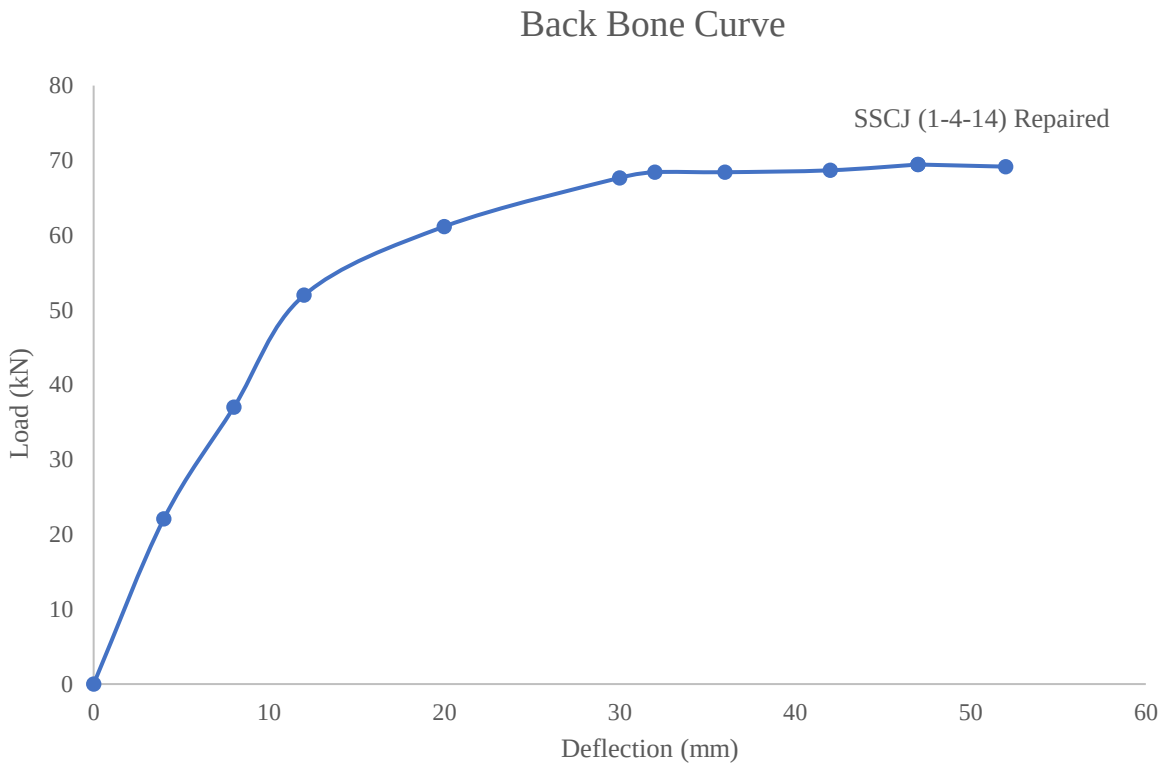

Figure 4.3: SSCJ 02 (1-4-14) Curves

Testing of SSCJ 02 (2-4-14)

In 7th cycle of loading 20% degradation was achieved. The deformation in the joint started at 16 KN load during the 1st cycle and achieved a displacement of 1 mm, while for repaired specimen at the load of 21 KN displacement was 2mm, with the appearance of a hair line crack at a distance of 8 mm from joint. In the 7th cycle peak load of 62 KN was recorded, while for repaired peak load was 74 KN. The residual displacements became significant after 4th cycle. The residual displacement was 15 mm at the completion of test. The hysteresis response and backbone curve are shown below.

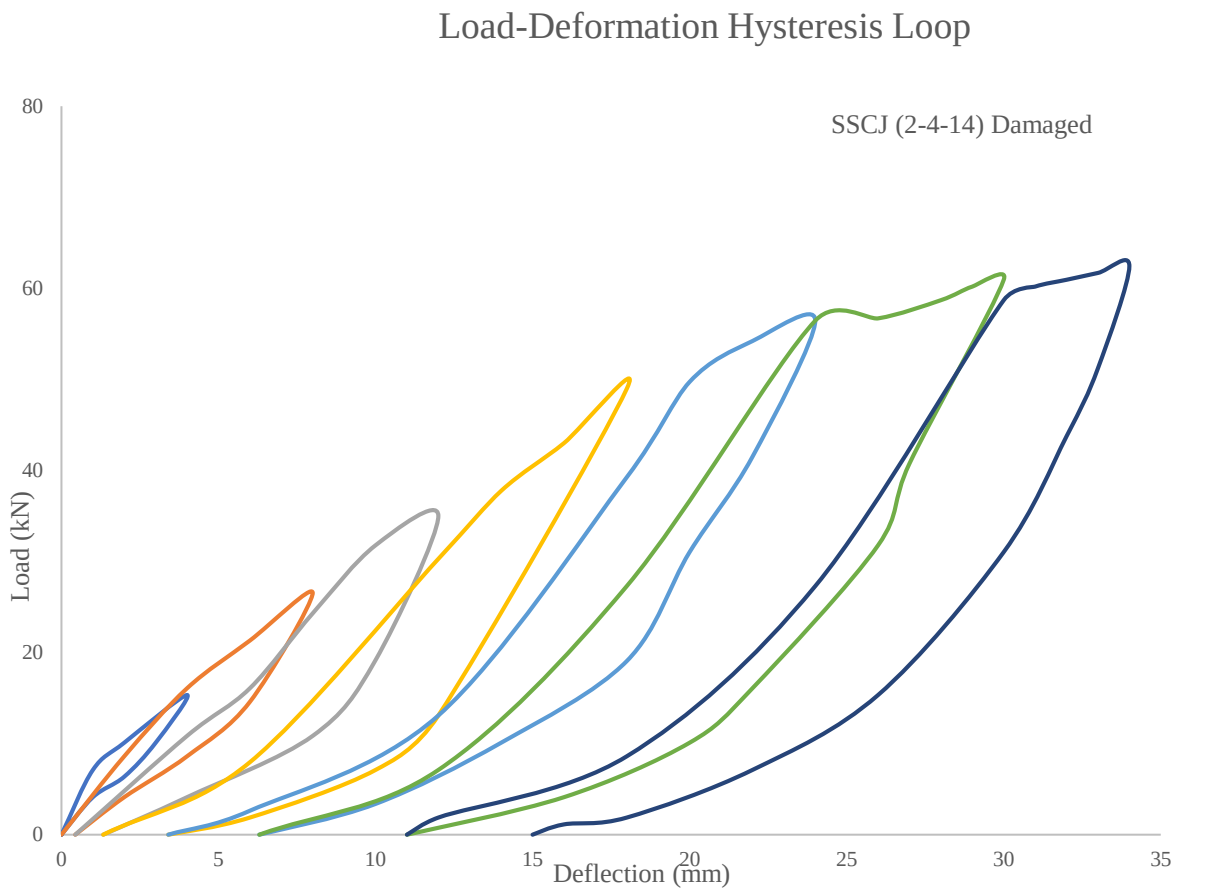
Load-Deformation Hysteresis Loop
SSCJ (2-4-14) Damaged
Load (kN)
Deflection (mm)
0
20
40
60
80
0
5
10
15
20
25
30
35

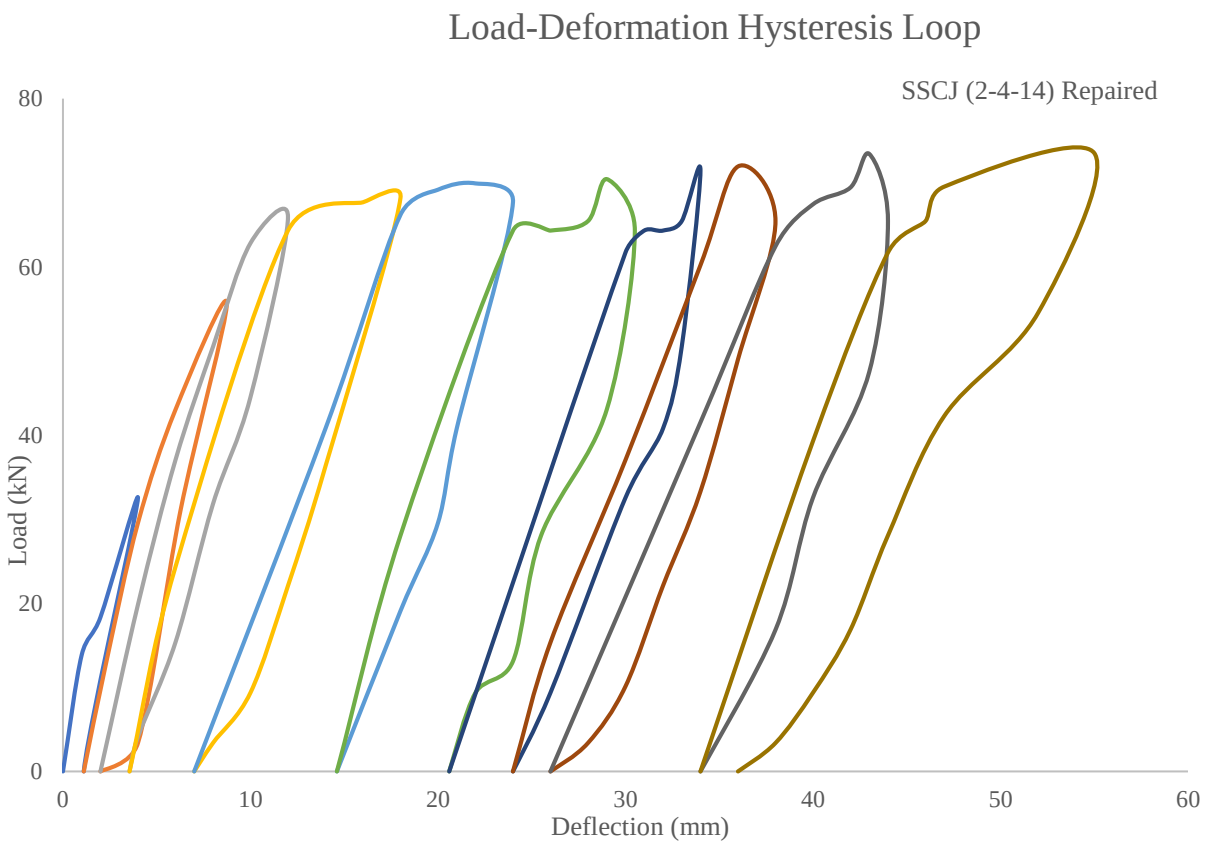
Load-Deformation Hysteresis Loop
SSCJ (2-4-14) Repaired
Load (kN)
Deflection (mm)
0
20
40
60
80
0
10
20
30
40
50
60

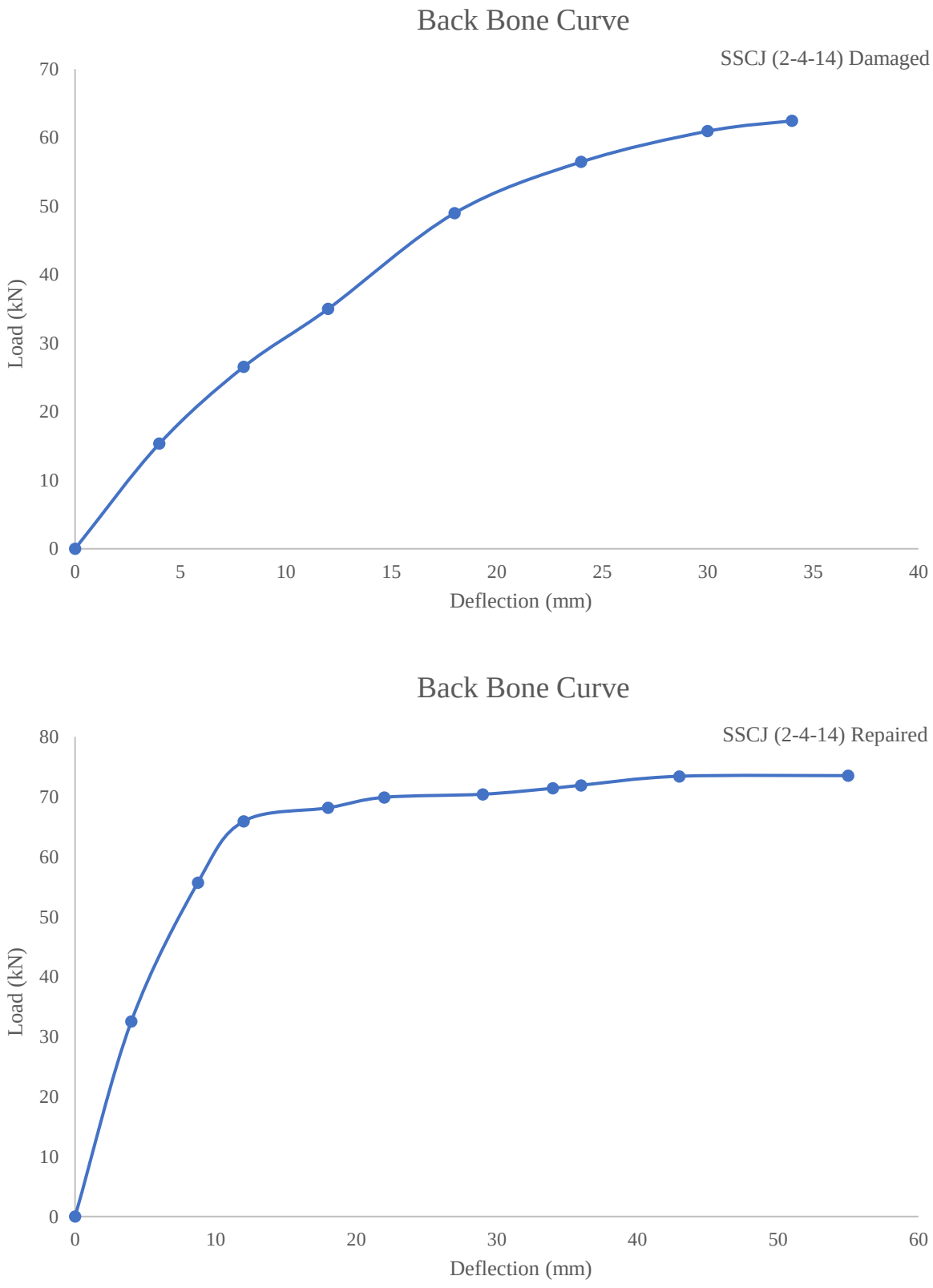

Figure 4.4: SSCJ 02 (2-4-14) Curves

Testing of SSCJ 1.3 (1-4-18)

In 10th cycle of loading 20% degradation was achieved. The deformation in the joint started at 9 KN load during the 1st cycle and achieved a displacement of 2 mm, while for repaired specimen at the load of 16 KN displacement was 4mm, with the appearance of a hair line crack at a distance of 12 mm from joint. In the 10th cycle peak load of 58 KN was recorded, while for repaired peak load was 64 KN. The residual displacements became significant after 5th cycle. The residual displacement was 15.5 mm at the completion of test. The hysteresis response and backbone curve are shown below.

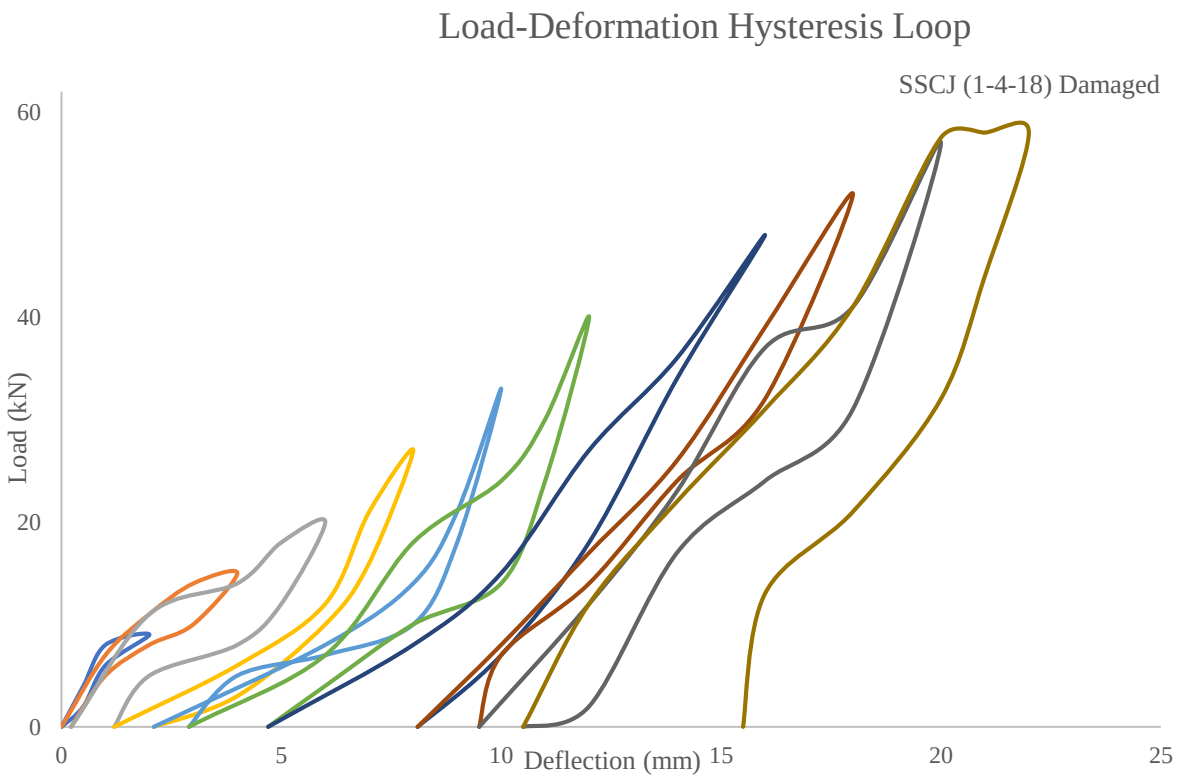

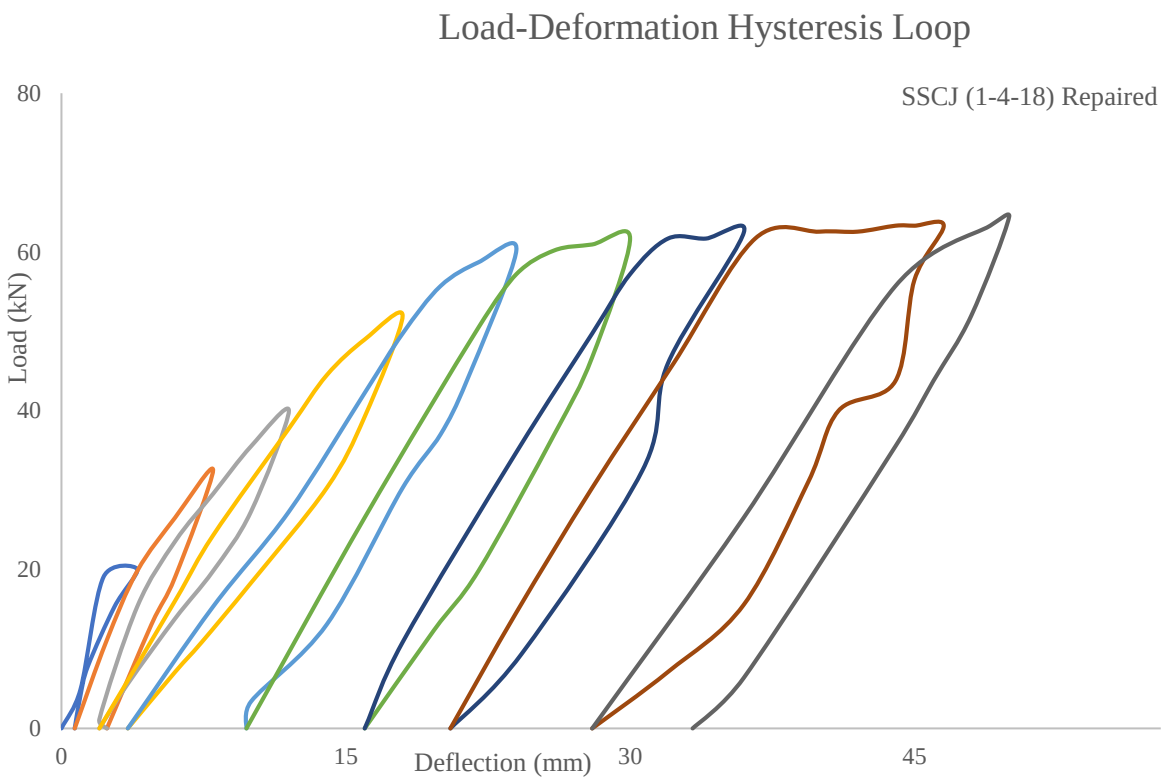
Load-Deformation Hysteresis Loop
SSCJ (1-4-18) Repaired
Load (kN)
80
60
40
20
0
0
15
30
45
Deflection (mm)

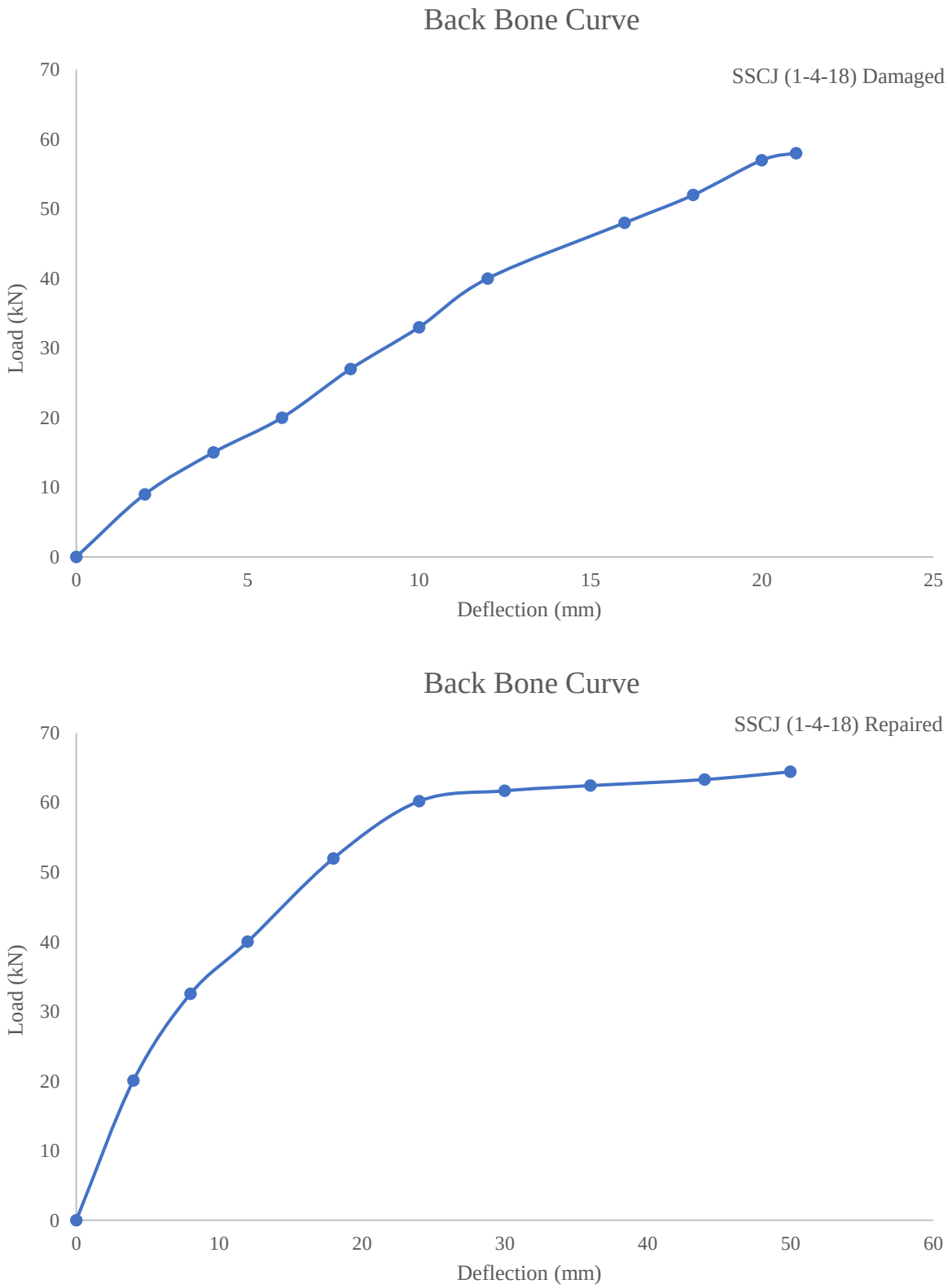

Figure 4.5: SSCJ 1.3 (1-4-18) Curves

Testing of SSCJ 1.3 (2-4-18)

In 7th cycle of loading 20% degradation was achieved. The deformation in the joint started at 16 KN load during the 1st cycle and achieved a displacement of 4 mm, while for repaired specimen at the load of 24 KN displacement was 6mm, with the appearance of a hair line crack at a distance of 10 mm from joint. In the 9th cycle peak load of 59 KN was recorded, while in case of repaired peak load was 68 KN. The residual displacements became significant after 5th cycle. The residual displacement was 18.7 mm at the completion of test. The hysteresis response and backbone curve are shown below.

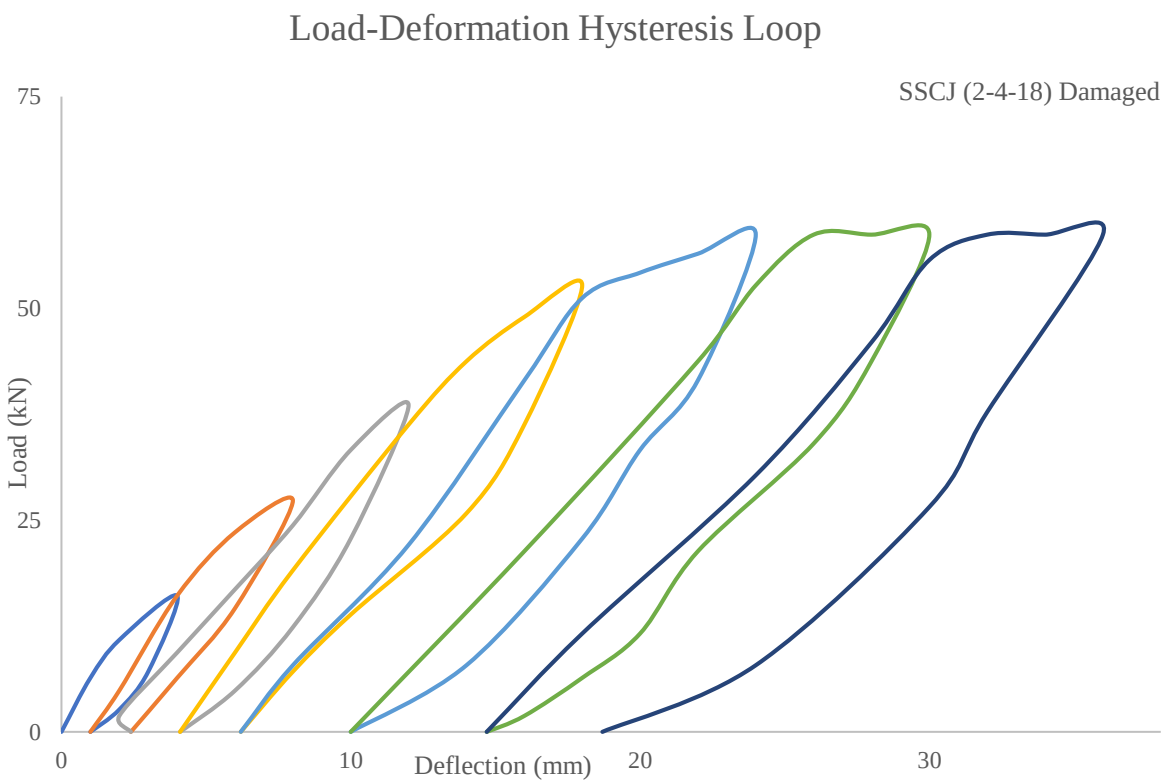

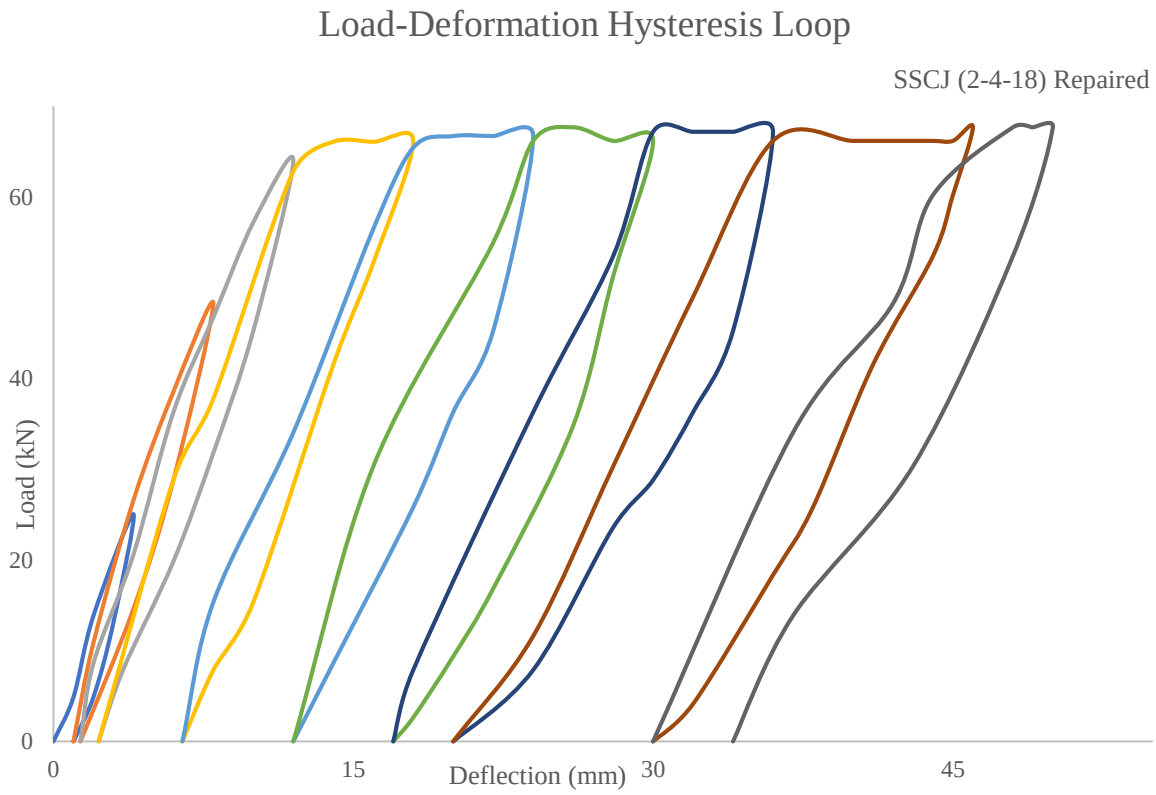
Load-Deformation Hysteresis Loop
SSCJ (2-4-18) Repaired
Load (kN)
0
20
40
60
0
15
30
45
Deflection (mm)

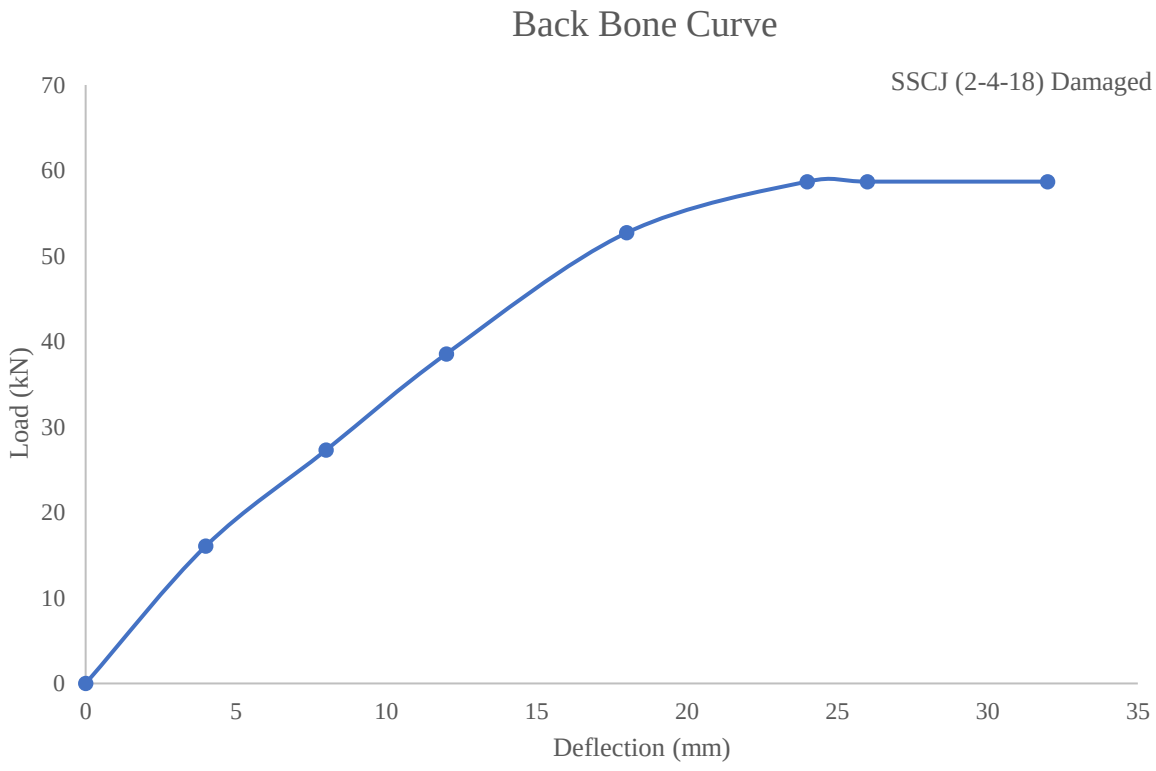
Back Bone Curve
SSCJ (2-4-18) Damaged
Load (kN)
0
10
20
30
40
50
60
70
0
5
10
15
20
25
30
35
Deflection (mm)

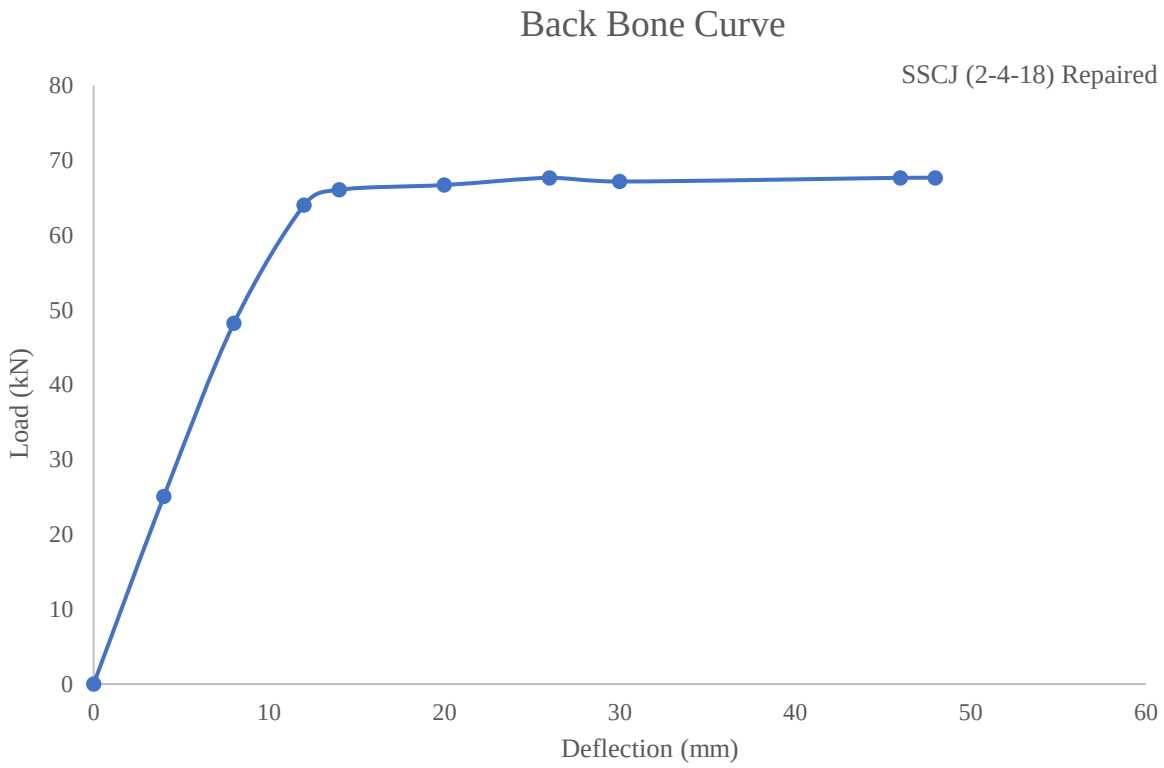

Figure 4.6: SSCJ 1.3 (2-4-18) Curves

Testing of CRCJ (1-3#3)

In 9th cycle of loading 20% degradation was achieved. The deformation in the joint started at 16 KN load during the 1st cycle and achieved a displacement of 4 mm, while for repaired specimen at the load of 19 KN displacement was 5mm, with the appearance of a hair line crack at a distance of 32 mm from joint. In the 9th cycle peak load of 59 KN was recorded, while for repaired peak load was 62 KN. The residual displacements became significant after 4th cycle. The residual displacement was 22 mm at the completion of test. The hysteresis response and backbone curve are shown below.

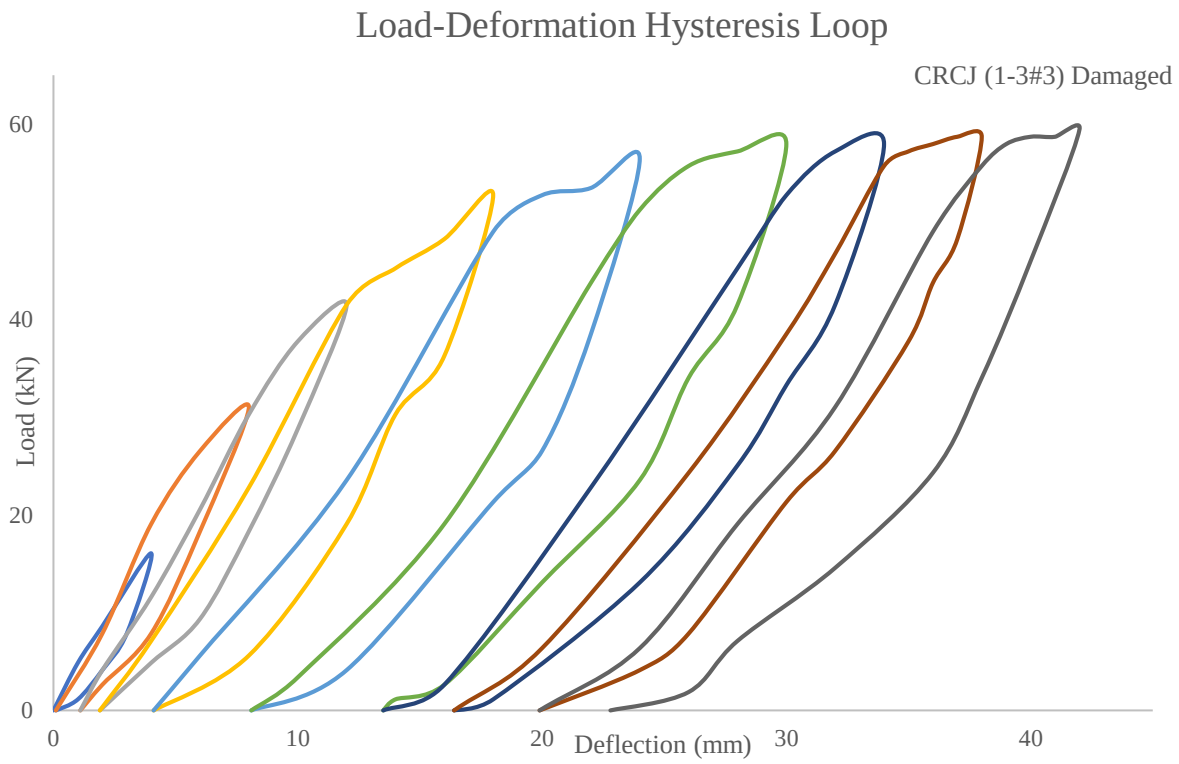
Load-Deformation Hysteresis Loop
CRCJ (1-3#3) Damaged
Load (kN)
0
20
40
60
0
10
20
30
40
Deflection (mm)

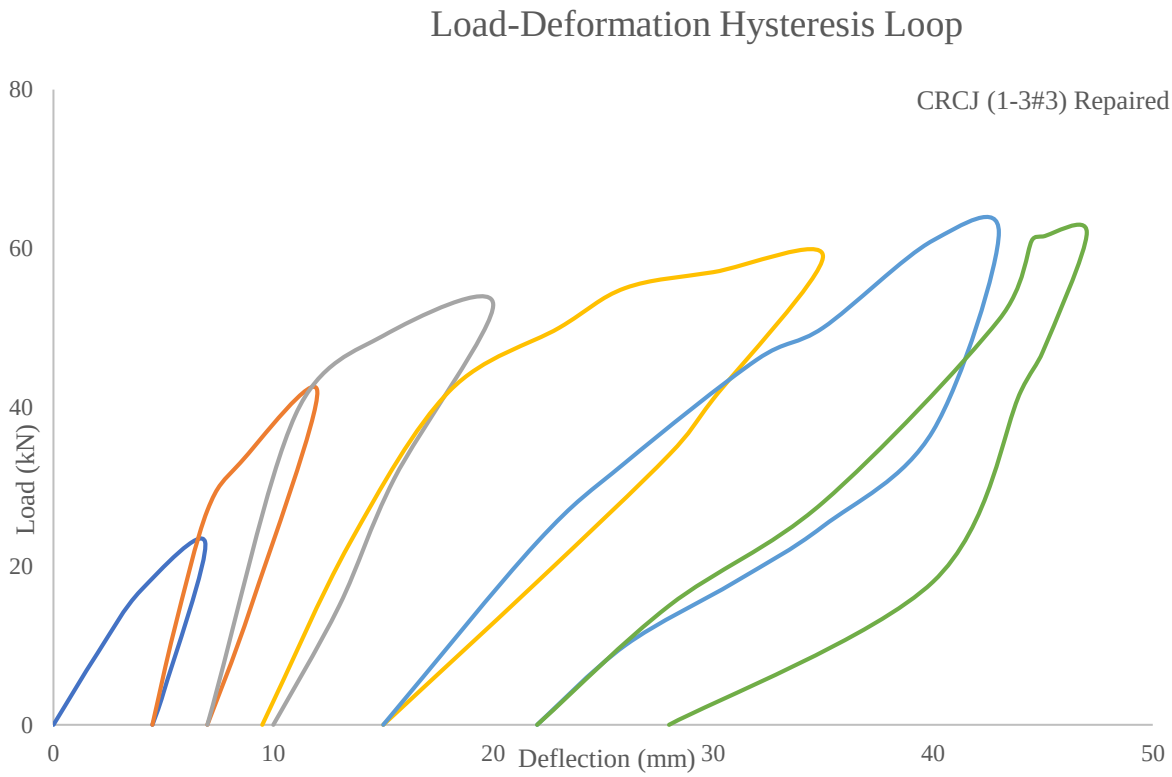
Load-Deformation Hysteresis Loop
CRCJ (1-3#3) Repaired
Load (kN)
0
20
40
60
80
0
10
20
30
40
50
Deflection (mm)

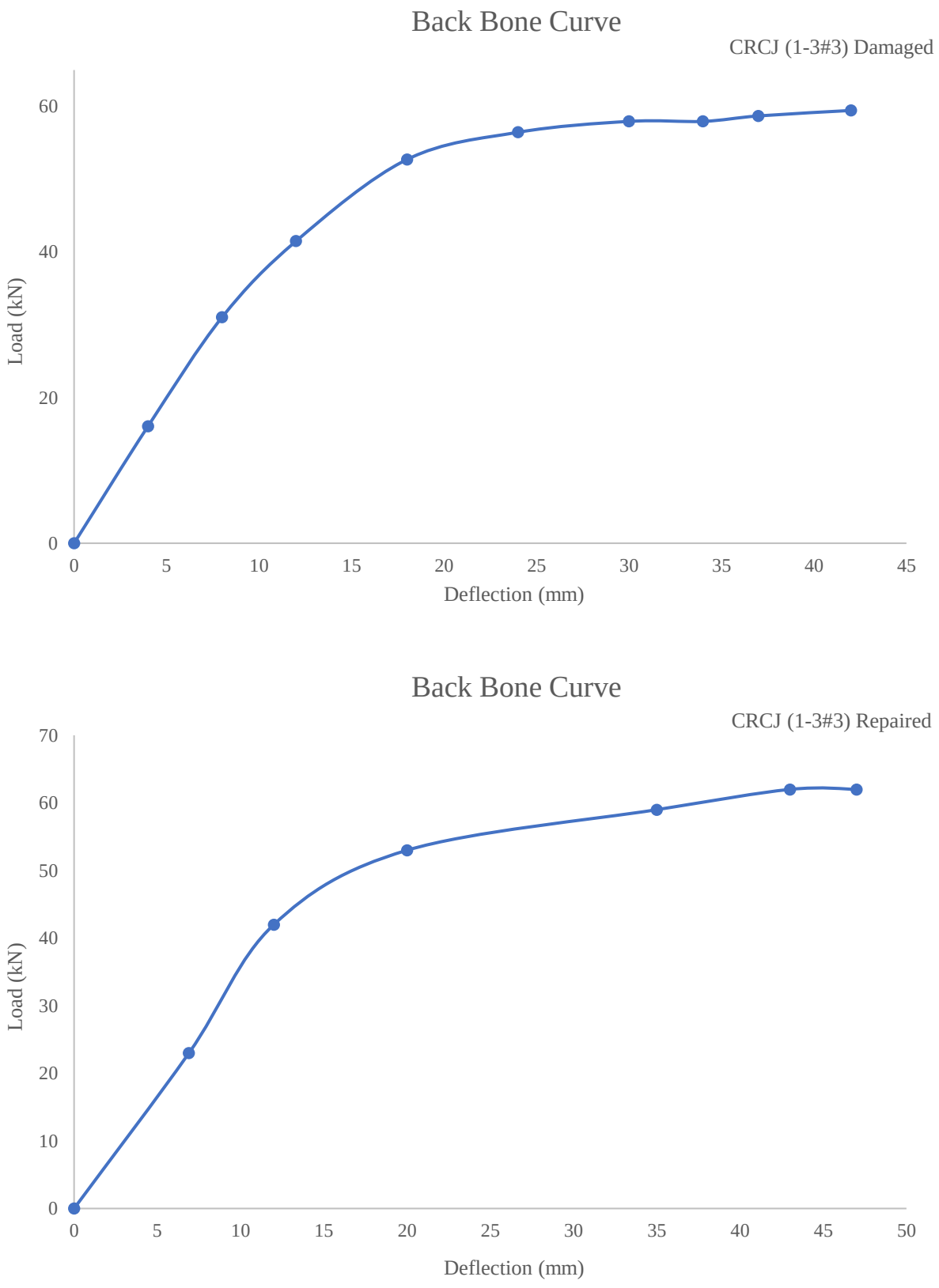

Figure 4.7: CRCJ (1-3#3) Curves

Testing of CRCJ (2-3#3)

In 5th cycle of loading 20% degradation was achieved. The deformation in the joint started at 22 KN load during the 1st cycle and achieved a displacement of 5 mm, while for repaired specimen at the load of 26 KN displacement was 6mm, with the appearance of a hair line crack at a distance of 9 mm from joint. In the 5th cycle peak load of 55 KN was recorded, while in case of repaired peak load was 64 KN. The residual displacements became significant after 3rd cycle. The residual displacement was 10.5 mm at the completion of test. The hysteresis response and backbone curve are shown below.

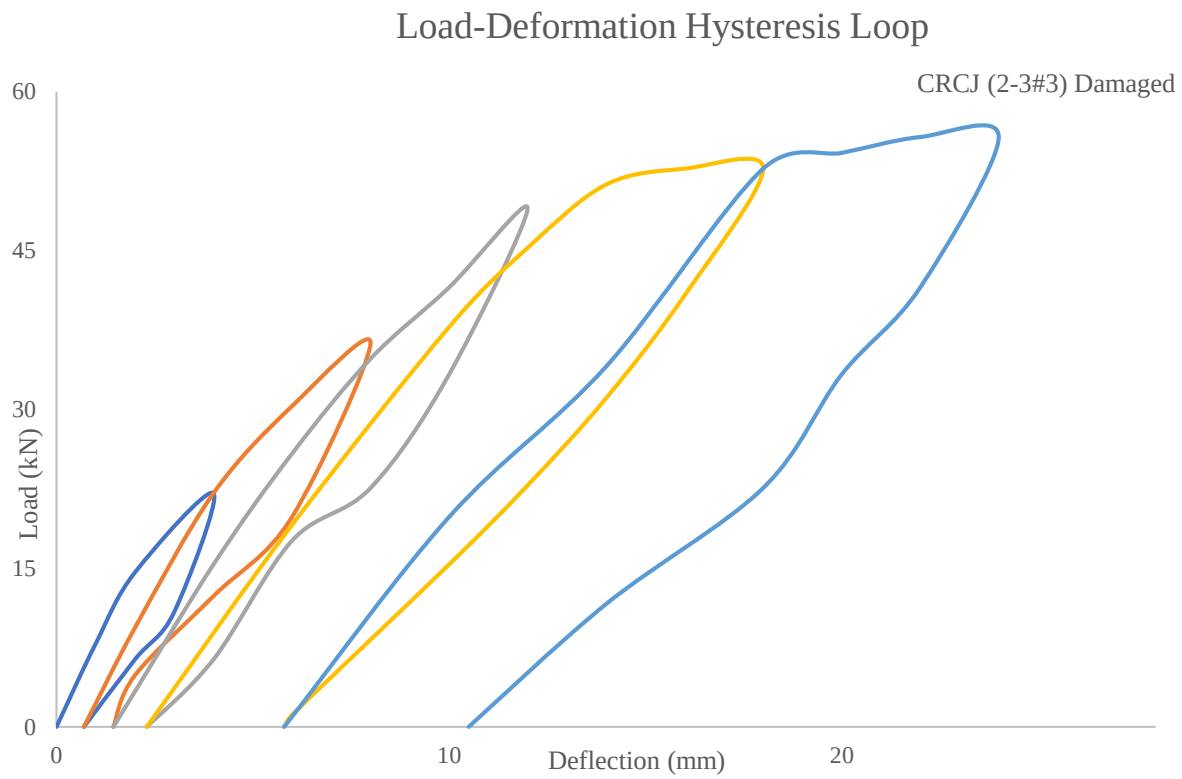

Load-Deformation Hysteresis Loop

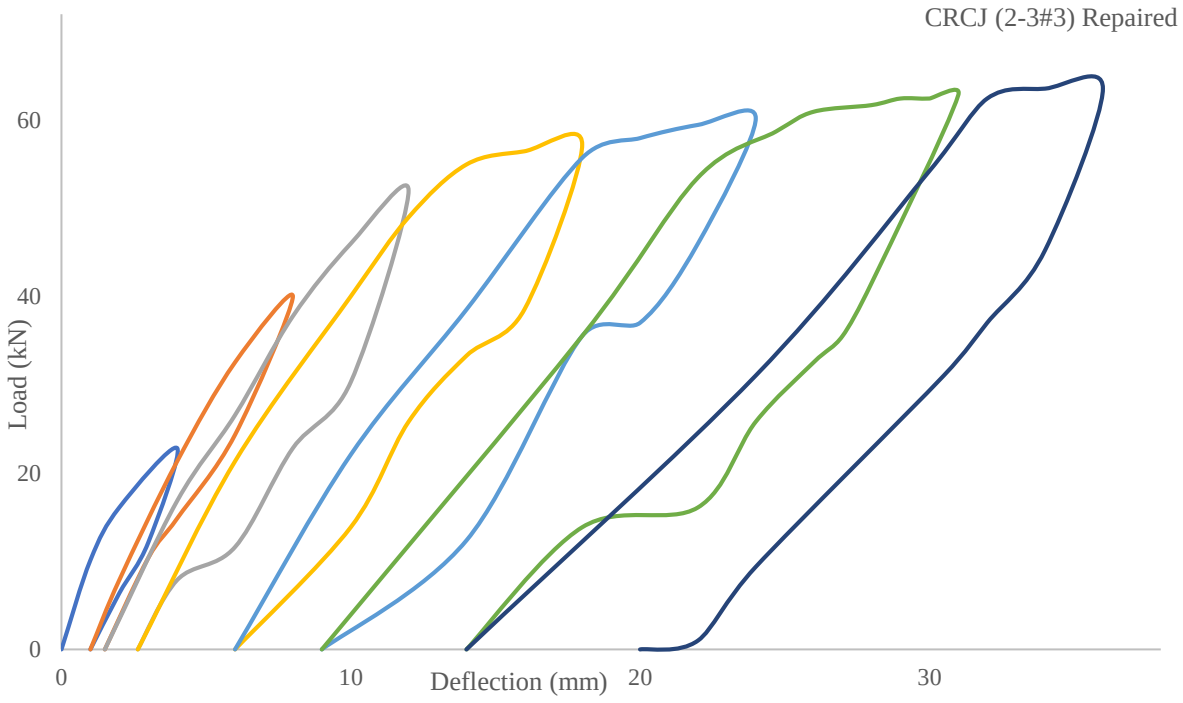

Back Bone Curve

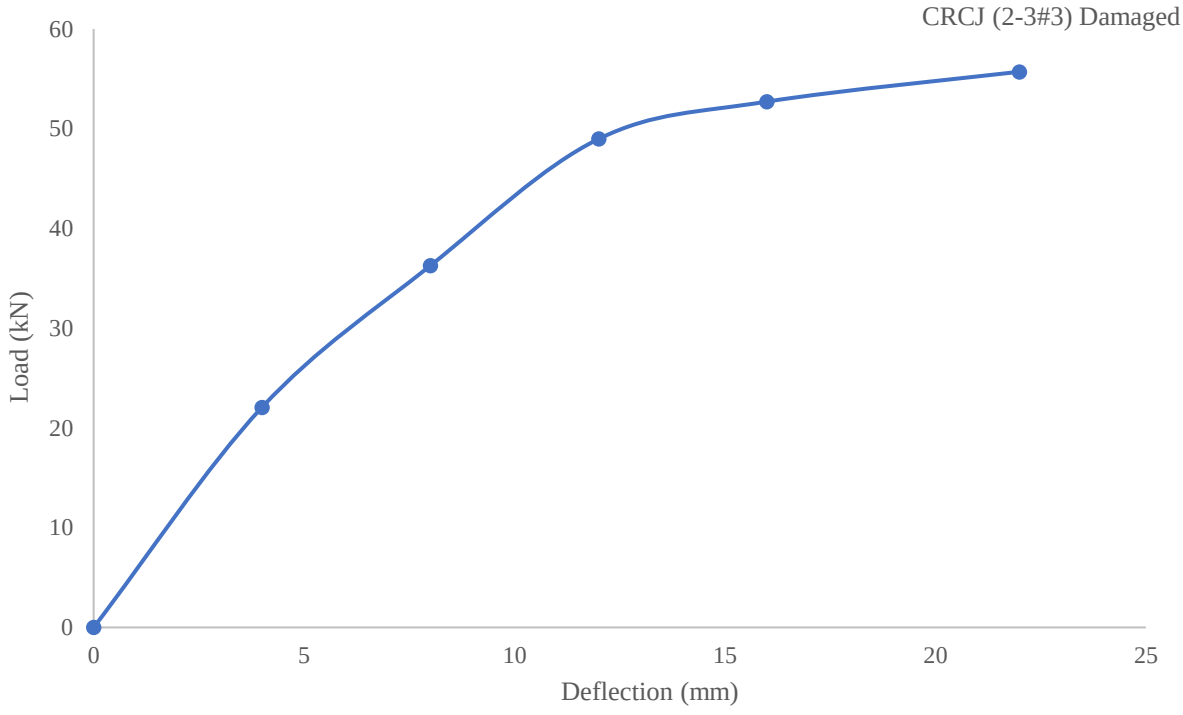

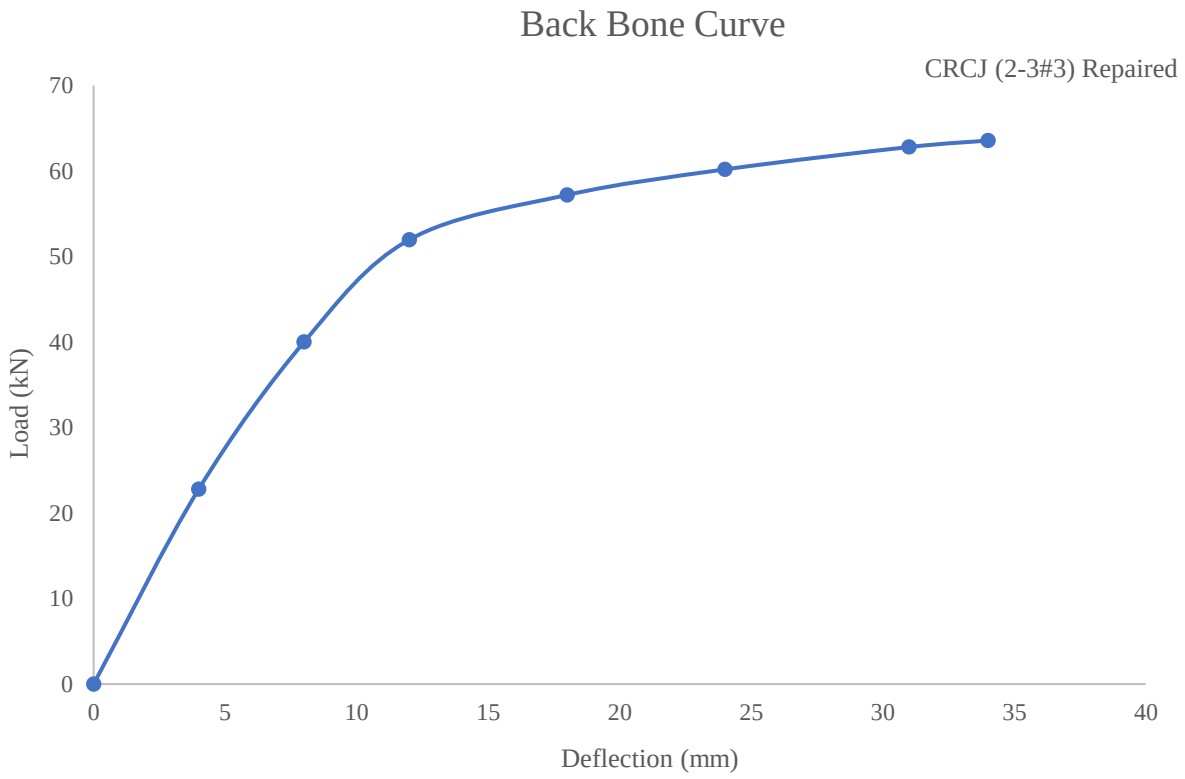

Figure 4.8: CRCJ (2-3#3) Curves

Testing of SSCJ 2 (1-3-14)

In 8th cycle of loading 20% degradation was achieved. The deformation in the joint started at 21 KN load during the 1st cycle and achieved a displacement of 3 mm, while for repaired specimen at the load of 24 KN displacement was 5mm, with the appearance of a hair line crack at a distance of 12 mm from joint. In the 9th cycle peak load of 57 KN was recorded, while in case of repaired specimen peak load was 61 KN. The residual displacements became significant after 4th cycle. The residual displacement was 12 mm at the completion of test. The hysteresis response and backbone curve are shown below.

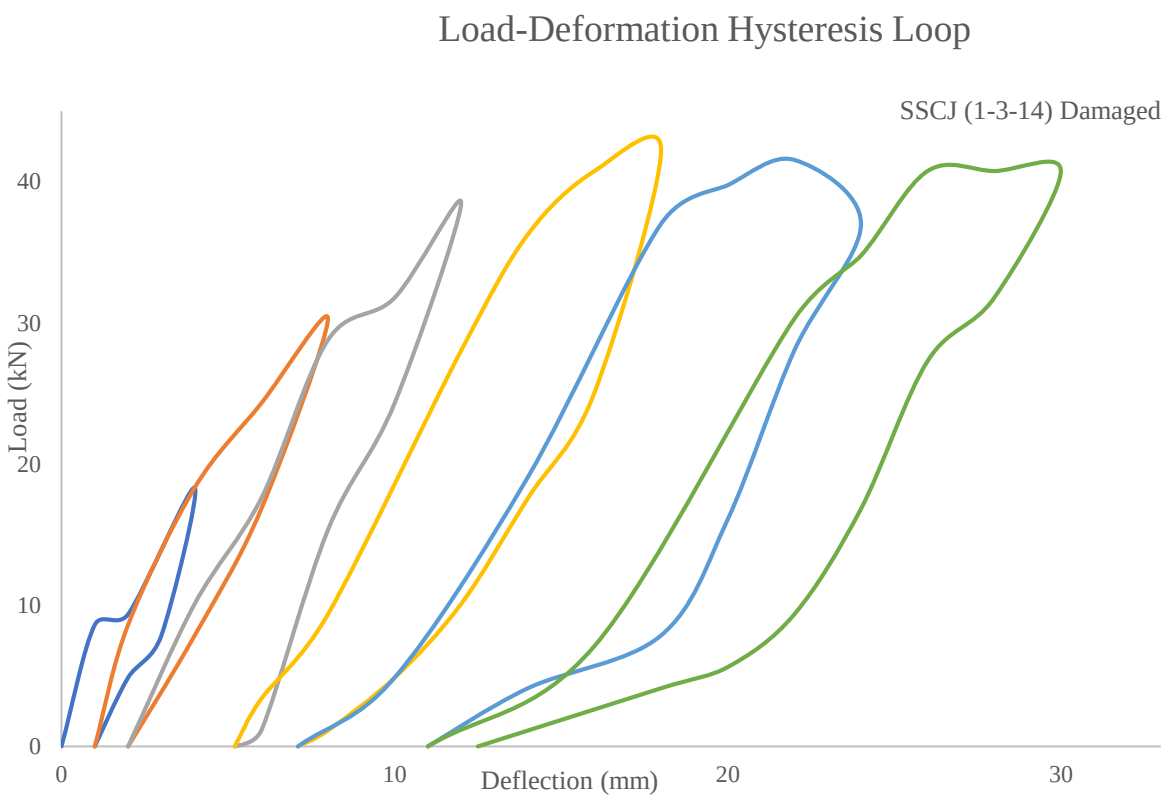
Load-Deformation Hysteresis Loop
SSCJ (1-3-14) Damaged
Load (kN)
40
30
20
10
0
0
10
20
30
Deflection (mm)

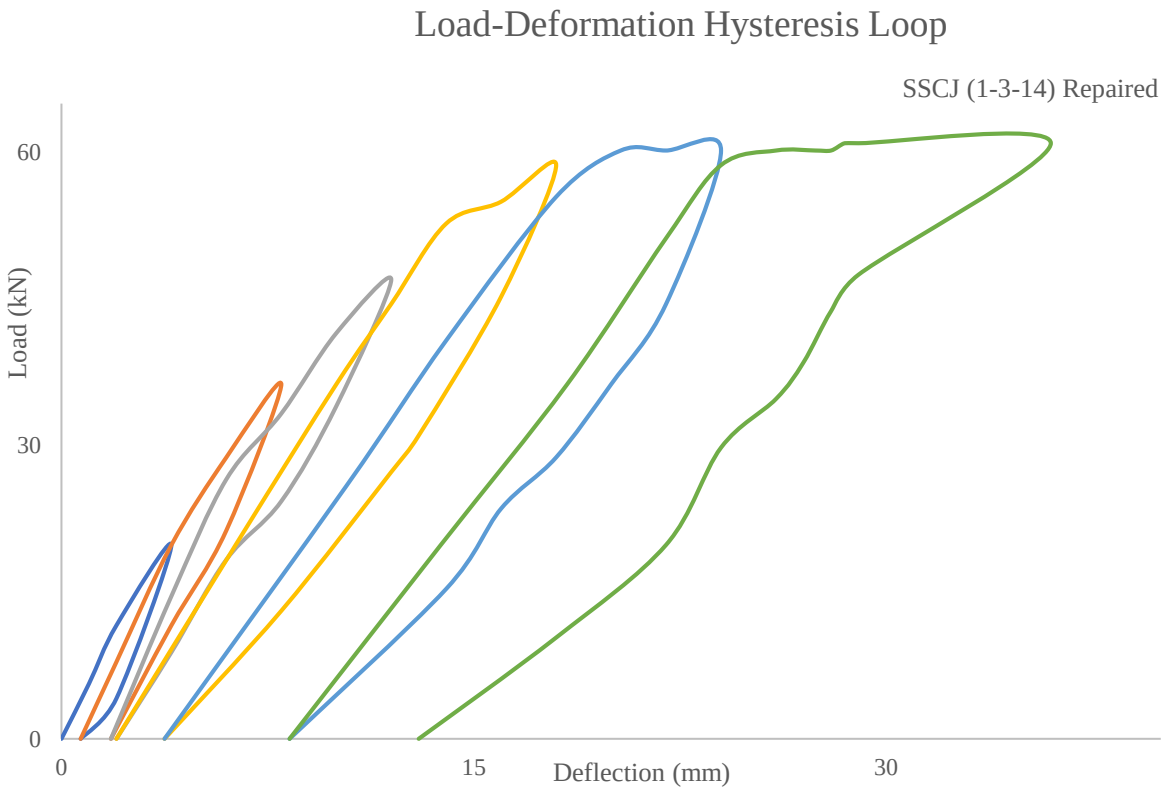
Load-Deformation Hysteresis Loop
SSCJ (1-3-14) Repaired
Load (kN)
60
30
0
0
15
30
Deflection (mm)

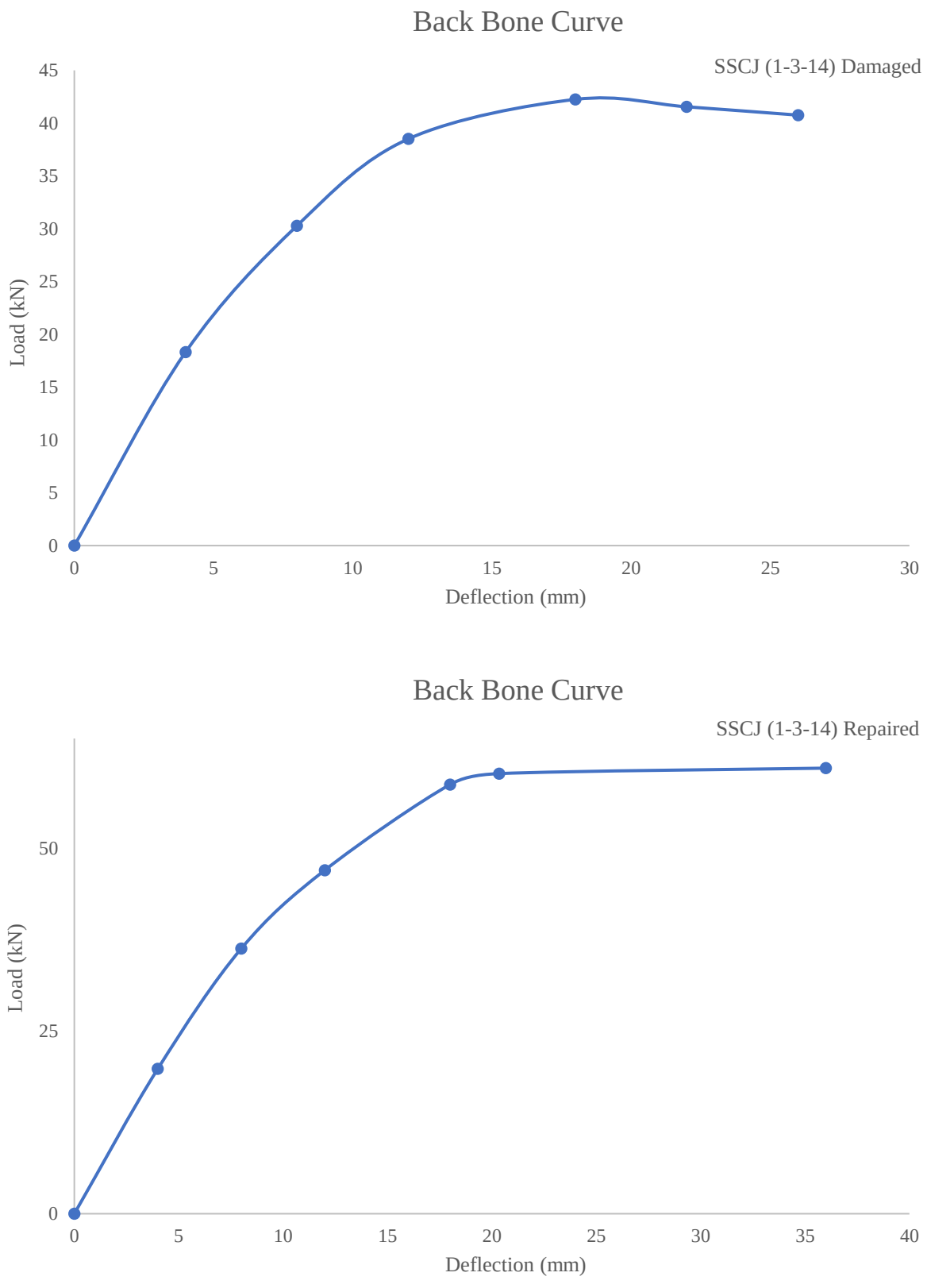

Figure 4.9: SSCJ 2 (1-3-14) Curves

Testing of SSCJ 2 (2-3-14)

In 8th cycle of loading 20% degradation was achieved. The deformation in the joint started at 18 KN load during the 1st cycle and achieved a displacement of 2 mm, while for repaired specimen at the load of 19 KN displacement was 4mm, with the appearance of a hair line crack at a distance of 9 mm from joint. In the 8th cycle peak load of 41 KN was recorded, while in case of repaired peak load was 69 KN. The residual displacements became significant after 4th cycle. The residual displacement was 12 mm at the completion of test. The hysteresis response and backbone curve are shown below.

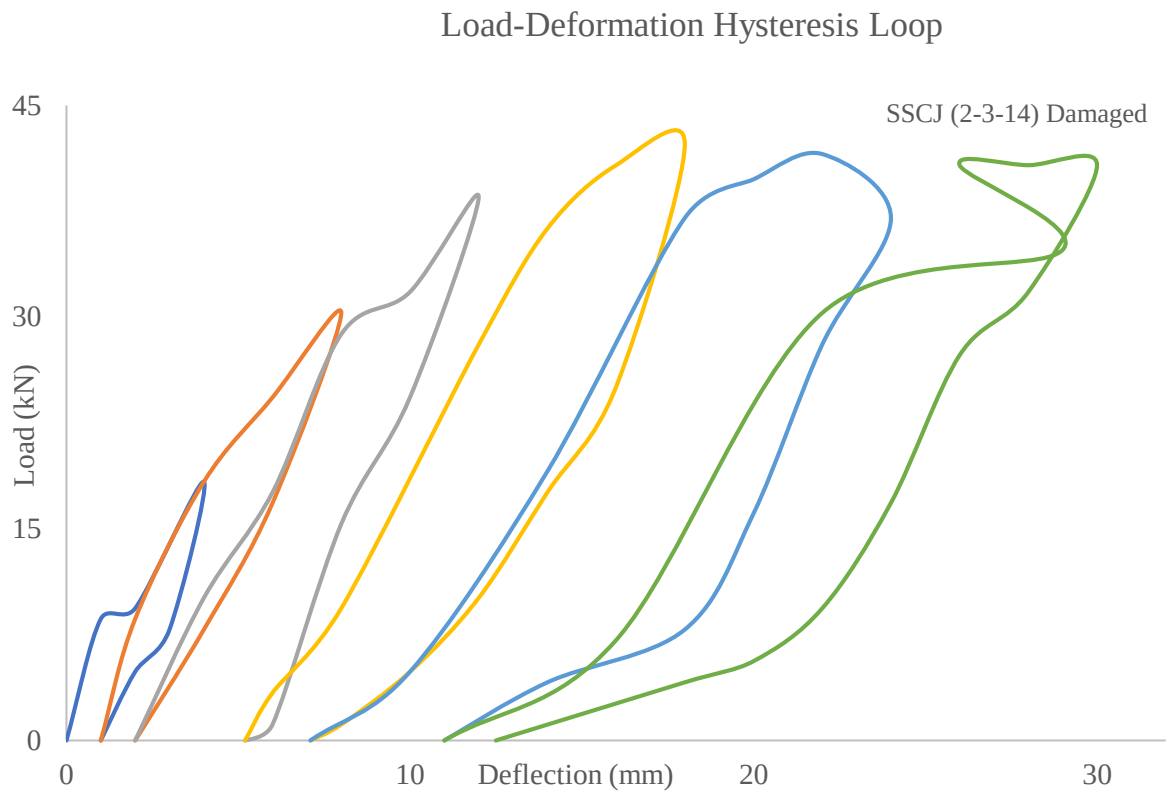

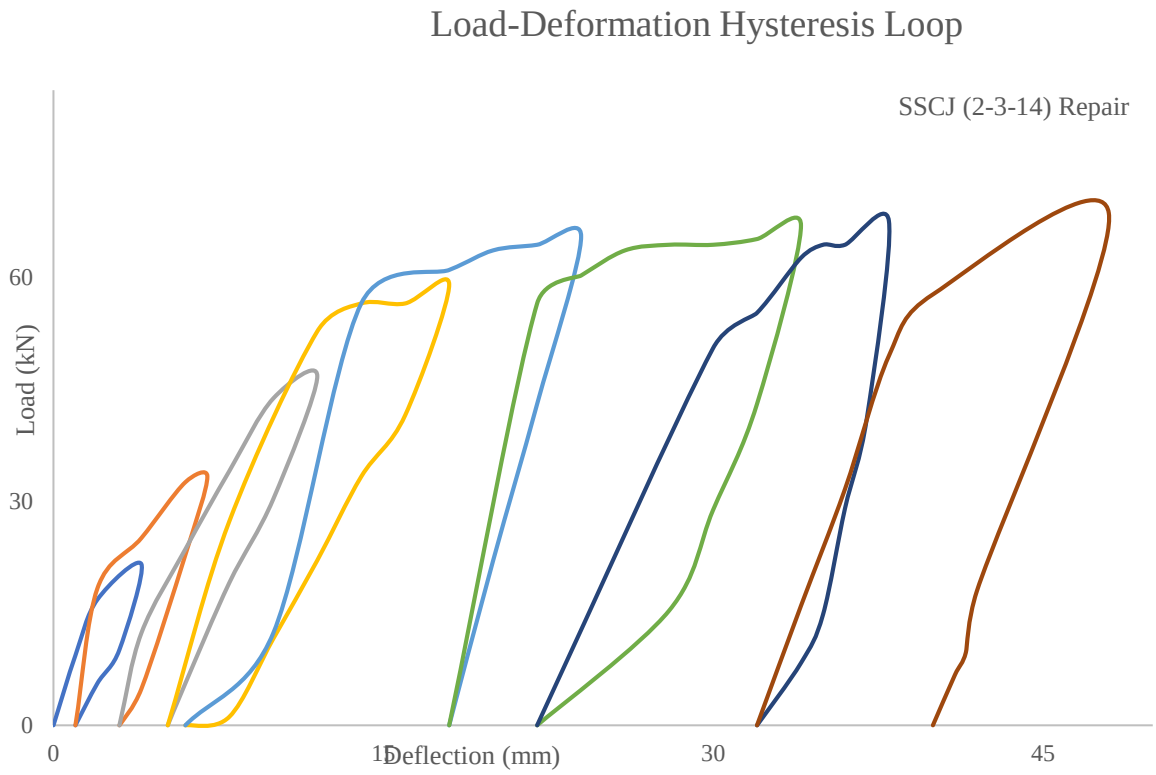
Load-Deformation Hysteresis Loop
SSCJ (2-3-14) Repair
60
30
0
Load (kN)
0
15
Deflection (mm)
30
45

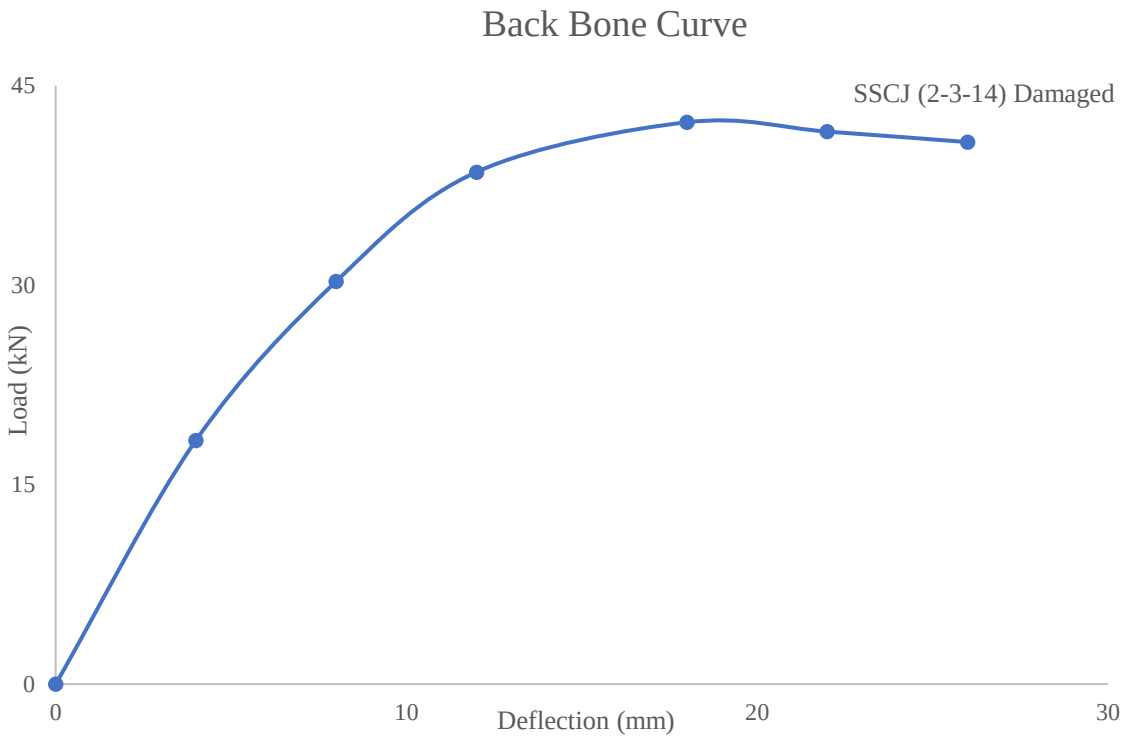
Back Bone Curve
SSCJ (2-3-14) Damaged
45
30
15
0
Load (kN)
0
10
Deflection (mm)
20
30

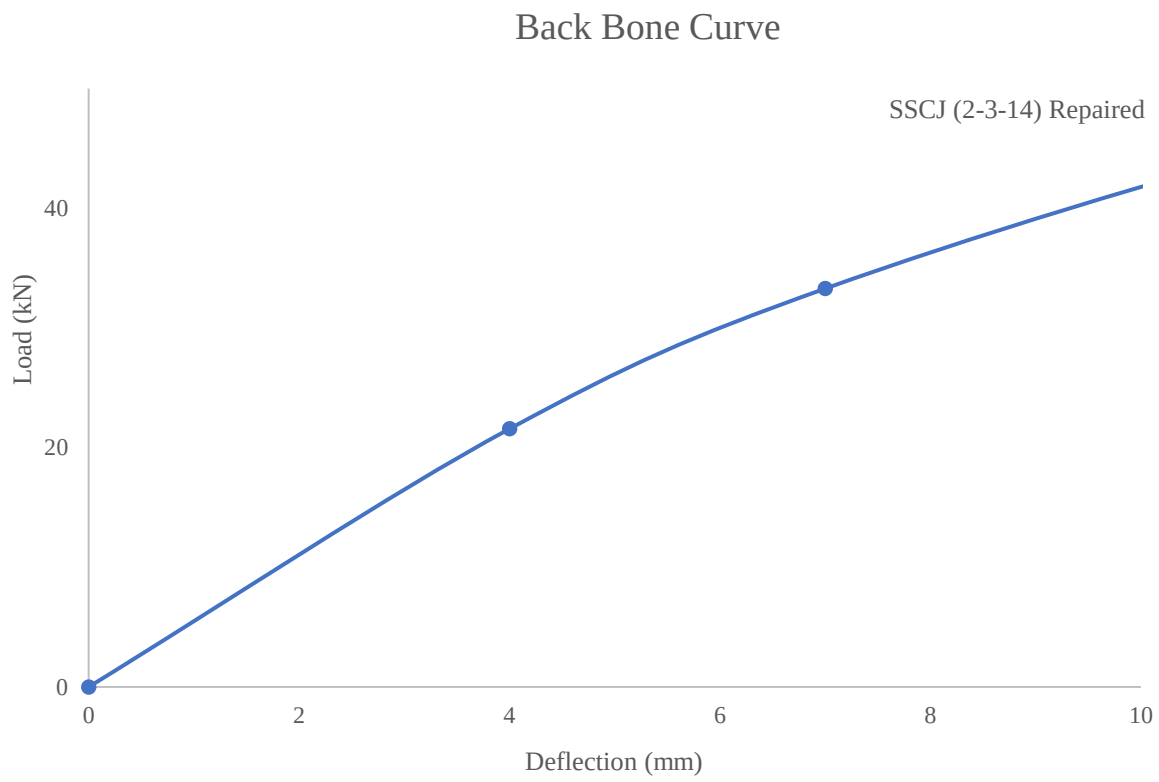

Figure 4.10: SSCJ 2 (2-3-14) Curves

Testing of SSCJ 1.3 (1-3-18)

In 7th cycle of loading 20% degradation was achieved. The deformation in the joint started at 18 KN load during the 1st cycle and achieved a displacement of 3 mm, while for repaired specimen at the load of 20 KN displacement was 4mm, with the appearance of a hair line crack at a distance of 9 mm from joint. In the 7th cycle peak load of 60 KN was recorded, while in case of repaired peak load was 69 KN. The residual displacements became significant after 4th cycle. The residual displacement was 20 mm at the completion of test.

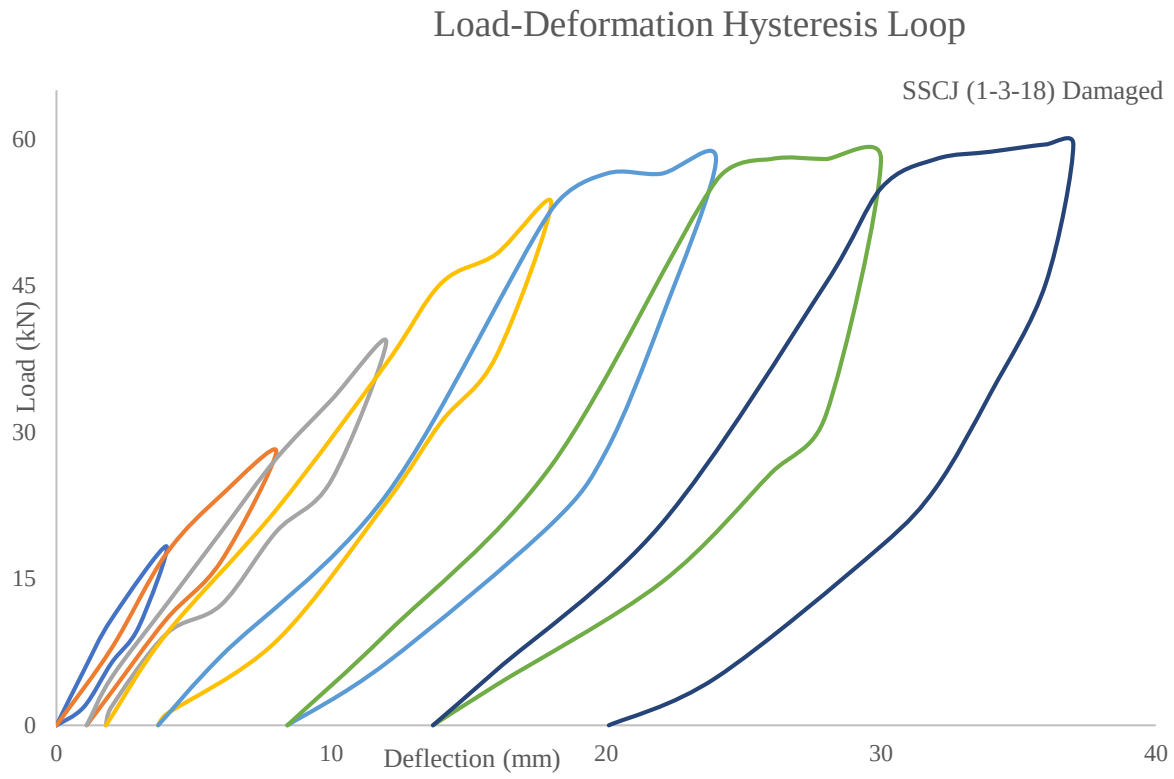
Load-Deformation Hysteresis Loop
SSCJ (1-3-18) Damaged
Load (kN)
60
45
30
15
0
0
10
20
30
40
Deflection (mm)

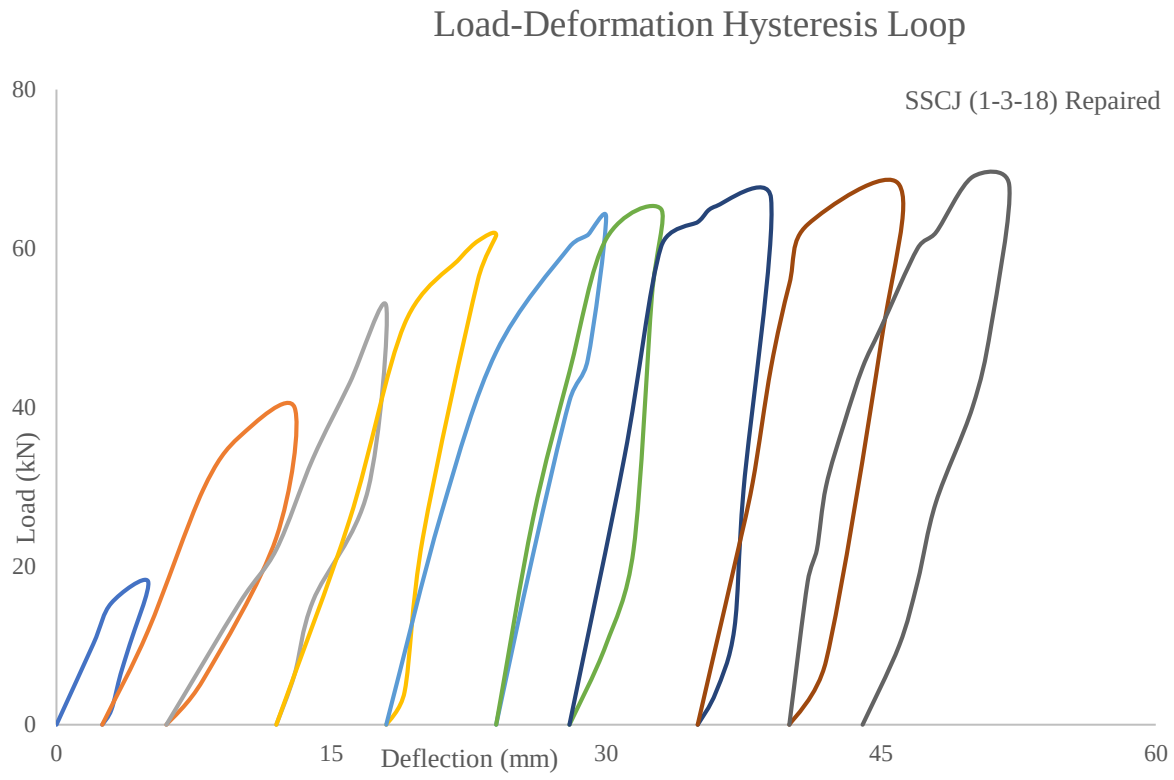
Load-Deformation Hysteresis Loop
SSCJ (1-3-18) Repaired
Load (kN)
80
60
40
20
0
0
15
30
45
60
Deflection (mm)

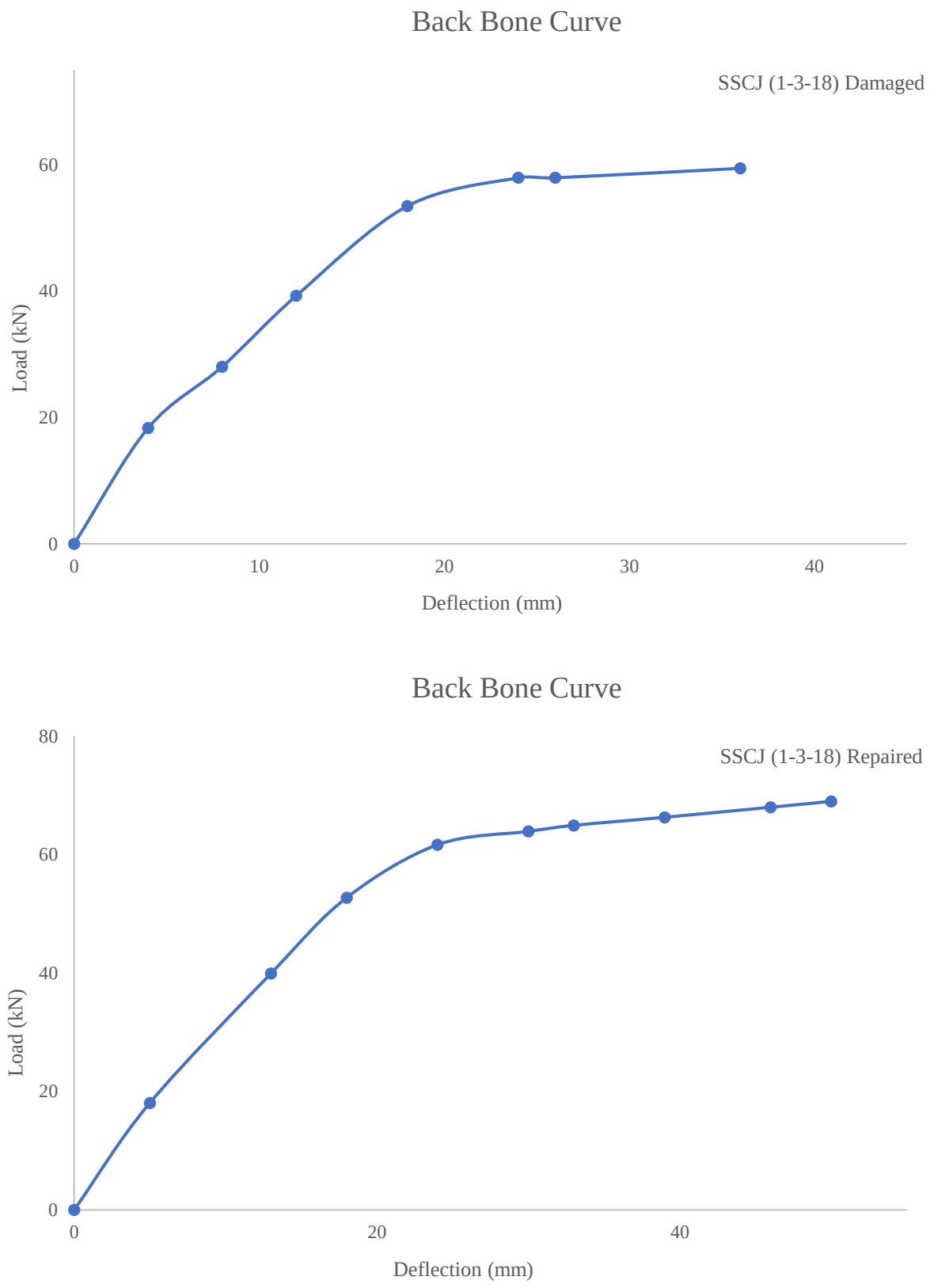

Figure 4.11: of SSCJ 1.3 (1-3-18) Curves

Testing of SSCJ 1.3 (2-3-18)

In 8th cycle of loading 20% degradation was achieved. The deformation in the joint started at 12 KN load during the 1st cycle and achieved a displacement of 3 mm, while for repaired specimen at the load of 18 KN displacement was 5mm, with the appearance of a hair line crack at a distance of 9 mm from joint. In the 8th cycle peak load of 61 KN was recorded, while in case of repaired peak load was 68 KN. The residual displacements became significant after 4th cycle. The residual displacement was 19 mm at the completion of test. The hysteresis response and backbone curve are shown below.

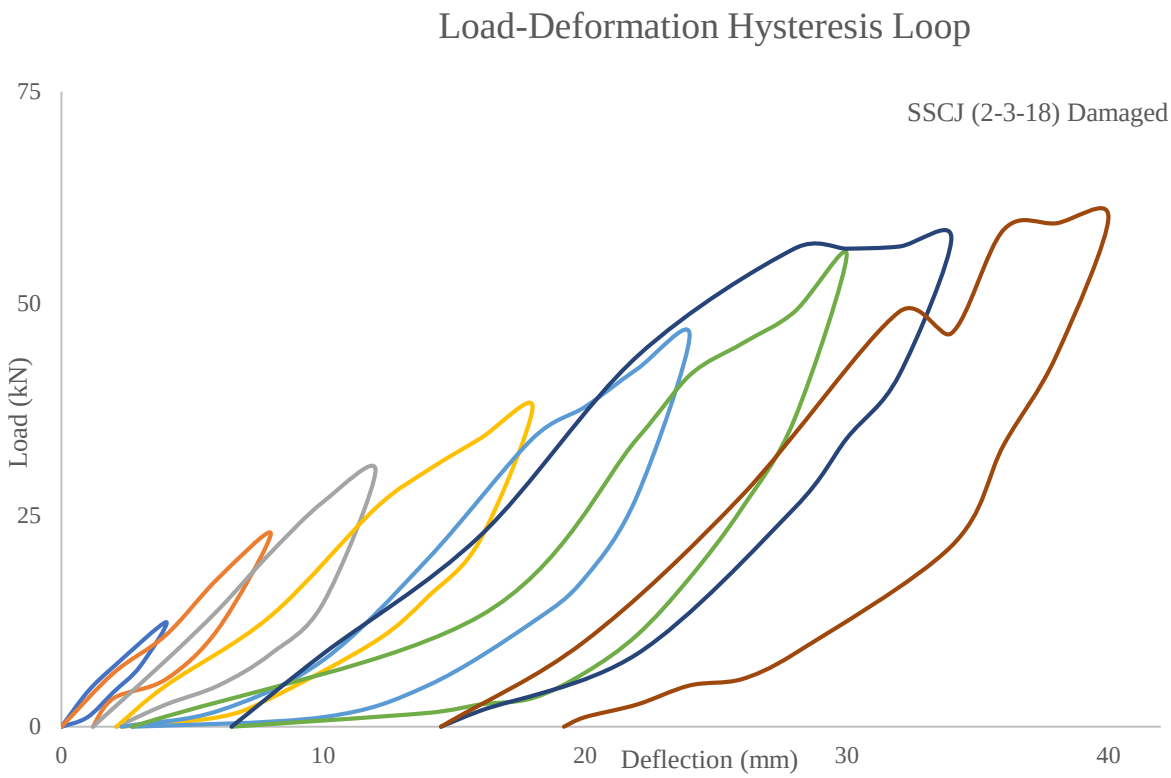

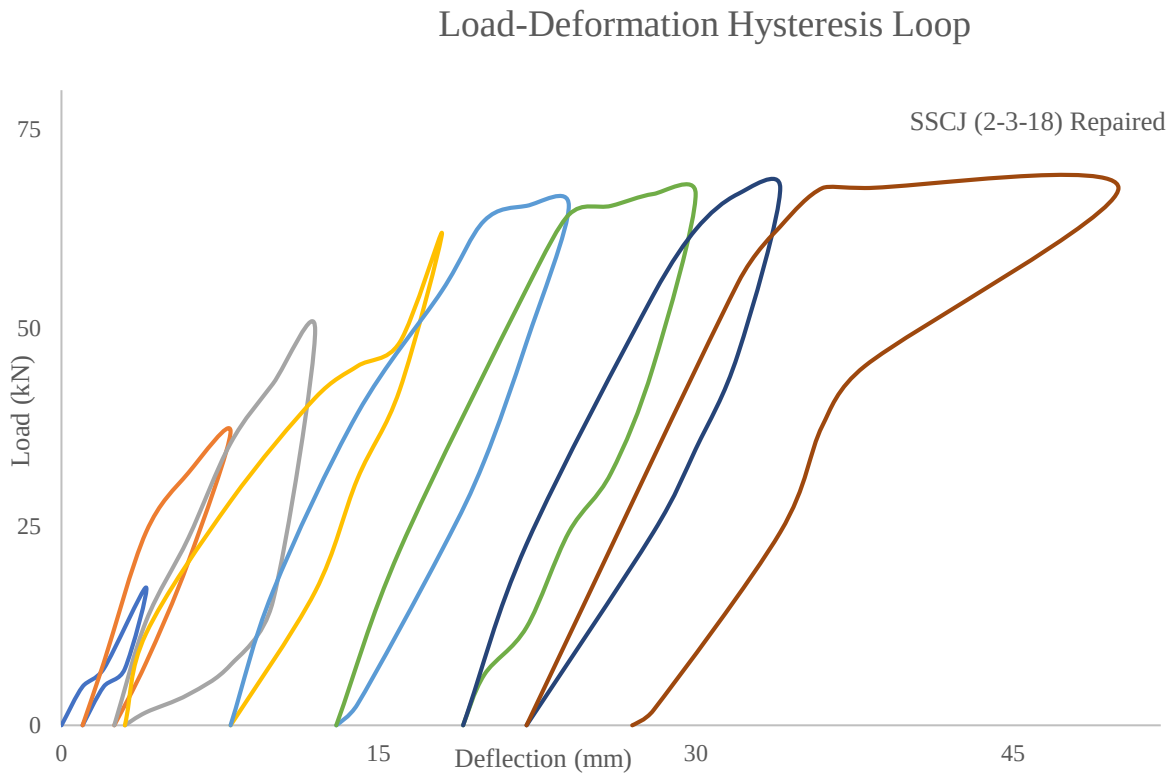
Load-Deformation Hysteresis Loop
SSCJ (2-3-18) Repaired
75
50
25
0
Load (kN)
0
15
30
45
Deflection (mm)

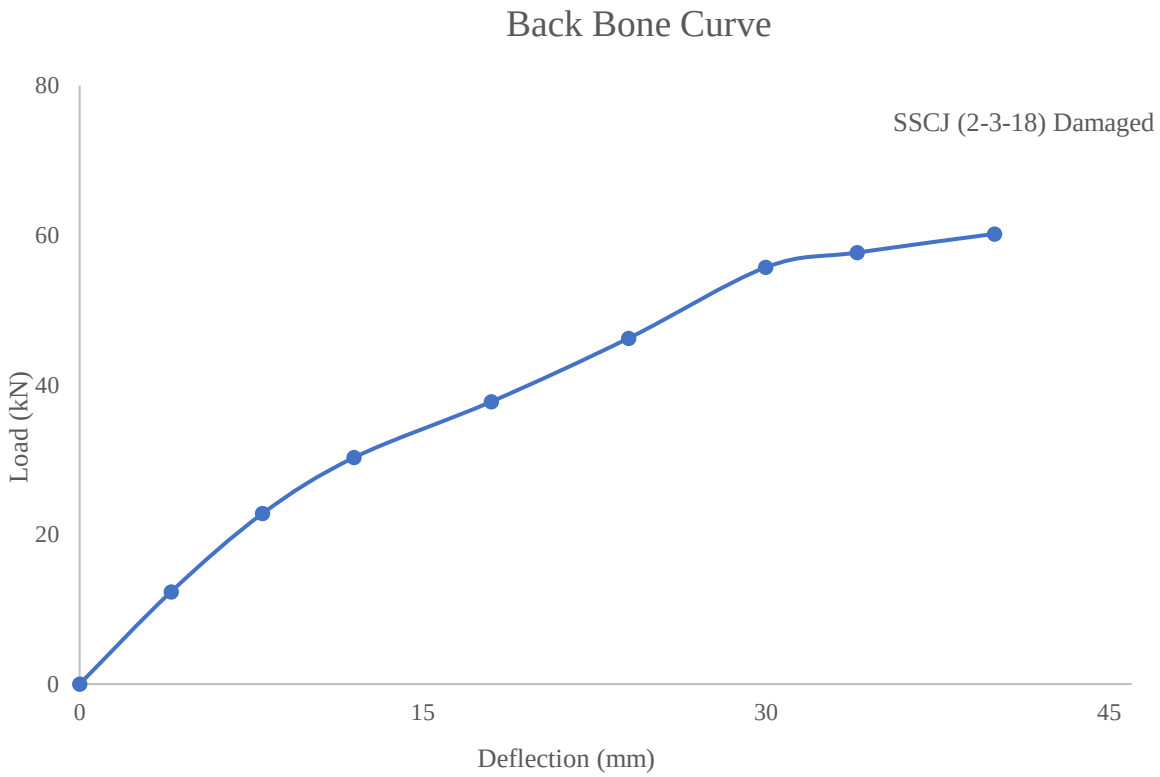
Back Bone Curve
SSCJ (2-3-18) Damaged
80
60
40
20
0
Load (kN)
0
15
30
45
Deflection (mm)

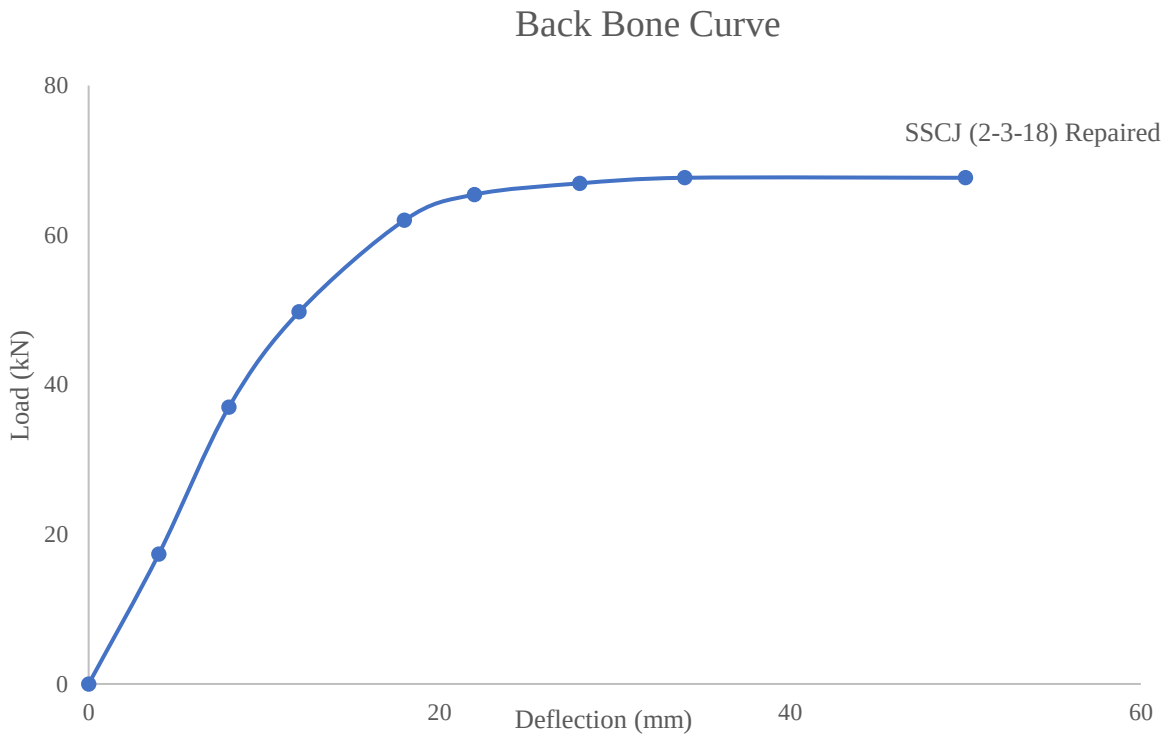

Figure 4.12: of SSCJ 1.3 (2-3-18) Curves

4.1.3 Yield, Peak and Ultimate Load Displacement Points

The backbone curves obtained from the hysteresis loops of the beam column repaired and control joint samples of 28 MPa strength are superimposed in Figure 4.13. It is observed that the control joints response is approximately identical up to 30 KN. Control specimen for SSCJ-02 (2-4-14) gave a higher peak load and exhibits better ductile response. After specimen repair, initially structure remained in elastic region and steel was not yielded. When load and deflection started to increase then initially the CFRP de-bonding took place, and with the increase in deflection, CFRP cracks initiated. But in case of repaired joints deflection became almost double with significant increase in load carrying capacity.

Table 13 and 14 shows a comparison of the yield load, peak load and ultimate displacement points, of control as well as repaired specimen. It is clear that SSCJ-02 resisted average 12.5% and 7% greater load at peak load points as compared to CRCJ and SSCJ-1.3 respectively.

Damaged Specimen 4-Ksi			Repaired Specimen 4-Ksi		
Parameter	**Displacement (mm)**	**Load (kN)**	**Parameter**	**Displacement (mm)**	**Load (kN)**
CRCJ			**CRCJ**		
Yield point	5	25	Yield point	6.5	28
Peak load	20	53	Peak load	48	63
Ultimate displacement	28	52.5	Ultimate displacement	47.5	62.5
SSCJ-02			**SSCJ-02**		
Yield point	4	20	Yield point	5.5	42.5
Peak load	34	62	Peak load	55	74
Ultimate displacement	28	60.5	Ultimate displacement	53.5	71.5
SSCJ-1.3			**SSCJ-1.3**		
Yield point	6	18.5	Yield point	7	41
Peak load	32	59	Peak load	48	68
Ultimate displacement	26.5	58	Ultimate displacement	49	66

Table 4.1: Yield, peak and ultimate load-displacement points for 28 MPa original/control and repaired specimens.

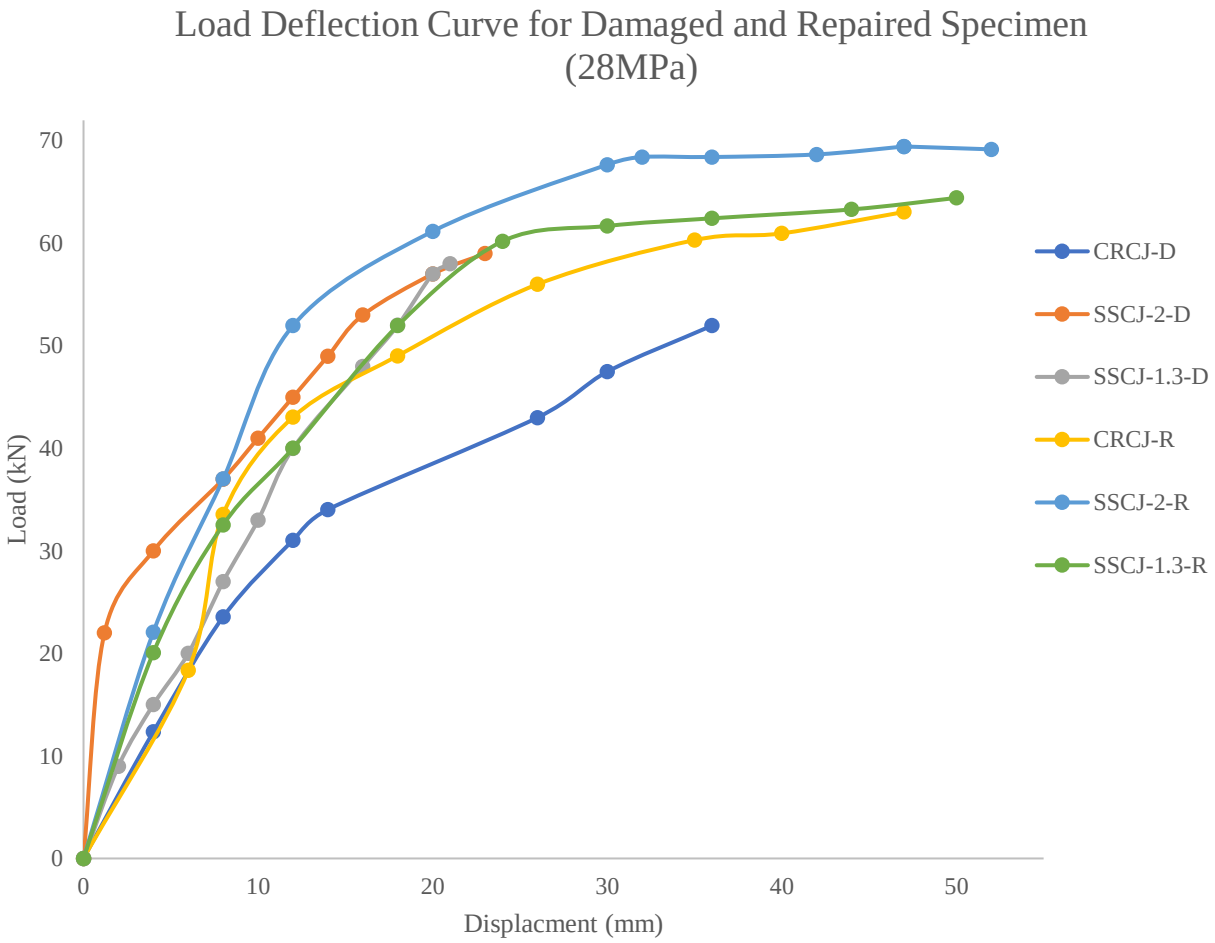

Figure 4.13: Load-displacement points of 28 MPa damaged and repaired Samples

Damaged Specimen 3-Ksi			Repaired Specimen 3-Ksi		
Parameter	**Displacement**	**Load**	**Parameter**	**Displacement**	**Load**
CRCJ			**CRCJ**		
Yield point	7.5	26.5	Yield point	9	37
Peak load	42	59	Peak load	34	63.5
Ultimate displacement	32	57	Ultimate displacement	40	62.5
SSCJ-02			**SSCJ-02**		
Yield point	4	19.5	Yield point	10.5	40.5
Peak load	20	56	Peak load	48	69
Ultimate displacement	23	48	Ultimate displacement	41.5	65
SSCJ-1.3			**SSCJ-1.3**		
Yield point	4.5	22.5	Yield point	9.5	36
Peak load	40	60	Peak load	50	69
Ultimate displacement	38	60	Ultimate displacement	50	68.5

Table 4.2: Yield, peak and ultimate load-displacement points for 21 MPa original/control and repaired specimens.

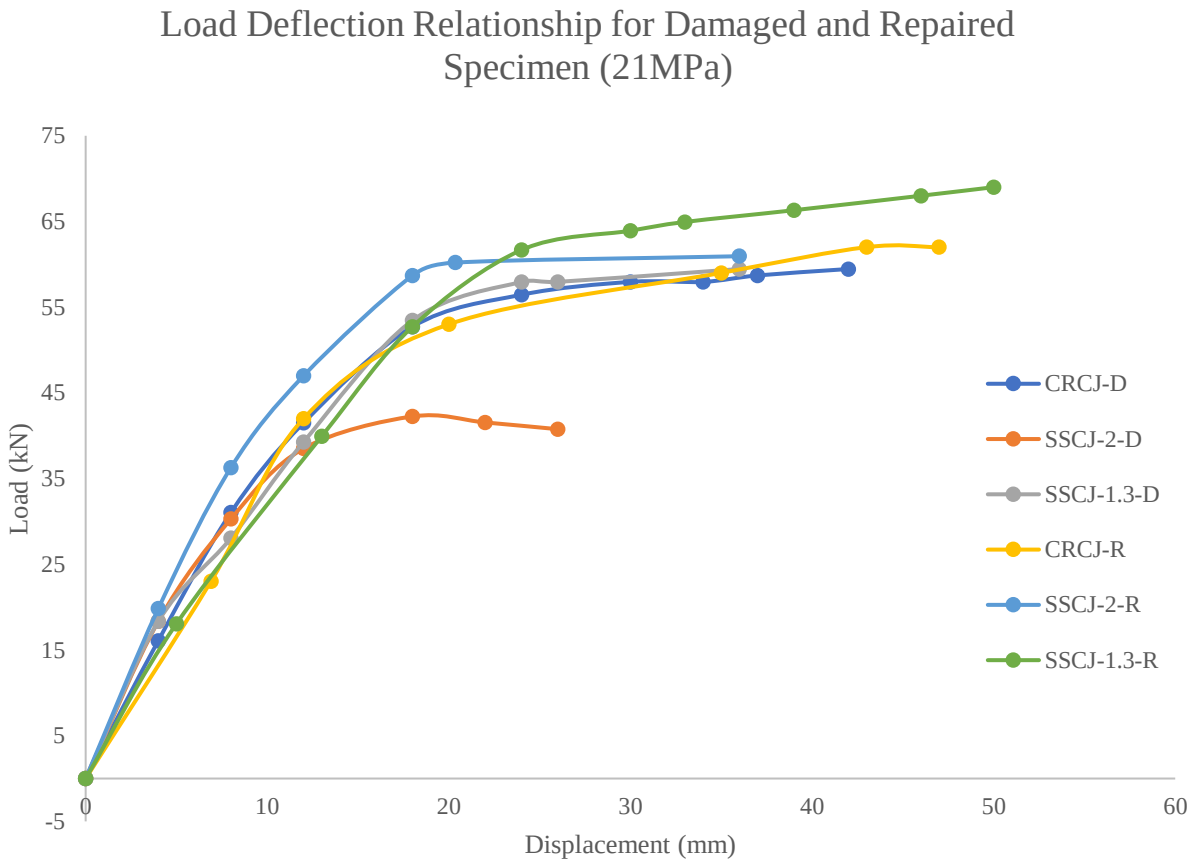

Figure 4.14: Load-displacement points of 21MPa damaged and repaired samples

4.1.4 Residual Displacement

The residual displacement was recorded for original and repaired specimens, and shown in tables below. CRCJ and SSCJ samples depicted the same trend. Comparatively lesser residual displacement of SSCJ-02 samples indicates a higher confining pressure as compared to CRCJ and SSCJ-1.3 samples.

JOINT	YIELD POINT (mm)	PEAK LOAD (kN)	ULTIMATE DISPLACEMENT (mm)
CRCJ	5	20	28
SSCJ-02	4	34	28
SSCJ-1.3	6	32	26.5

Table 4.3 : Residual displacements of 28 MPa Samples of control specimen

JOINT	YIELD POINT (mm)	PEAK LOAD (kN)	ULTIMATE DISPLACEMENT (mm)
CRCJ	7.5	42	32
SSCJ-02	4	20	23
SSCJ-1.3	4.5	40	38

Table 4.4 : Residual displacements of 21 MPa Samples of control specimen

JOINT	YIELD POINT (mm)	PEAK LOAD (kN)	ULTIMATE DISPLACEMENT (mm)
CRCJ	6.5	48	47.5
SSCJ-02	5.5	55	53.5
SSCJ-1.3	7	48	49

Table 4.5 : Residual displacements of 28 MPa Samples of repaired specimen

JOINT	YIELD POINT (mm)	PEAK LOAD (kN)	ULTIMATE DISPLACEMENT (mm)
CRCJ	9	34	40
SSCJ-02	10.5	48	41.5
SSCJ-1.3	9.5	50	50

Table 4.6 : Residual displacements of 21 MPa Samples of repaired specimen

4.1.5 Energy Dissipation

Hysteresis response of structural members under cyclic loading can be used for calculation of their energy. The area in a hysteresis cycle/ loop is the total energy dissipated in a cycle. The addition of damping and damage energy gives us the total energy. Figure 4.15 shows the total, damage, damp and strain energy on the hysteresis loop. These energies are calculated from the backbone curves of the samples. The amounts of energies dissipated by different samples are compared in Table 17 and 18. It is pertinent to mention that due to improved post peak behavior SSCJ-02, it has dissipated 23.1 to 27.1% higher energy as compared to CRCJ.

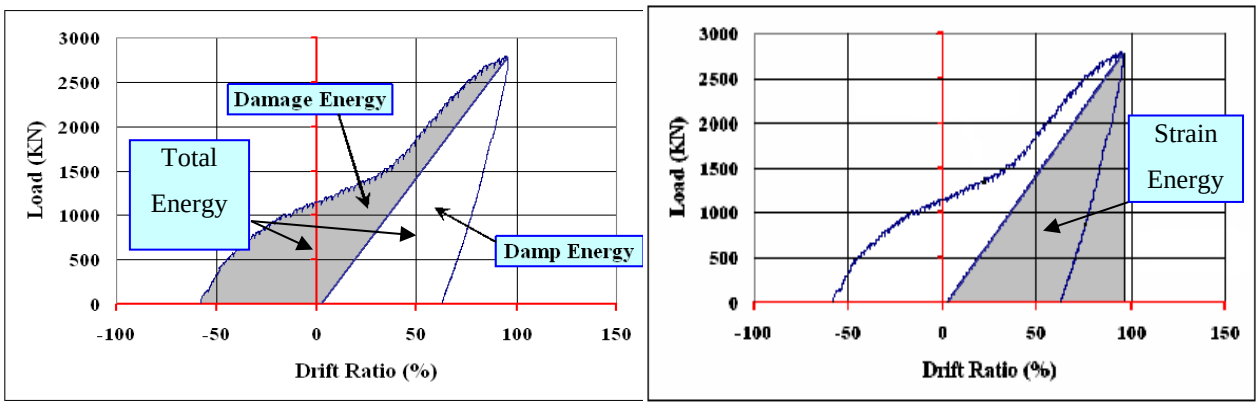

Figure 4.15 Categories for Energy Dissipation

ENERGY DISSIPATED	CRCJ (KN/mm)	SSCJ-02 (KN/mm)	SSCJ-1.3 (KN/mm)	GAIN/LOSS SSCJ-02	GAIN/LOSS SSCJ-1.3
Total energy	711	900	651	26.6%	8.4%
Damping energy	418	531	314	27%	24.9%
Damage energy	293	369	337	25.9%	8.7%
Strain energy	722	824	708	14.1%	1.9%

Table 4.7: Energy Dissipated by Joints of 28 MPa of control specimen

ENERGY DISSIPATED	CRCS-40 (KN/mm)	SSCJ-02 (KN/mm)	SSCJ-1.3 (KN/mm)	GAIN/LOSS SSCJ-02	GAIN/LOSS SSCJ-1.3
Total energy	1052	659	1083	37.4%	2.9%
Damping energy	586	365	449	37.7%	23.4%
Damage energy	466	248	449	46.8%	3.6%
Strain energy	999	583	1133	41.6%	13.4%

Table 4.8: Energy Dissipated by Joints of 21 MPa of original specimen

ENERGY DISSIPATED	CRCJ (KN/mm)	SSCJ-02 (KN/mm)	SSCJ-1.3 (KN/mm)	GAIN/LOSS SSCJ-02	GAIN/LOSS SSCJ-1.3
Total energy	1470	2356	2452	60.3%	66.8%
Damping energy	812	1393	1358	71.6%	67.2%
Damage energy	658	1163	1092	76.7%	65.9%
Strain energy	1215	1823	1757	50%	44.6%

Table 4.9 : Energy Dissipated by Joints of 28 MPa of repaired specimen

ENERGY DISSIPATED	CRCS-40 (KN/mm)	SSCJ-02 (KN/mm)	SSCJ-1.3 (KN/mm)	GAIN/LOSS SSCJ-02	GAIN/LOSS SSCJ-1.3
Total energy	1559	1786	1630	14.56%	4.6%
Damping energy	771	962	692	24.8%	10.2%
Damage energy	792	810	933	2.3%	17.8%
Strain energy	1311	1452	1276	8.7%	2.7%

Table 4.10: Energy Dissipated by Joints of 21 MPa of repaired specimen

4.1.6 Ultimate Strength

Ultimate strength of repaired specimen was experimented by applying cyclic loading. Cyclic loading was applied a certain load and then remove it the procedure is continued until the ultimate load is reached, where the load started decreasing or remains constant with the increase in displacement.

For pre-damaged joints the ultimate strength of 14-gauge (2mm) strips was 10 - 12% higher than that of stirrups likewise strength of 18-gauge (1.3mm) strips was 7 - 10% higher that of stirrups. Whereas, for repaired joints ultimate strength of 14-gauge (2mm) strips 15-20% while 10 – 13% increase in strength was observed for 18-gauge (1.3mm) strips.

We also tested three concrete cylinders to check the compressive strength of concrete and 28 days compressive strength of concrete is found to be 28 MPa and 21 MPa respectively for both the specimen groups. Non-destructive test of beam column joints was also conducted by Schmidt-hammer test and the average compressive strength at joints and top of specimen was found to be more than the desired range.

4.1.6 Ductility

Performance of a structure beyond its peak load point is measured by its ductility. The ductile behavior of RC structures is greatly influenced by the use of steel reinforcement and confinement. Ductility of members is termed as the ability to deform after the yield point, it is also the ability to dissipate energy. In general, ductility is a structural property which is governed by fracture and depends on structure size. Figure below shows a typical comparison of ductility curves of confined and un-confined concrete. It is evident that with increase in confinement the ductility of the concrete member/ structure increases. Mathematically it is the ratio of prescribed displacement beyond yield to the displacement at yield. Hence, in general terms the ductility of a structure can be defined by the ductility factor:

$$\mu = \frac{\Delta_u}{\Delta_y}$$

Δu = the ultimate deflection of member

Δy = the deflection at the yield point

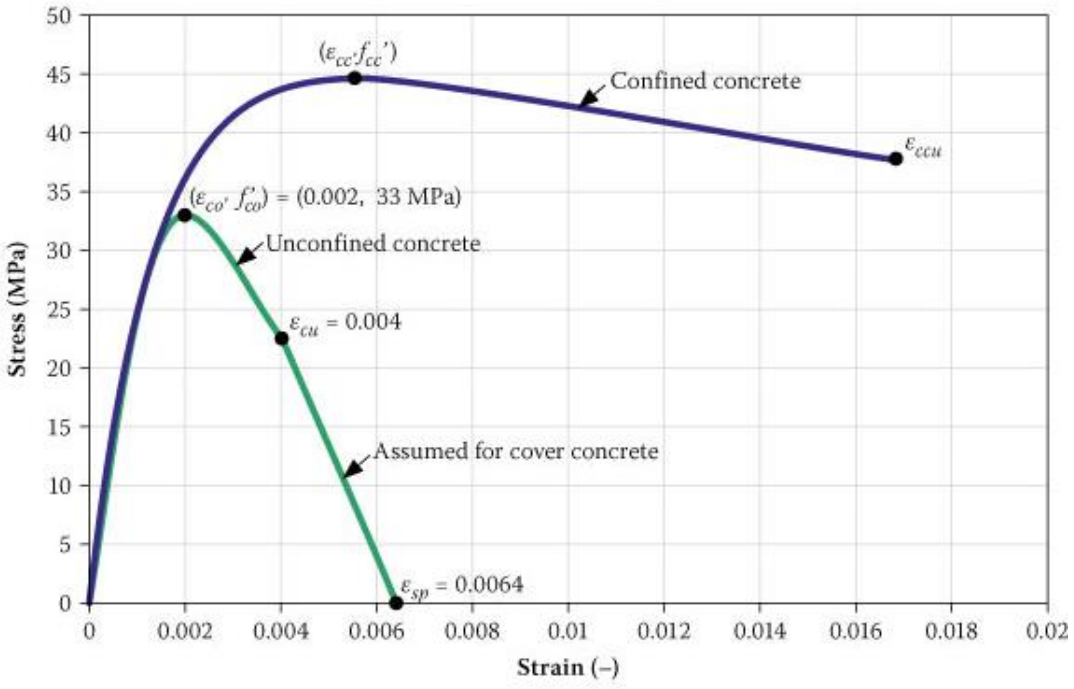

Figure 4.16 Ductility of Concrete

Ductility of different samples (28 MPa and 21 MPa samples consisting of CRCJ, SSCJ-02 and SSCJ-1.3) is calculated and compared in Table 4.11.

Table 4.11 Summary of Test Result for Control Specimens with 28MPa and 21 Mpa Concrete Strengths

Sample		**Load and Deflection at first crack**		**Load and Displacement at Yield**		**Ultimate Load P_U (KN)**	**Ulti-mate Deflec-tion Δ_U (mm)**	**Energy Dissipated (KN-mm)**				**Stiff. P_U / Δ_U (KN/mm)**	**Ductility Δ_U / Δ_y (mm/mm)**
		Load (KN)	**Def. (mm)**	**Load (KN)**	**Def. Δ_y (mm)**			**Total**	**Damping**	**Damage**	**Strain**		
CRCJ	1-4#3	12.5	2	22	6	52	36	802	470	332	860	1.44	6
	2-4#3	18	2	28	4	53	20	619	366	253	548	2.65	5
Average		**15.2**	**2**	**25**	**5**	**52.50**	**28.00**	**710.5**	**418.00**	**292.50**	**704.0**	**2.05**	**5.5**
SSCJ-2	1-4-14	18	1	22	2	59	22.5	878	512	367	608	2.62	11.25
	2-4-14	16	1	18	6	62	34	922	550	372	1040	1.82	5.6
Average		**17**	**1**	**20**	**4**	**60.50**	**28.25**	**900**	**531**	**369.50**	**824**	**2.22**	**8.46**
SSCJ-1.3	1-4-18	9	2	20	5.5	58	21	345	105	240	450	2.76	3.8
	2-4-18	16	4	17	6	58.7	32	957	522	434	966	1.83	5.3
Average		**12.5**	**3**	**18.50**	**5.75**	**58.35**	**26.50**	**651**	**313.5**	**337**	**708**	**2.30**	**4.58**
CRCJ	1-3#3	16	4	28	11	59	42	1458	773	685	1361	1.40	3.5
	2-3#3	22	5	25	4	55.7	22	645	399	247	637	2.53	5.5

Average		**19**	**4.50**	**26.50**	**7.50**	**57.35**	**32**	**1051**	**586**	**466**	**999**	**1.97**	**4.66**
SSCJ-2	1-3-14	21	3	21	4	56	20	645	399	167	637	2.80	5
	2-3-14	18	2	18	4	40.7	26	672	330	330	528	1.57	6.5
Average		**19.5**	**2.5**	**19.5**	**4**	**48.35**	**23**	**658.5**	**364.5**	**248.5**	**582.5**	**2.18**	**5.75**
SSCJ-1.3	1-3-18	18	3	20	5	59.5	36	1219	519	519	1021	1.65	7.2
	2-3-18	12	3	25	4	60	40	946	378	378	1244	1.50	10
Average		**15**	**3**	**22.5**	**4.50**	**59.75**	**38.00**	**1083**	**448.5**	**448.50**	**1133**	**1.58**	**8.60**

Table 4.12 Summary of Test Results for Repaired Specimen 28MPa and 21 MPa Concrete Strengths

Sample		Load and Deflection at first crack		Load and Displacement at Yield		Ulti-mate Load (KN) P_U	Ultimate Deflec-tion Δ_y (mm)	Energy Dissipated (KN-mm)				Stiffness (KN/mm) Pu/Δu	Ductility (mm/mm) Δu/ Δy
		Load (KN)	Deflection (mm)	Load (KN)	Deflection (mm) Δ_y			Total	Damping	Damage	Strain		
CRCJ	1-4#3	16	2	27	7	63	48	1796	1041	755	1506	1.3	6.9
	2-4#3	23	2	29	6	62	47	1144	583	561	924	1.3	7.8
Average		**19**	**2**	**28**	**6.5**	**62.5**	**47.5**	**1470**	**812.0**	**658.0**	**1215**	**1.3**	**7.3**
SSCJ-2	1-4-14	23	1.5	30	6	69	52	2450	1445	1005	1935	1.3	8.7
	2-4-14	20	1.5	55	5	74	55	2261	1341	1320	1711	1.3	11.0
Average		**21**	**1.5**	**42.5**	**5.5**	**71.5**	**53.5**	**2356**	**1393.0**	**1162.5**	**1823**	**1.3**	**7.1**
SSCJ-1.3	1-4-18	11	2	32	8	64	50	2224	1353	871	1737	1.3	6.3
	2-4-18	20	4	50	6	68	48	2680	1363	1313	1776	1.4	8.0
Average		**16**	**3**	**41**	**7.0**	**66.0**	**49.0**	**2452**	**1358.0**	**1092.0**	**1757**	**1.3**	**7.1**
CRCJ	1-3#3	20	4	42	12	62	46	1785	774	1012	1511	1.3	3.8
	2-3#3	28	6	32	6	63.5	34	1333	768	572	1110	1.9	5.7

Average		**24**	**5**	**37**	**9.0**	**62.8**	**40.0**	**1559**	**771.0**	**792.0**	**1311**	**1.6**	**4.8**
SSCJ-2	1-3-14	26	3	40	8	61	35	1450	750	670	1147	1.7	6.9
	2-3-14	23	2	41	13	69	48	2122	1174	949	1703	1.4	5.6
Average		**24**	**3**	**40.5**	**10.5**	**65.0**	**41.5**	**1786**	**962**	**809.5**	**1425**	**1.6**	**6.7**
SSCJ-1.3	1-3-18	23	3	34	11	69	50	1838	1062	767	1791	1.4	9.5
	2-3-18	15	3	38	8	68	50	1421	321	1100	761	1.4	8.3
Average		**19**	**3**	**36**	**9.5**	**68.5**	**50.0**	**1630**	**691.5**	**933.5**	**1276**	**1.4**	**9.4**

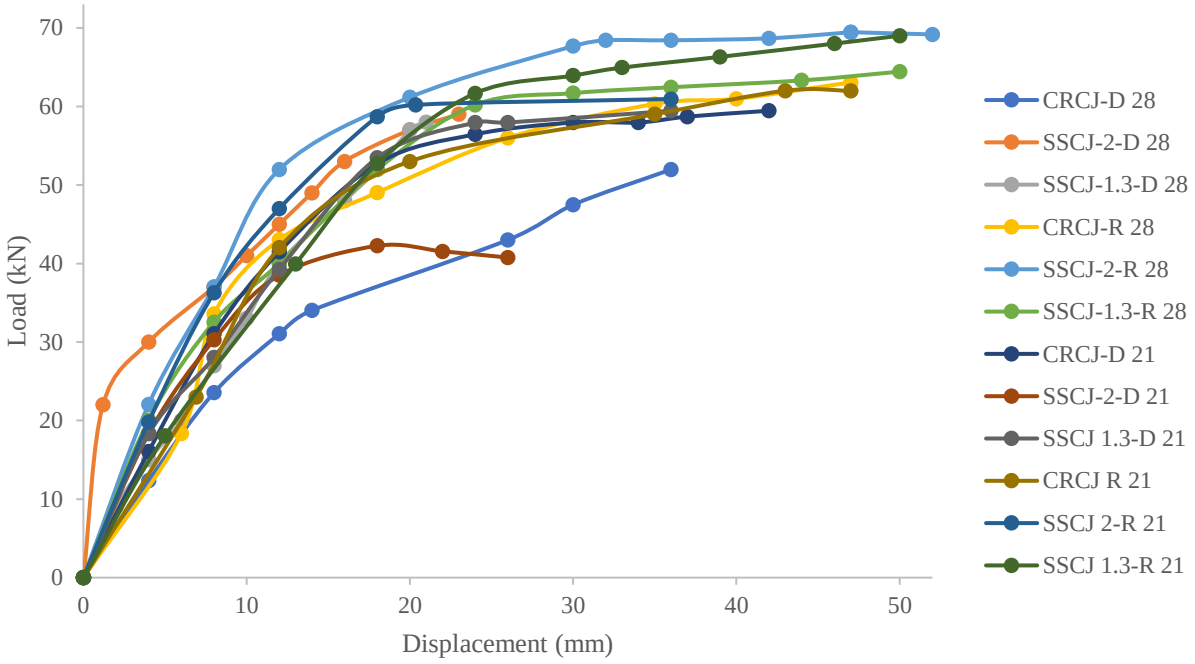

Figure 4.17 Load Deflection Curve for 28 and 21MPa Series Damaged and Repaired Specimen

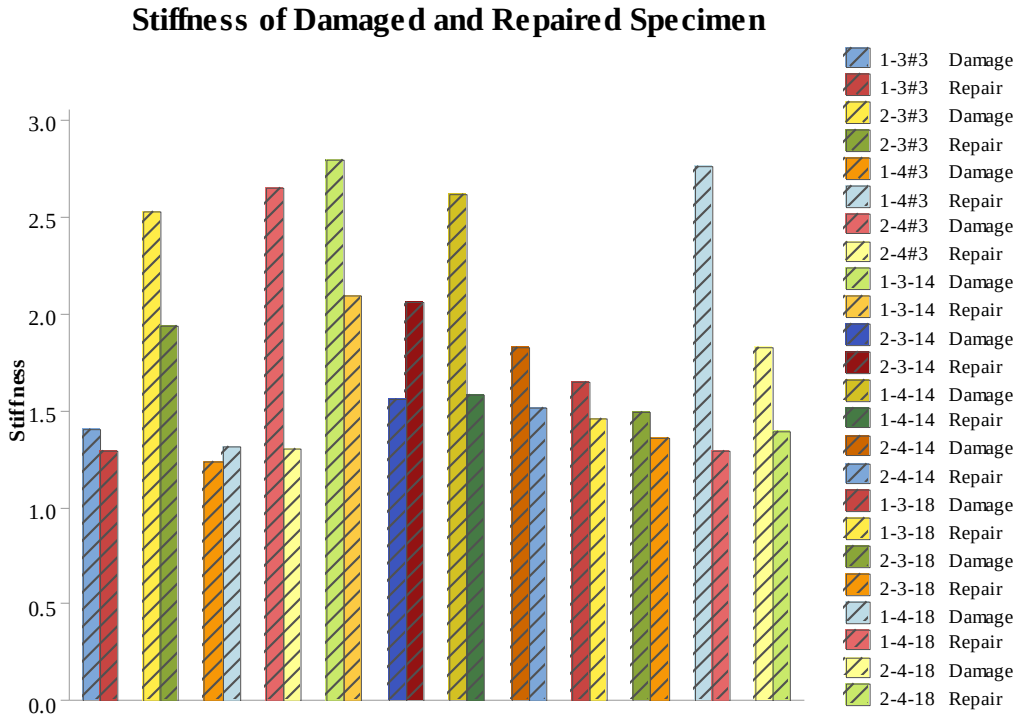

Figure 4.18 Stiffness of Damaged and Repaired Specimen

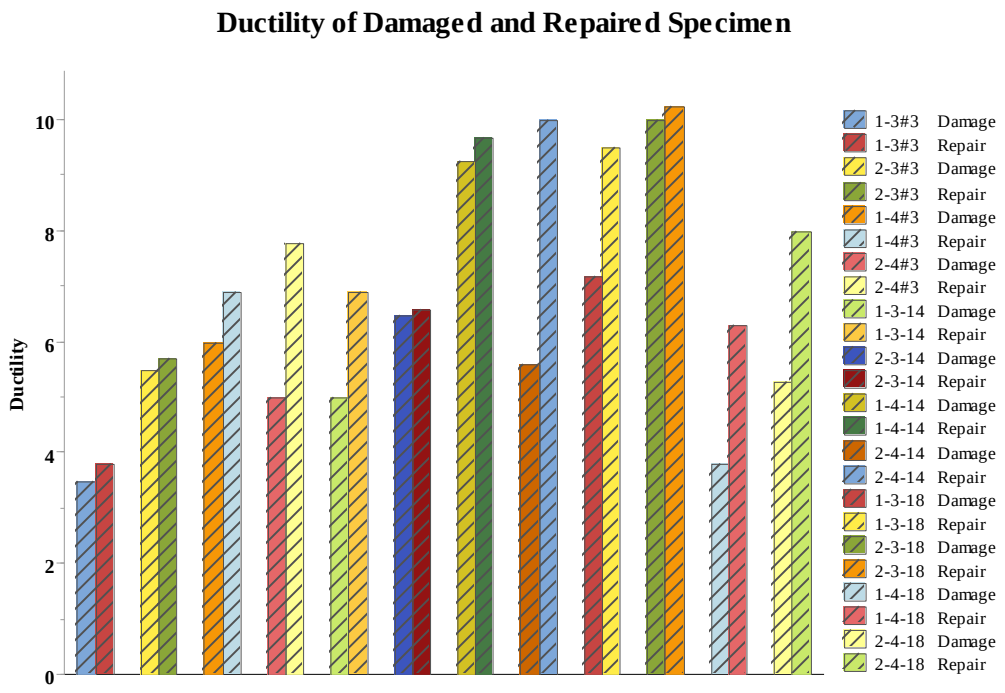

Figure 4.19 Ductility of Damaged and Repaired Specimen

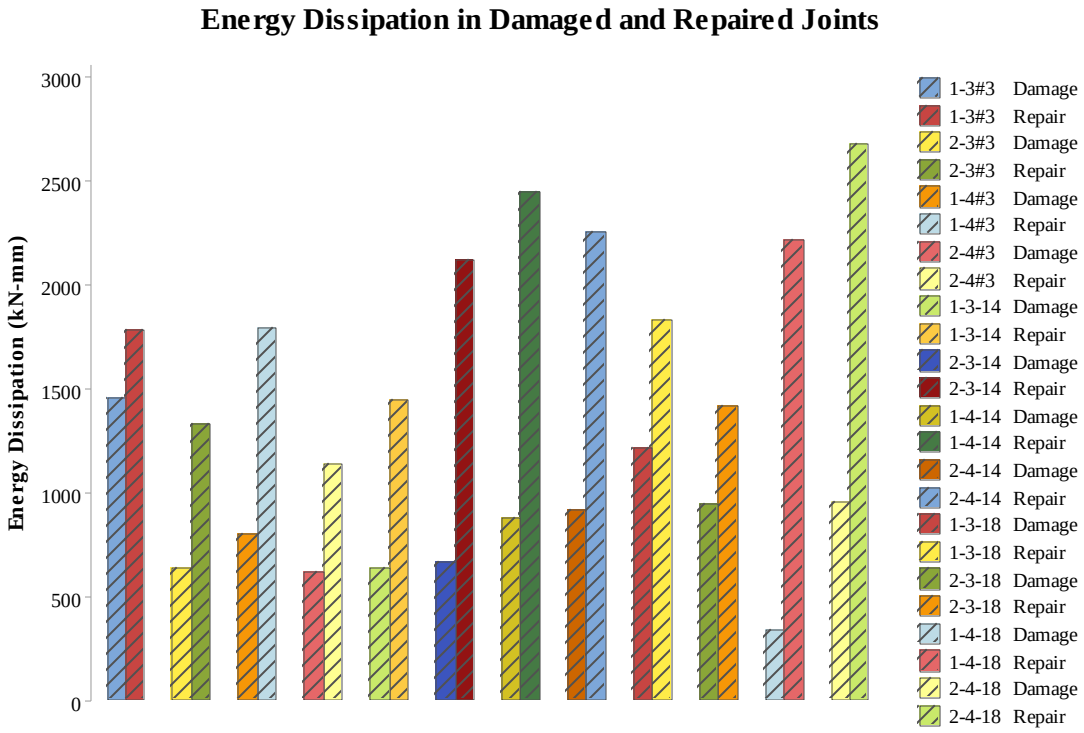

Figure 4.20 Energy Dissipation in Damaged and Repaired Joints

RESULT DISCUSSION AND CONCLUSION

CFRP was employed to repair damaged RC beam column joints. Initially, all specimens were tested under quasi static cyclic loading. These specimens were then repaired with CFRP layers. Repaired joints showed that CFRP laminates significantly improved load carrying capacity. Few findings of this investigation are as follows:

1. Debonding dominates the behavior of external reinforcement unless very low area fractions are employed or proper mechanical anchorages are provided.
2. Improvement in ultimate load in specimens repaired with CFRP was 19%, 16% and 13% respectively for CRCJ, 28 MPa, whereas this increase was observed to be 8%, 17% and 15% for 21 MPa repaired specimens.
3. Role of CFRP laminates in improving ultimate deflection was pivotal. Ultimate deflection in specimens with CFRP was significantly higher with all repaired joints, as compared to pre-damaged control specimen.
4. Generally, using CFRP as a strengthening material led to increased ultimate capacity and decreased ductility compared to those of un-strengthened damaged joints.
5. Stiffness of specimens repaired with CFRP was reduced significantly due to bar slips and damaged concrete structure under repeated load cycles. This indicates that, after retrofitting, the failure pattern of weak beam strong column joint is achieved.

Chapter 5

RECOMMENDATIONS

Following Recommendations are suggested for future research projects.

1. In present study, the beams were repaired with CFRP, wrapped in the with single unique configuration for all joints. Other orientations of CFRP need to study to predict the maximum strength of CFRP repaired joints. Thus, optimization in use CFRP can be achieved which can reduce the cost of repair.
2. This experimental study was focused on repair for exterior RC beam column joints, further research on interior joints with high strength concrete can be carried out.
3. The results of the present study infer that, for field applications, it is very much necessary to decide judiciously and carefully which scheme is suitable for strengthening a deteriorated or deficient beam-column joint. This is because strengthening of a joint and its adjacent members with CFRP sheets may also shift the failure mode from the joint to the adjacent member (e.g., beam or column) or vice versa.
4. The experimental studies and subsequent analyses provide the basis for the next stage of the study involving finite element modelling and analysis.
5. The retrofit schemes proposed in the literature require different levels of intensive labor and artful detailing. Besides, all these specimens have been tested on isolated beam-column sub-assemblages with no floor members (i.e., transverse beams and floor slabs). This limits the range of their applicability, and therefore inhibits their adoption in practice. On the other hand, most of the tests were performed on exterior joints. Additional investigations, with particular emphasis on these aspects, are strongly recommended.

REFERENCE

1. Dr Muhammad Rizwan (2015) - Modelling steel-strip-confined reinforced-concrete columns. Proceedings of the Institution of Civil Engineers - Structures and Buildings 2016 169:4, 245-256.

2. Tahir, M. (2015). Response of Seismically Detailed Beam Column Joints Repaired with CFRP Under Cyclic Loading. Arabian Journal for Science and Engineering. 41.. 10.1007/s13369-015-1943-z.

3. Eythor Thorhallsson (2011) - Test of Rectangular Confined Concrete Columns for Strength and Ductility.

4. Pasala Nagaprasad (2009) - Seismic strengthening of RC columns using external steel cage. Earthquake Engineering & Structural Dynamics. 38. 1563 - 1586. 10.1002/eqe.917.

5. Giuseppe Campione (2012) - Strength and ductility of R.C. columns strengthened with steel angles and battens. Construction and Building Materials. 35. 800–807. 10.1016/j.conbuildmat.2012.04.090.

6. G. Campione (2012) – Reinforced Concrete columns externally strengthened with RC jackets. Mater Struct 2014- 47: 1715.

7. Hasan Moghaddam (2010) - Axial compressive behavior of concrete actively confined by metal strips; part A: experimental study. Mater Struct 2010 - 43: 1369. https://doi.org/10.1617/s11527-010-9588-6.

8. Richart, F. E., Brandzaeg, A. and Brown, R. L. (1928) - A study of the failure of concrete under Combined Compressive Stresses. University of Illinois Engineering Station, Bulletin No. 185, 1928, 104 pp.

9. Balmer, G.G., Shearing Strength of Concrete under High Triaxial Stresses – Computation of Mohr's Envelope as a Curve". Structural Research Laboratory Report No. SP-23, U.S. Bureau of Reclamation, 1943, 13 pp. plus tables and figures.

10. Sundara Raja Iyengar, K.T., Parakash Desayi and Nagi Reddy, K., "Stress-Strain Characteristics of concrete Confined in Steel Binder", Magazine of Concrete Research, Vol. 22, No 72: September 1970, pp. 173-184.

11. Parakash Desayi, Sundara Raja Iyengar, K.T. and Sanjeeva Reddy, T., "Equation for Stress-Strain Curve of Concrete Confined in Circular Steel Spiral", Matériau et Constructions, Vol. 11 – No 65, September/October 1978, pp. 339-345.

12. Muguruma, H., Watanabe, F., Tanaka, H., Sakurai, K. and Nakamura, E., "Effect of Confinement by High Yield Strength Hoop Reinforcement upon the Compressive Ductility of Concrete", Proceedings of the Twenty-Second Japan Congress on Material Research, The Society of Material Science, Japan, 1979, pp. 377-382.

13. Muguruma, H., Watanabe, F., Tanaka, H., Sakurai, K. and Nakamura, E., "Study on Improving the Flexure and Shear Deformation Capacity of Concrete Member by Using Lateral Confining Reinforcement with High Yield Strength", Comité Euro-International du Béton, BULLETIN D'INFORMATION N◦ 132, Volume 2 – Technical Papers, AICAP-CEB Symposium, Rome, May 1979, pp. 37-44.

14. Watanabe, F., Muguruma, H., Tanaka, H. and Katsuda, S., "Improving the Flexural Ductility of Prestressed Concrete Beam by Using the High Yield Strength Lateral Hoop Reinforcement", FIP, Symposia on Partial Prestressing and Practical Construction in Prestressed and Reinforced Concrete, Proceedings: Part 2, Sept. 1980, Bucuresti-România, pp. 398-406.

15. Mander, J. B., Priestley, M.J.N. and Park, R., "Theoretical Stress Strain Model for Confined Concrete" Journal of Structural Engineering, American Society of Civil Engineers, vol. 114, No. 8 August 1988, pp. 1804-1826.

16. Mander, J. B., Priestley, M.J.N. and Park, R., "Observed Stress-Strain Behavior of Confined Concrete" Journal of Structural Engineering, American Society of Civil Engineers, vol. 114, No. 8 August 1927, pp. 1804-1849.

17. Popovics, S., “A Numerical Approach to the complete Stress-Strain Curves of Concrete”, Cement and Concrete Research, Vol. 3, No. 5, September 1973, pp. 583-599.

18. Roy, H.E.H. and Sozen, M.A., “Ductility of Concrete”, Proceedings of the International Symposium on Flexural Mechanics of Reinforced Concrete, ASCE-ACI, Miami, November 1964, pp. 213-224.

19. Soliman, S.A. and Uzumeri, S.M., “Properties of Concrete Confined by Rectangular Tie”, AICAP-CEB Symposium on Structural Concrete under Seismic Actions (Rome, May 1979), Bulletin d'Information No. 132, Comité Euro-International du Beton, Paris, 1979, pp-53-60.

20. Park, R., Priestley, M.J.N. and W.D. Gill, “Ductility of Square Confined Concrete Columns” Proceedings ASCE, Vol. 108, ST4, April 1982, pp-929-950.

21. Kent, D. C. and Park, R., “Flexural Members with Confined Concrete”, Proceedings of ASCE, Vol. 97, No. ST 7, July 1971, pp. 1969-1990.

22. Sheikh S. A. and Uzumeri, S. M., “Strength and ductility of tied concrete columns”, Journal of the structure division, ASCE 1980, 106(5), pp 1079-1102.

23. Sheikh S. A. and Yeh C.C., “Flexural behavior of confined concrete columns”, ACI Journal May–June 1982, pp-389–404.

24. Saatcioglu, M. and Razvi, S. R., “Strength and ductility of confined concrete”, Journal of Structural Engineering, ASCE 1992, 118 (6), pp. 1590-1607.

25. Razvi, S. R. and Saatcioglu, M., “Design of RC columns for confinement based on lateral drift”, Ottawa-Carleton Earthquake Engineering Research Center, Report OCEERC 96-02 1996, Dept. of Civil Engineering, Univ. of Ottawa, Ottawa, Canada, pp. 92.

26. Razvi, S. R. and Saatcioglu, M., “Stress-strain relationship for confined high strength concrete”, Journal of Structural Engineering, ASCE 1999, 125 (3).

27. Hoshikuma, J., Kawashima, K., Nayaga, K. and Taylor, A.W., "Stress–strain model for confined RC in bridge piers", Journal of Structural Engineering 1994, Vol.123(5), pp-624–633.

28. EL-Dash. K. M. and Ahmad. S. H., "A model for the stress-strain relationship of rectangular confined normal and high strength concrete columns", Material and structures 1994 No. 27, pages 572-579.

29. Bousalem, B. and Chikh, N., "Development of a confined model for rectangular ordinary reinforced concrete columns", Journal of Material and Structures 2006, DOI 10.1617/s11527-06-9172-2.

30. Bing, L., Park, R. and Tanaka, H. (2001). Stress–strain behavior of high strength concrete confined by ultra-high and normal strength transverse reinforcements. Structural Journal, ACI, May–June, pp-395–406.

31. Muguruma H., Nishiyama, M., Watanabe, F. and Tnaka, H. (1991). Ductile behavior of high strength concrete columns confined by high strength transverse reinforcement. ACI Special Publication: Evaluation and Rehabilitation of concrete structures and innovation in design Vol.128-54(88-AB).